Impact of surface properties of polymers on the cytocompatibility

Bc. Leona Mahelová

Master's thesis
2020

Tomas Bata University in Zlín
Faculty of Technology

Univerzita Tomáše Bati ve Zlíně
Fakulta technologická
Ústav inženýrství polymerů

Akademický rok: 2019/2020

ZADÁNÍ DIPLOMOVÉ PRÁCE

(projektu, uměleckého díla, uměleckého výkonu)

Jméno a příjmení:	**Bc. Leona Mahelová**
Osobní číslo:	**T18245**
Studijní program:	**N2808 Chemie a technologie materiálů**
Studijní obor:	**Inženýrství polymerů**
Forma studia:	**Prezenční**
Téma práce:	**Povrchové vlastnosti polymerů a jejich vztah k buněčné kompatibilitě**

Zásady pro vypracování

Student/ka zpracuje literární rešerši zaměřenou na charakterizaci povrchových vlastností polymerních materiálů, možnosti jejich modifikací a vztah k buněčné kompatibilitě. Samostatnou kapitolu pak věnuje vlivu isotropie. Dále se zaměří na vliv povrchové energie a elektrické vodivosti. V rámci praktické části provede sérii experimentů zaměřenou na úpravu povrchových vlastností, tvorbu vzorků s různou isotropií a následně provede test buněčné kompatibility.

Forma zpracování diplomové práce: **Tištěná/elektronická**
Jazyk zpracování: **Angličtina**

Seznam doporučené literatury:

SNUSTAD, D.P., SIMMONS, M.J., RELICHOVÁ, J. et al. Genetika. Brno: Masarykova univerzita, 2009.
ALBERTS B. et al. Molecular Biology of the Cell 5th ed. Garland Science.
DAVID A.P. BIZIOS R. Biological Interactions on Material Surfaces. ISBN 978-0-387-98160-4

Vedoucí diplomové práce: **doc. Ing. Petr Humpolíček, Ph.D.**
Centrum polymerních materiálů

Datum zadání diplomové práce: **2. ledna 2020**
Termín odevzdání diplomové práce: **15. května 2020**

L.S.

prof. Ing. Roman Čermák, Ph.D.
děkan

doc. Ing. Tomáš Sedláček, Ph.D.
ředitel ústavu

Ve Zlíně dne 17. února 2020

PROHLÁŠENÍ AUTORA
DIPLOMOVÉ PRÁCE

Beru na vědomí, že:

- diplomová práce bude uložena v elektronické podobě v univerzitním informačním systému a dostupná k nahlédnutí;
- na moji diplomovou práci se plně vztahuje zákon č. 121/2000 Sb. o právu autorském, o právech souvisejících s právem autorským a o změně některých zákonů (autorský zákon) ve znění pozdějších právních předpisů, zejm. § 35 odst. 3;
- podle § 60 odst. 1 autorského zákona má Univerzita Tomáše Bati ve Zlíně právo na uzavření licenční smlouvy o užití školního díla v rozsahu § 12 odst. 4 autorského zákona;
- podle § 60 odst. 2 a 3 autorského zákona mohu užít své dílo – diplomovou práci nebo poskytnout licenci k jejímu využití jen s předchozím písemným souhlasem Univerzity Tomáše Bati ve Zlíně, která je oprávněna v takovém případě ode mne požadovat přiměřený příspěvek na úhradu nákladů, které byly Univerzitou Tomáše Bati ve Zlíně na vytvoření díla vynaloženy (až do jejich skutečné výše);
- pokud bylo k vypracování diplomové práce využito softwaru poskytnutého Univerzitou Tomáše Bati ve Zlíně nebo jinými subjekty pouze ke studijním a výzkumným účelům (tj. k nekomerčnímu využití), nelze výsledky diplomové práce využít ke komerčním účelům;
- pokud je výstupem diplomové práce jakýkoliv softwarový produkt, považují se za součást práce rovněž i zdrojové kódy, popř. soubory, ze kterých se projekt skládá. Neodevzdání této součásti může být důvodem k neobhájení práce.

Prohlašuji,

- že jsem diplomové práci pracoval samostatně a použitou literaturu jsem citoval. V případě publikace výsledků budu uveden jako spoluautor.
- že odevzdaná verze diplomové práce a verze elektronická nahraná do IS/STAG jsou obsahově totožné.

Ve Zlíně dne:

Jméno a příjmení studenta:

.....
podpis studenta

ABSTRAKT

V dnešní době začíná využití polymerů v biomedicíně, zejména v perspektivním oboru tkáňového inženýrství, převládat nad tradičními materiály, jako je kov, keramika či sklo. Předložená diplomová práce pojednává o vlivu povrchových charakteristik polymerů, jako je chemická struktura, fyzikální a mechanické vlastnosti, včetně (an)izotropie a různých způsobů povrchových úprav na buněčnou kompatibilitu. V rámci praktické části proběhly analýzy zaměřené na polyuretanové nanovlákenné netkané textilie vyrobené electro-spinningem. Byly hodnoceny účinky orientace vláken a polypyrrolových, albuminových a želatinových povrchových povlaků na chování myších fibroblastů a embryonálních kmenových buněk a to vše za účelem rozšíření báze znalostí, která může pomoci zlepšit optimalizaci scaffoldů pro dosažení růstu specifických tkání.

Klíčová slova: polymerní biomateriál, buněčná kompatibilita, anizotropie, povrchové modifikace

ABSTRACT

Nowadays, the utilization of polymers in biomedicine, especially in the promising field of tissue engineering, starts to predominate over traditional materials such as metal, ceramics, or glass. The submitted master's thesis discusses the impact of surface characteristics of polymers, such as chemical structure, physical and mechanical properties, including the (an)isotropy and various ways of surface modifications, on the cytocompatibility. In the experimental part, analyzes focused on electrospun polyurethane nanofibrous nonwoven mats. The effects of fiber alignment and polypyrrole, albumin, and gelatin surface coatings on the behavior of mouse fibroblasts and mouse embryonic stem cells were assessed for the purpose of knowledge base expansion that may improve scaffold design optimization for specific tissue growth achievement.

Keywords: polymeric biomaterial, cytocompatibility, anisotropy, surface modifications

I would like to thank the supervisor of my master's thesis doc. Ing. Petr Humpolíček, Ph.D. for providing valuable advice, and doctoral students Ing. Kateřina Skopalová and Ing. Thanh Huong Truong for their help in biological laboratories. I would also like to express my gratitude to my loving parents Ing. Zbyněk Mahel and Dana Mahelová and my life partner Bc. Danila Gorgol for their support during my studies.

I hereby declare that the print version of my Master's thesis and the electronic version of my thesis deposited in the IS/STAG system are identical.

CONTENTS

INTRODUCTION **9**

I THEORY **10**

1 POLYMERS USED AS BIOMATERIALS **11**

2 BIOMATERIAL SURFACE CHARACTERISTICS AFFECTING THE CYTOCOMPATIBILITY **15**

2.1 ABILITY TO ADSORB ADHESIVE PROTEINS TO THE SURFACE 15

2.1.1 Chemical structure of the surface 17
2.1.2 Physical properties of the surface 18
2.1.3 Vroman effect 19

2.2 ELECTRICAL CONDUCTIVITY 20

2.3 TOPOGRAPHY AND MORPHOLOGY 22

2.4 MECHANICAL PROPERTIES OF THE SURFACE 24

3 BIOMATERIAL ISOTROPY VERSUS ANISOTROPY **27**

3.1 EFFECT ON CELL BEHAVIOR 28

3.1.1 Under static cultivation conditions 29
3.1.2 Under dynamic cultivation conditions 33

3.2 FABRICATION TECHNIQUES FOR ANISOTROPIC SCAFFOLDS 36

3.2.1 Electrospinning 38

4 SURFACE MODIFICATIONS OF POLYMERIC BIOMATERIALS **41**

4.1 CHEMICAL MODIFICATIONS 41

4.2 BIOLOGICAL MODIFICATIONS 43

4.3 PHYSICAL MODIFICATIONS 44

4.4 MECHANICAL MODIFICATIONS 46

4.5 COMBINED AND SPECIAL MODIFICATIONS 47

II ANALYSIS **48**

5 AIMS AND OBJECTIVES **49**

6 MATERIALS AND METHODS **50**

6.1 SAMPLES PREPARATION AND MODIFICATION 50

6.1.1 Production 50
6.1.2 Extraction 51
6.1.3 Purification and orientation 51
6.1.4 Coating with polypyrrole 51
6.1.5 Coating with albumin and gelatin 52

6.2 CELL LINES AND CULTIVATION MEANS 52

6.2.1 Mouse fibroblast cell line 52
6.2.2 Mouse embryonic stem cell line 53
6.2.3 Cultivation with sample extracts 54

6.2.4 Cultivation on sample surfaces under static conditions 54
6.2.5 Cultivation on sample surfaces under tensile-dynamic and electric conditions 54
6.3 OBTAINING OF RESULTS 56
6.3.1 Scanning electron microscopy 56
6.3.2 Optical microscopy 56
6.3.3 Fluorescence microscopy 56
6.3.4 MTT assay 56
6.4 USED CHEMICALS 57
6.5 USED APPARATUS AND EQUIPMENT 58
7 RESULTS 59
7.1 ELECTROSPUN SAMPLES AND ORIENTATION 59
7.1.1 Sample 1 60
7.1.2 Sample 2 63
7.1.3 Sample 3 66
7.2 SURFACE COATINGS 69
7.3 CONDITIONS OF CELL CULTIVATION 72
7.3.1 Cultivation under static conditions 72
8 DISCUSSION 78
CONCLUSION 82
BIBLIOGRAPHY 83
LIST OF ABBREVIATIONS 91
LIST OF FIGURES 93
LIST OF EQUATIONS 96

INTRODUCTION

After polymers showed up in the field of biomedicine, the use of traditional materials such as metals, ceramics, and glass decreased considerably. Recently polymers became the most important and largest family of materials used in medical technologies, including today's very promising field of tissue engineering research. In comparison to the other biomaterials, polymers gained their popularity mainly due to the ability to easily and widely modify not only shapes but also the chemical structure, physical and mechanical properties. However, it has to be kept in mind that all of these mentioned characteristics and their changes have a certain impact on biological systems and although many studies were already carried out, this problematics is still not wholly understood. Since the missing pieces of this puzzle may have a great effect on the biocompatibility, it is essential to deepen current knowledge about how polymeric surface properties affect cellular behavior and how they can be modified and functionalized.

In addition to general information about which polymeric biomaterials are utilized and where and review of how their surface properties affect cytocompatibility and the ways they can be modified, this master's thesis also focuses on less studied areas that are expected to have a substantive impact on the success rate of polymeric biomaterial application too, such as structural and mechanical anisotropy and cell cultivation in dynamic *in vitro* conditions that are important to mimic the natural environment *in vivo*. The analysis attention was particularly driven to polyurethane nonwoven mats produced by electrospinning that were preferably chosen due to its specific properties, such as biocompatibility, viscoelasticity, and nanofibrous structure, which are supposed to mimic the natural cell surroundings – extracellular matrix. The effect of nanofiber alignment and several surface modifications, specifically polypyrrole, albumin, and gelatin coatings, on the behavior of mouse fibroblasts and mouse embryonic stem cells was observed for the purpose of knowledge base expansion that may improve scaffold design optimization for specific tissue growth achievement.

I. THEORY

1 POLYMERS USED AS BIOMATERIALS

Biomaterial refers to any material designed to interact with biological systems within or on the human body. (Schmalz et al., 2009) Polymers have great potential as biomaterials due to the ability to easily and broadly modify their chemical structure, physical and mechanical properties, and also shapes. It allows us to adapt polymers to the specific needs of individual biological systems and to develop such combinations of properties that cannot be achieved by using other materials, such as metal or ceramic. In addition to its tailoring-ability, polymers also have easy manufacturing, easy secondary processability, and reasonable cost. (Bronzino & Peterson, 2015) In this section, biomedical applications of the most commonly used polymers will be briefly discussed.

Polyethylene (PE) is the most common thermoplastic in the world and it is classified by its density, crystallinity, molecular weight, and type of branching in several classes, each having different applications due to the differences in mechanical properties. For example, high-density polyethylene (HDPE) is used in pharmaceutical bottles and medical nonwoven fabrics, in contrast with low-density polyethylene (LDPE), which is used in medical disposable supply and flexible packaging. (Bronzino & Peterson, 2015) However, of all PE classes, ultra-high molecular weight polyethylene (UHMWPE) plays a major role in biomedical applications as it is used in orthopedic implants due to great abrasion resistance and high load-bearing capacity. As shown in Figure 1, UHMWPE is utilized (a) in an acetabular cup of a hip joint prosthesis and (b) in a tibial plateau in a knee joint prosthesis. (Paita & Dahotre, 2008)

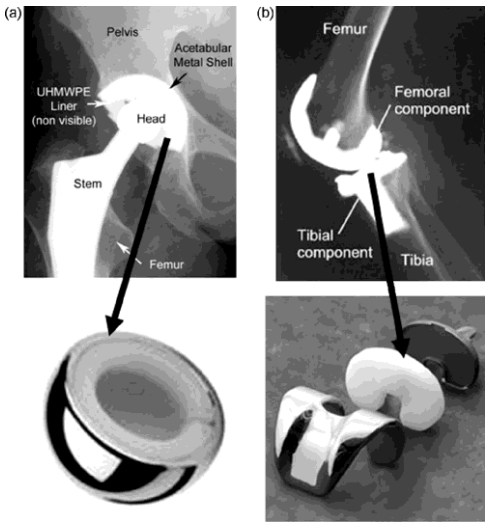

Figure 1 Application of UHMWPE in (a) hip joint and (b) knee joint prostheses. (Paita & Dahotre, 2008)

Polypropylene (PP) is possible to apply in finger joints prostheses due to its high flex life and stress-cracking resistance. PP also has received significant importance as disposable hypothermic syringes, blood oxygenator membranes, packaging for medical devices, nonwoven fabrics (Bronzino & Peterson, 2015), wound dressing, surgical suture, hernia repair, and blood transfusion bags (Gogoi et al., 2014).

Polystyrene (PS) is mostly utilized in the fabrication of tissue culture flasks for use in biological laboratories. (Bronzino & Peterson, 2015) Also, PS latex particles can serve as carriers for the immobilization of proteins in various diagnostic systems and assays. (Bousalem et al., 2003)

Polyvinylchloride (PVC) is used in different shapes. Sheets and films, made of PVC, are used for surgical packaging, blood and solution storage bags. PVC tubes can be found in catheters, cannulae, and connectors, for example serving as an intravenous set (Bronzino & Peterson, 2015) or can be used for artificial blood vessel production (Paita & Dahotre, 2008).

Polymethylmethacrylate (PMMA) is one of the most used polymers in medical applications. Due to its excellent optical properties, PMMA is used in conventional hard contact lenses and used in implantable ocular lenses. Due to good physical and coloring properties, it is used for the production of dentures and facial prostheses. Other applications of PMMA are in intravenous systems, blood dialyzers, pumps, and reservoirs, but its most specific use is in bone cement[1] earmarked for joint prostheses fixation. PMMA together with other acrylates, such as polyhydroxyethylmethacrylate (PHEMA), are used for the manufacture of medical hydrogels that are popularly utilized as soft contact lenses. (Bronzino & Peterson, 2015)

Polyurethane (PU) occurs in various implants, mostly in the cardiovascular system, such as pacemakers, artificial heart valves, or intra-aortic balloon pumps, but also in other devices, for example, artificial tympanic membrane or stent-like extensions for the esophagus. Recently, PU is attractive in the field of regenerative medicine, where PU scaffolds have already been used for engineering of nerve tissue, cartilage tissue (Kupka, 2015), skin tissue, and bone tissue. (Mani et al., 2019)

[1] However, a condition of functionality is the filling with hydroxyapatite particles, since PMMA itself does not promote bone adhesion. (Chauhan et al., 2019)

Polytetrafluoroethylene (PTFE), commonly known as Teflon (DuPont), is non-adhesive, hydrophobic, and it has superior chemical and physical properties than other fluorocarbon polymers. Hence PTFE has found the utilization as a biomaterial in artificial heart valves. (Chauhan et al., 2019)

Polyamides may have different properties depending on the number and distribution of –CONH– (amide) groups in polymer chains. These factors affect interchain hydrogen bonding, degree of crystallinity, thus fiber-forming ability, and hygroscopicity, thus *in vivo* strength. Polyamides are mostly used for sutures, catheters, and packaging films. (Bronzino & Peterson, 2015)

Liquid crystal polymers (LCPs) are also used as biomaterials, especially as retinal and neural prosthetic implants (Chauhan et al., 2019). LCPs are suitable for mentioned applications in reason of the dependency of molecular alignment and physical properties of LCPs on temperature, electric or magnetic fields, and molecular or surface interactions (Adamow et al., 2020).

Polyesters have also found widespread use in medicine. Polyethyleneterephthalate (PET), the most common representative of polyesters, is frequently used in non-biodegradable sutures, artificial vascular graft and heart valves, or catheter housings. Moreover, there is an important subgroup: poly-α-hydroxy acids that are mainly represented by polylactic acid (PLA), polyglycolic acid (PGA), and their copolymer poly(lactic-co-glycolic) acid (PLGA). In reason of their good biocompatibility and controllable biodegradability, those acids are used primarily for bioresorbable sutures, tissue-engineered repair scaffolds, and drug delivery systems. (Bronzino & Peterson, 2015)

Polyethers are highly thermally, chemically, and mechanically resistant polymers with various applications. Since the 1990s, polyetheretherketone (PEEK) has been commercially used as spinal implants (Kersten et al., 2015). Polyethersulfone (PES) is mostly used for the fabrication of separation membranes for micro- and ultra-filtration, which are employed in the field of medical applications for hemodialysis. (Michaljaničová et al., 2016) Polyetherimide (PEI) is not yet widely used as a biomaterial, although it is a potential candidate for parts of biosensors, neuroprostheses, intraocular lenses, and oxygenators. (Seifert et al., 2002)

Electrically conductive polymers, specifically polyaniline (PANI), polypyrrole (PPy), and polyethylenedioxythiophene (PEDOT), are preferably used in scaffolds for

regeneration of neural lesioned tissue. (Shrestha et al., 2019) Conductive polymers, as well as conductive hydrogels, are also utilized in biosensors. (Gajendiran et al., 2017)

Rubbers have also found their medical applications. Natural rubber in its genuine form is compatible with blood. After vulcanization, its biocompatibility depends on the type of used crosslinking initiator, for example, X-rays and organic peroxides are preferable than conventional sulfur. (Bronzino & Peterson, 2015) Of synthetic rubbers, only silicone rubber was developed for medical use, especially for finger joint prosthesis, tracheal tubes, and gastrointestinal segments. (Paita & Dahotre, 2008)

Natural polymers are frequently used in clinical practice. Silk and cellulose (cotton) are non-degradable biopolymers that are used as semipermeable membranes for hemodialysis or drug delivery systems. On the other hand, degradable biomaterials could be made of collagen (Chauhan et al., 2019), fibrin, alginate, silk, hyaluronic acid and chitosan (Bose et al., 2018), or natural polyhydroxyalkanoates, such as poly(3-hydroxybutyrate) (PHB), poly(4-hydroxybutyrate) (P4HB), poly(3-hydroxyvalerate) (PHV), poly(3-hydroxyhexanoate) (PHHx), poly(3-hydroxyoctanoate) (PHO) and their copolymers, that are produced by bacterial biosynthesis. They are suitable for bioresorbable products, for example, sutures, coronary stents, or porous membranes and scaffolds for soft tissue, cartilage or bone tissue regeneration. (Bonartsev et al., 2019)

Many other polymers that are used in biomedical applications have not been mentioned before mainly because of their rarity, less use, high price, or unknownness. For example, polysulfones and also polyacetals are being tested as implant materials; polycarbonates are used in the heart/lung assist device; polycaprolactone (PCL) has found its application as a biocompatible and biodegradable coating for conventional polyester fibers (Bronzino & Peterson, 2015); polyvinylpyrrolidone (PVP) was originally used as a blood plasma expander, but these days it is rather an ingredient in drug manufacture (Chauhan et al., 2019); and other polymers.

2 BIOMATERIAL SURFACE CHARACTERISTICS AFFECTING THE CYTOCOMPATIBILITY

It should be understood that the interaction of any biomaterial with cells, tissues, biological fluids, or immune system always begins on the surface of the material. Often, this interaction is not ideal and there are many properties of biomaterial that affect it:

- **ability to adsorb adhesive proteins** to the surface, which is an essential property to ensure cytocompatibility and is controlled primarily by chemical structure and physical properties of the surface (Wilson et al., 2005),
- **electrical conductivity** and magnetic properties that help cells communicate with each other (Gajendiran et al., 2017),
- **topography and morphology** that are also capable of eliciting specific cellular responses (Unadkat et al., 2011),
- **mechanical properties** of the surface that enhance the mimicking the natural environment of cells - extracellular matrix, (Ma, 2008).

2.1 Ability to adsorb adhesive proteins to the surface

The most crucial property of biomaterials is an ability to adsorb adhesive proteins to the surface. The explanation is traceable in the natural environment of the cells, as showen in Figure 2. In a living multicellular organism, cells are anchored in the natural extracellular matrix (ECM), which is composed of a network of fibril proteins and proteoglycans. The binding between cells and macromolecules of the ECM is ensured by receptors in the cell membrane called integrins and adhesive proteins, mainly fibronectin and vitronectin, located in the ECM. (Wilson et al., 2005) These adhesive proteins contain a tripeptide consisting of amino acids Arginine, Glycine, and Aspartate (Arg-Gly-Asp, RGD) that can be recognized by the integrin in the cell membrane. Following binding of integrin to RGD sequence initiates signal transduction cascades in the cell, which positively influences its attachment and proliferation. (Ke et al., 2017)

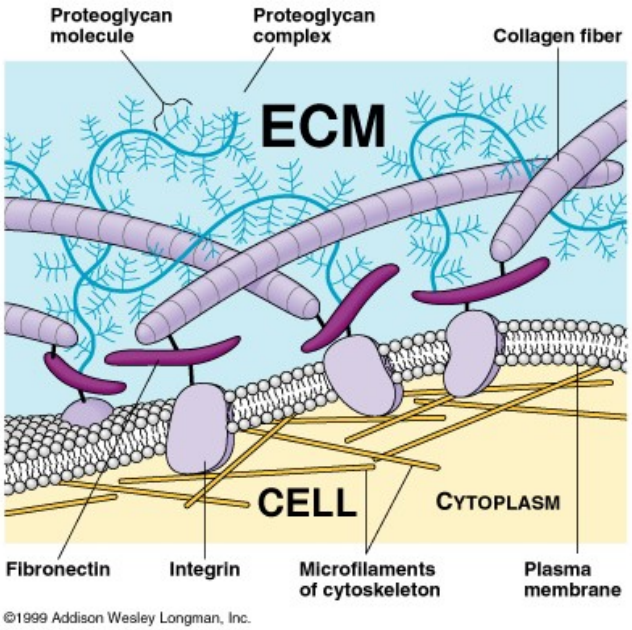

Figure 2 A schematic illustration of a cell anchored in its natural environment. (Imbeau, online)

The binding between cells and cultivation surfaces *in vitro* works similarly. It is typically mediated by the binding of integrins to adhesive proteins, especially fibronectin and vitronectin, which are contained in a cell culture medium. It means that the cell adhesion *in vitro* depends primarily on the ability of the material to adsorb these adhesive proteins (in the active state) from serum to the surface[2]. (Wilson et al., 2005) Lack of adherence of anchorage-dependent cells to the substrate surface results in apoptosis termed anoikis. (Nikkhah et al., 2012) Various components such as growth factors and other signal molecules that contribute to cell proliferation or differentiation may also bind to the surface of the material or the already adsorbed proteins. (Wilson et al., 2005) Exactly these interactions of proteins and other molecules with the surface are the first events that occur once a biomedical device is placed in the biological environment and they have a significant impact on further biological responses, such as the aforementioned adsorption of proteins to the biomaterial surface, as well as cell attachment, biofilm formation, and biomineralization, or triggering of biological cascades, for example, blood coagulation. Thus, biomedical surface sciences are the basis of both *in vitro* and *in vivo* tissue engineering. (Vogler, 1998; Castner, 2017)

[2] Cell adhesion may occur even in the absence of serum proteins, in which case these are non-physiological interfaces. Nevertheless, these interactions are not desirable as they exhibit reduced cellular activity and may contribute to cell death. (Wilson et al., 2005)

The ability of biomaterials to adsorb the adhesive proteins and other components to the surface is driven by the affinity of those molecules for the surface of the observed biomaterial, and it may be affected by:

- **chemical structure** of the surface of the biomaterial and its polarity (Curtis et al., 1983; Maitz et al., 2019),
- **physical properties**, such as surface energy, wettability and the nature of the surface charge (Schmalz et al., 2009; Vogler, 1998),
- **environmental conditions**, such as pH, temperature, types of adhesive proteins, their size, charge, affinity to the surface, concentrations, and rate of diffusion, presence of detergents/surfactants or flow rate (Puleo & Bizios, 2009),
- **time** because there are often time-dependent changes in conformation and spatial orientation of the surface-bound proteins as well as in the distribution of the proteins and composition of the protein films. (Castner, 2017).

2.1.1 Chemical structure of the surface

As mentioned above, it is essential to understand how proteins interact with surfaces and there are many bonding mechanisms, including both covalent and non-covalent binding formations, which are controlled by the chemical structure of the proteins and the surfaces of materials simultaneously. (Castner, 2017) In the field of tissue engineering, glass was used for many years as a culture surface *in vitro* until 1965 when polymers proved to be good enough to replace the glass. Polystyrene (PS), which is currently used most, is non-polar in its natural state, so for cultivation purposes, it is necessary to modify its surface. (Curtis et al., 1983) Surface modifications can be made in a variety of ways, which is discussed in chapter no. 4 ‘Surface modifications of polymeric biomaterials’. In this case, the necessity of surface treatment is that the oxidized surface of the biomaterials adsorbs more adhesive proteins from the serum and better preserves their bioactivity, which is reflected by the higher number of adhered cells. (Curtis et al., 1983; Wilson et al., 2005) This positive effect on the cytocompatibility is attributed mostly to formed hydroxyl and carboxyl groups[3]. (Curtis et al., 1983) Limits appear when there are too many hydroxyl or other polar groups on the surface together bounding water molecules by hydrogen bond

[3] In the case of viable neuronal stem cells, surfaces functionalized with amino groups provide under physiological conditions higher efficiency than surfaces functionalized with hydroxyl and carboxyl groups. (Ke et al., 2017)

and hence creating a strongly bound hydration layer that suppresses protein interaction with the surface. However, this effect may be useful when enhancing the hemo-compatibility of biomaterials is desired. It may be achieved by using selected polymers, such as polyhydroxyethylmethacrylate (PHEMA) or polyethyleneglycol (PEG). (Maitz et al., 2019)

2.1.2 Physical properties of the surface

Adhesion of proteins is influenced not only by the chemical properties of the material but also by its physical properties, such as surface energy and wettability. (Schmalz et al., 2009) The measured values of surface energy or surface tension correlate with the values of the so-called contact angle, which is the angle of contact of a water drop with a solid surface that characterizes the wettability of the observed biomaterial. If the contact angle is greater than 65°, the surface is hydrophobic; if the contact angle is less than 65°, the surface is hydrophilic. (Vogler, 1998)

The adsorption of proteins (and various surfactants) from water to the mildly hydrophobic surface is driven by the reduction of surface energy while replacing water molecules on the surface with the adhesive proteins, this is so-called surface dehydration. (Vogler, 1998) However, when the observed surface shows high hydrophobicity, which is determined by its chemical composition, or superhydrophobicity, which also depends on specific nanostructured geometry of the surface, suppression of protein interactions with the surface appears. The reason is an energy barrier that prevents liquid from entering the cavities of the nanostructure, resulting in water droplets rolling off from the surface. However, the repelling capacity of these surfaces dwindles in physiological conditions since the high protein concentration in blood decreases the surface tension. (Maitz et al., 2019)

On the other hand, the hydrophilic surface does not promote adsorption by surface dehydration since the water molecules are bound to the surface strong enough to make the process energetically unfavorable. (Vogler, 1998) However, the adsorption can be assumed to occur in an alternative manner, for example, charges on mildly hydrophilic surfaces are capable of binding adhesive proteins due to electrostatic interactions. The positivity or negativity of the charge may then affect the selectivity and orientation of the bounded proteins. (Wilson et al., 2005) Still, it should be remembered that highly increasing hydrophilicity decreases protein interaction with the surface. (Maitz et al., 2019)

Nevertheless, this could be useful in applications where biomaterials are in contact with blood, such as prosthetic valves, artificial vascular grafts, heart and heart-lung machines, or hemodialysis membranes and tubes, because it prevents the formation of blood clots. (Bronzino & Peterson, 2015)

2.1.3 Vroman effect

Once a biomedical device is placed in a biological environment, a protein film is formed on its surface within a few seconds. A question is the composition of the protein film. Molecules in a protein mixture solution (blood or a culture medium) diffuse to the surface of biomaterial at different rates. Proteins of a smaller molecular weight and more highly concentrated in a solution adsorb first to the surface but after some time, these proteins may be displaced by proteins, typically of a larger molecular weight and/or lower concentration in the solution, due to the higher affinity for the surface. (Horbett, 2018)

This competitive displacement of earlier adsorbed proteins by other proteins with stronger binding affinities was first observed with dilute blood plasma protein mixtures (Vroman & Adams, 1969) and nowadays it is a general phenomenon known as the Vroman effect. Three possible protein exchange processes (illustrated in Figure 3) have been identified and are well-accepted in the literature as interpretations of this phenomenon. The simplest explanation of the protein exchange process is a desorption/adsorption model shown in Figure 3A, in which a surface adsorbed protein (blue) naturally desorbs back into the solution and leaves a vacancy on the surface for a different protein (red) to adsorb. However, this desorption/adsorption model was only found to be consistent at long time scales. The protein displacement observed at shorter time scale may be due to a so-called competitive exchange, shown in Figure 3B, in which a surface adsorbed protein (blue) is displaced by the spreading of a different protein (red) on the surface due to its large and flexible structure, which enables them to adhere with greater attachment strength through broader surface contacts. Both of these models predict that the concentration of the first blue protein on the surface continually decreases and the second red protein continually increases. If not, this could be described by the third protein exchange process which is illustrated in Figure 3C in three steps: (1) an initial layer of protein (blue) adsorbs and then a different protein (blue) embeds itself into the initial layer forming a joint structure, which was termed as a “transient complex” (2) the transient complex turns itself and exposes the earlier adsorbed protein layer (blue); (3) proteins from the earlier adsorbed layer (blue) desorb into the solution resulting in a final adsorbed protein composition that is enriched in

proteins from the second layer (red). The atomic force microscopy (AFM) images (see Figure 4) support the above interpretation for the "transient complex" facilitated protein exchange. (Hirsh et al., 2013)

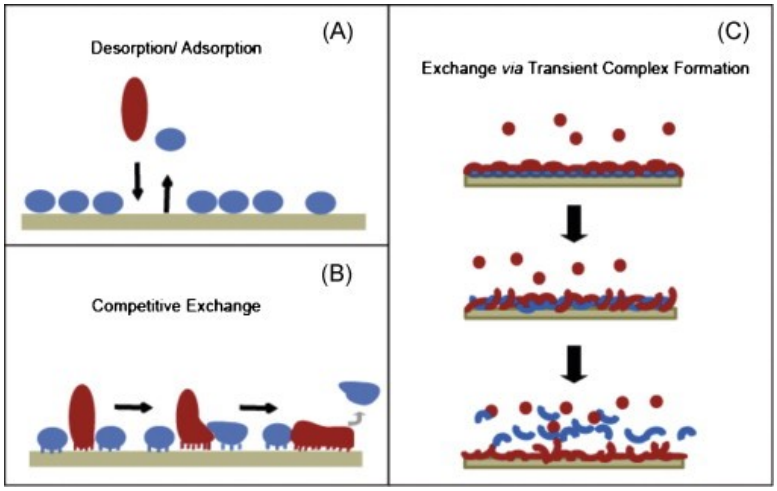

Figure 3 Schematic illustrations of three possible protein exchange processes as an interpretation of the Vroman effect. (Hirsh et al., 2013)

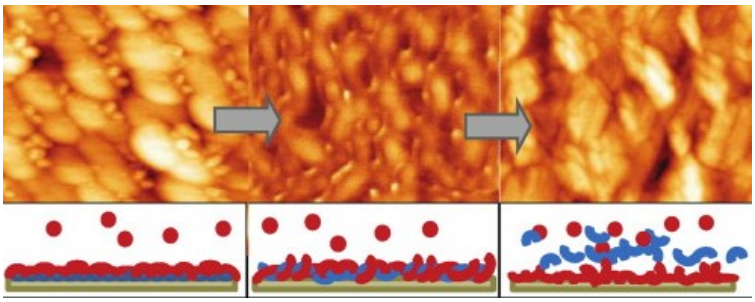

Figure 4 AFM images with the schematic illustration of the protein exchange process via transient complex. (Hirsh et al., 2013)

2.2 Electrical conductivity

The effects of externally applied electrical stimuli on tissues were demonstrated in the 1960s when low intense direct electrical stimuli were found to induce osteogenic differentiation and bone formation in adult dogs. (Bassett et al., 1964) Then the revolution in the biomedical fields began with the use of conductive biomaterials precisely because of their electrically conductive and magnetic properties, which affect cell activities, improve cell growth and help cells communicate with each other. (Gajendiran et al., 2017) Electrical conductivity is a property that is particularly important for biomaterials intended to be used in tissue engineering of cardiac or neural tissue. Therefore, it is preferable to investigate the interaction of conductive biomaterials with cardiomyocytes and neurocytes

or the effect of conductive substrates on cardiomyogenesis and neurogenesis from stem cells. (Humpolíček et al., 2015) In clinical practice, scaffolds integrated with these conductive polymers provide strong evidence of axonal regeneration after transplantation into the harmed tissue. (Shrestha et al., 2019)

The potential of polymers in the field of conductive materials has been proven by the Nobel Prize awarded in 2000 to three scientists, Heeger, MacDiarmid & Shirakawa, for the invention of polyacetylene-based polymer conductors. Other supervenient organic conductive polymers are polyaniline (PANI), polyethylenedioxythiophene (PEDOT), or polypyrrole (PPy). The conductive properties of organic polymers come from the presence of conjugated π-bonds, which are along the entire polymer chain, allowing electrons to delocalize relatively easily. (Gajendiran et al., 2017) The conductivity can also be greatly enhanced by so-called doping, incorporating dopants (anions or cations) into the neutral polymer during synthesis. This process produces charged polarons or bipolarons that serve as charge carriers which enable 'electron hopping' along and between the polymer chains. (Ravichandran et al., 2010) In addition to the ability of organic conductive polymers to respond to externally applied electrical stimuli and thereby control cell differentiation, their importance in tissue engineering is also due to their soft nature, which is capable of mimicking ECM and creating a more appropriate cellular environment than conventional electrically conductive inorganic materials, such as metals. (Gajendiran et al., 2017)

Among the conductive polymers, especially the PPy is promising for commercial applications due to its relatively high conductivity, facile synthesis, and flexibility of surface characteristics. (Padmapriya et al., 2019; Wang et al., 2004) However, in bio-medical applications, also the biocompatibility is a crucial material property that should be investigated. For example, researches have addressed cytocompatibility when an electric current is applied to the PPy, although evidence of cytotoxicity could be seen after long-term exposure to the current. (Ravichandran et al., 2010) The study of Wang et al., 2004, demonstrated that the PPy extraction solution *in vivo* has no evidence of acute and subacute toxicity, hemolysis, allergen, or mutagenesis. The PPy surface improves Schwann cell migration and neurite extension *in vitro* in comparison to bare glass. (Wang et al., 2004) On the other hand, other studies showed low cytotoxicity of PPy when in contact with various biological tissues. (Hsu et al., 2008) According to Ravichandran et al., 2010, the major limitation in the cytocompatibility of PPy (and conductive polymers in general) is its hydrophobicity that decreases successful entrapping of proteins to the surface.

(Ravichandran et al., 2010) However, specific properties of PPy, such as topography, electrical conductivity, surface chemistry, and physical properties, and hence its cytocompatibility, are influenced by a host of other variables: the polymerization technique, which could be chemical or electrochemical, and various synthesis parameters, for example, used solvent, dopant, and substrate as well as pH, temperature (Fonner et al., 2008), and polymerization initiators – $(NH_4)_2S_2O_8$ (ammonium persulfate, APS), $FeCl_3$, H_2O_2, $K_2Cr_2O_7$, and $CeSO_4$ that are the most commonly used oxidants. (Padmapriya et al., 2019)

An interesting area where conductive biomaterials, including conductive polymers, are applied is biosensors that are devices that transform biochemical information into an analytically useful signal. Sensors usually contain two basic components connected in series: a chemical molecular recognition system (receptor) and a physico-chemical converter (detector, sensor, or electrode). The main purpose of the receptor is to provide a high degree of selectivity for the component to be analyzed. Biosensors may be more or less selective for various analytes, which may be ions, gases, antibodies or antigens, proteins, and other different substrates. Transducers can be of various types, such as electrochemical, optical, piezoelectric, or thermal. The most commonly used converter is the electrochemical one, which provides bi-directional signal transmission - chemical to electrical and vice versa. (Thévenot et al., 2001) Electro-chemical converters must be conductive (or semiconductive) biomaterials. For example, some conductive polymers may act as excellent materials for the immobilization of biomolecules. Conductive hydrogels, that have unique properties such as swelling, high porosity, permeability, and hydro-philicity, are suitable for converters as well. (Gajendiran et al., 2017)

2.3 Topography and morphology

Topography is a term that describes surfaces from a quantitative perspective, for example, an amount and size of surface irregularities, whereas morphology describes surfaces from a qualitative point of view, such as surface appearance. (Maszybrocka et al., 2017)

Topography and morphology are other important properties of biomaterials that affect cells-surface interactions. Cytocompatibility is dependent on the topography primarily at the micro-scale but also at the nano-scale. For the best results, topography should be modified at both scales depending on the type of cultured cells. (Slepička et al., 2012)

Topographical treatments of materials are an economically effective way of improving the biological activity of any biomaterial surface, which is a great advantage. On the other hand, interactions between cells and surfaces are complex and still incompletely understood. (Unadkat et al., 2011)

The effect of topography on osteoblasts was studied by Woo, Chen & Ma (2003). Specifically, nanofibrous and smooth scaffolds made of polylactic acid (PLA) were compared. Nanofibrous scaffolds showed better bioactivity, because of a greater amount of adhered osteoblasts. This success has been attributed to an enlarged surface area, due to which a greater amount of fibronectin and vitronectin has been adsorbed, improving the adhesion of osteoblasts. (Woo et al., 2003)

Smooth polystyrene (PS) foils together with PS foils illuminated by a polarized UV laser beam, which induced formation of self-organized ripple structure on the surface of the PS foils with various periodicity, depth, and direction, were used to an investigation of the behavior of human embryonic kidney cells, Chinese hamster ovary cells, and skeletal myoblasts. In comparison to the cell activity on the pristine smooth PS, the adhesion and proliferation of observed cells were enhanced on surface-structured PS foils. Furthermore, it has been found that the cell alignment strongly depends on the ripple direction and the critical value of its periodicity that varies with cell type. (Rebollar et al., 2008)

In addition to cell adhesion, proliferation, and alignment, topography has also a major effect on other cell processes, including differentiation of stem cells. The principle is that a surface structure affects the availability of suitable binding sites for adhesive proteins, thereby affecting their surface distribution. As a result, biomaterials with topographic modifications acquire capabilities that were originally reserved for growth factors only. (Wilson et al., 2005) The study that used mathematical algorithms to design impartial, random topography features contributed considerably to the need for a broad mapping of this issue. A total of 2,176 PLA chips were produced, each having a different topography. Human mesenchymal stem cells (MSCs) were subsequently grown on these chips. As shown in Figure 5, the cells were induced by these surface structures to proliferate, differentiate, and develop different morphological structures. Based on the results of this study, correlations between topographic parameters and cellular responses were stated. (Unadkat et al., 2011)

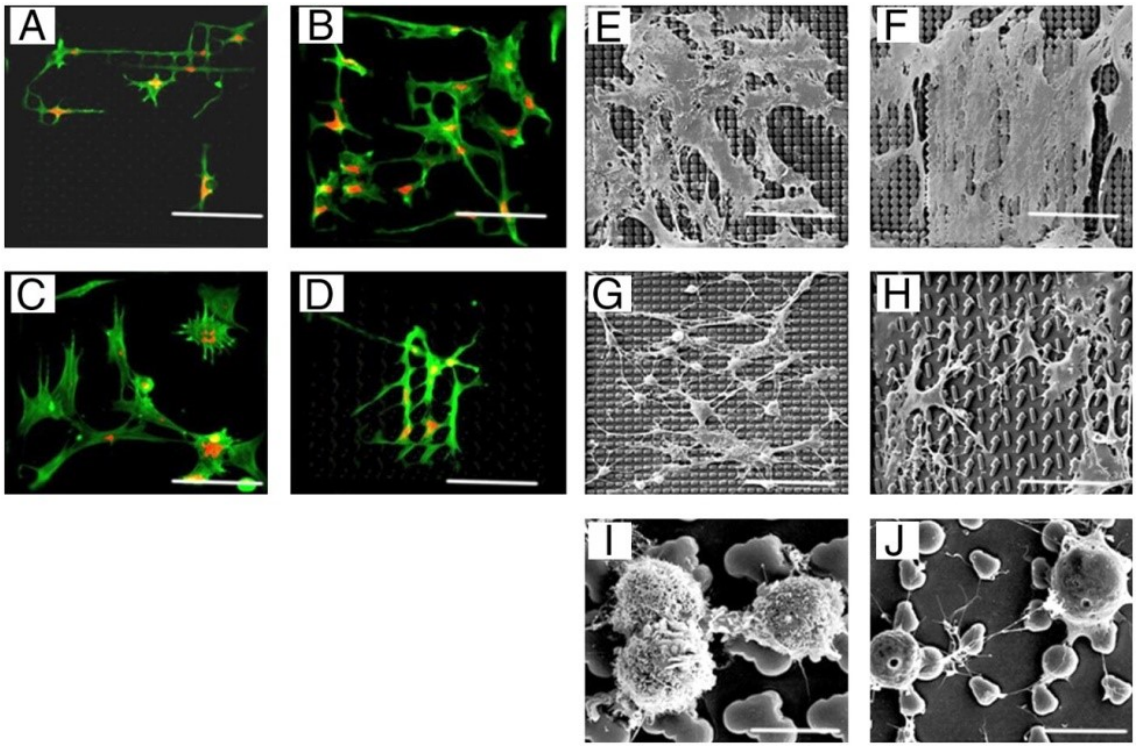

Figure 5 Morphology of human MSCs on different PLA chips. (A–D): Elongated cells aligned according to topographic features (fluorescence microscope, green - actin, red - nucleus, scale: 90 μm). (E–H): Cells with different morphologies (SEM scanning electron microscope, scale: 90 μm.) (I–J): Morphology of rounded cells on two different chips, which differ in cell membrane structure. (SEM, scale: 10 μm.) (Unadkat et al., 2011)

2.4 Mechanical properties of the surface

In addition to the chemical structure and physical properties, the mechanical cues also have a great influence on cell migration, proliferation, morphogenesis, and stem cell differentiation. These mechanical signals present themselves in the form of shear stress, hydrostatic pressure, environment (ECM or/and biomaterial) topography and stiffness, and also intercellular tugging. The effect of mechanical forces on cellular activities was first introduced in 1892 by Julius Wolff in describing the changes in bone structures in response to load-bearing. In the 20th century, mechanical factors were ignored until recent days, when their roles in embryogenesis, development, and many adult life pathological conditions, such as atherosclerosis, osteoporosis, myopathies, and cancer, have been studied. There are numerous of technologies currently being used for studying mechano-biology, including micropipette aspiration, optical or magnetic tweezers, and traction force microscopy. (Nikkhah et al., 2012) In tissue engineering, the purpose of scaffolds is to mimic the appropriate properties, including the mechanical properties, of natural ECM as

far as possible. (Ma, 2008) Polymers have a great advantage in this field compared to metal and ceramic, since their mechanical properties, such as strength, elasticity, or durability, can be controlled very significantly and relatively simply. (Bronzino & Peterson, 2015)

One of the breakthroughs in studying cell mechanics has been with the use of flexible microscale post or pillar arrays. For example, effects of surface rigidity on the cytocompatibility were researched in a study of Fu et al. (2010) which was based on micromolded elastomeric micropost arrays made of polydimethylsiloxane (PDMS). Each post behaves like a cantilever or a spring characterized by the nominal spring constant (Figure 6C). The microposts have the same top surface geometry but three different heights, determining the degree of the micropost deflection in response to the horizontal traction force (Figure 6A, 6B) which is exerted by cells adhered to these arrays. (Fu et al., 2010) The length of displacement can be used to quantify the traction force, as described by

$$F = k \cdot \Delta x = \left(\frac{3}{4}\pi E \frac{r^4}{L^3}\right) \cdot \Delta x \quad (1)$$

where F is the traction force, k is the spring constant, Δx is the micropost displacement length, E is Young's modulus, and r and L are the radius and height of each pillar. (Nikkhah et al., 2012)

Human MSCs were deployed on these elastomeric micropost arrays together with a differentiation medium promoting osteogenesis and adipogenesis. Cells cultivated on short rigid micropost arrays had high focal adhesion (Figure 6D) with highly organized actin fibers and osteogenic differentiation was favored. In contrast, cells on soft micropost arrays exhibited rounded morphology (Figure 6F) with disorganized actin fibers and low focal adhesion, adipogenic differentiation was favored. (Fu et al., 2010)

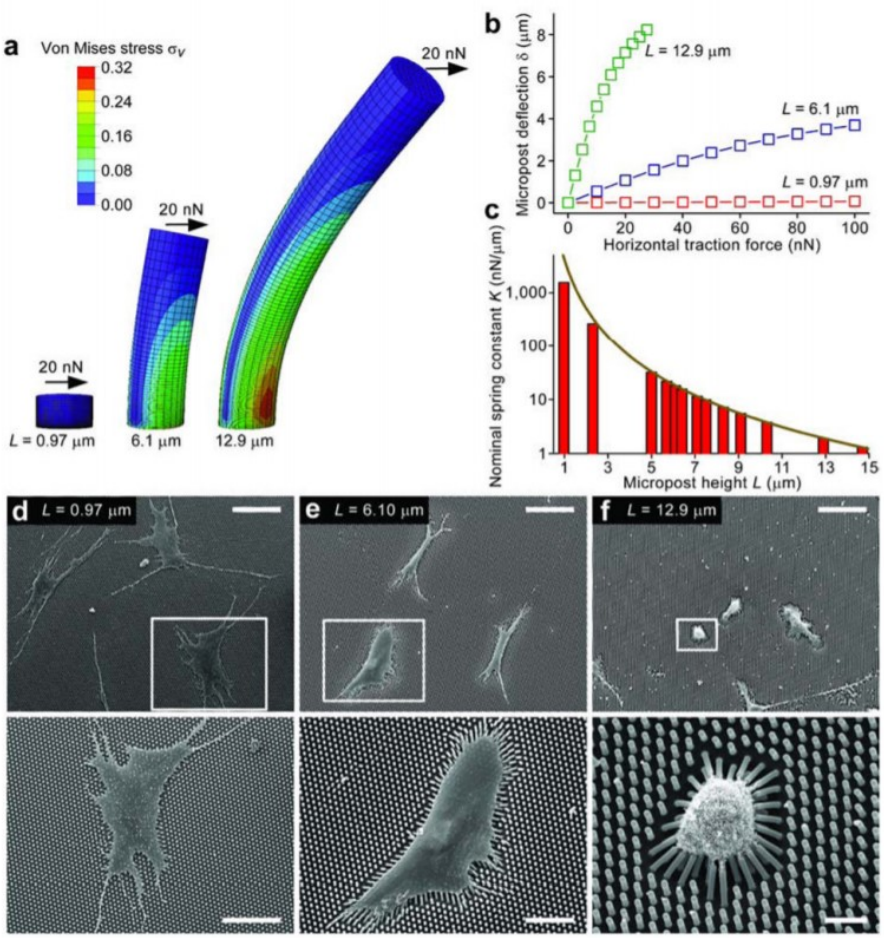

Figure 6 (a): PDMS micromolded elastomeric micropost arrays with three different heights in response to the horizontal traction force. (b): Dependence of the micropost deflection on the horizontal traction force. (c): Dependence of the nominal spring constant on the micropost height. (d–f): Human MSCs cultivated on the microposts of different heights and rigidity. SEM, scale: 100 µm (top), 50 µm (bottom left), 30 µm (bottom center) and 10 µm (bottom right). (Fu et al., 2010)

In addition to all the aforementioned chemical, physical, and mechanical properties of biomaterial surfaces, it has been found that isotropy and even more anisotropy of these properties have a considerable impact on cellular activities. The following chapter will be focused on this topic.

3 BIOMATERIAL ISOTROPY VERSUS ANISOTROPY

As discussed in the previous chapter, biomaterials such as scaffolds act as an artificial ECM due to mimicking its chemical composition and physical architecture with certain mechanical and conductive properties to ensure the surface cytocompatibility by facilitating cell adhesion, migration, proliferation, and differentiation. In the subsequent theoretical part, it is addressed the role of isotropic versus the anisotropic nature of the biomaterial systems in affecting cell behavior in the field of tissue engineering.

Isotropic material is one that exhibits the same properties or structures when viewed from any direction, for example, the shape of a sphere is isotropic because it has a single characteristic diameter the same in all directions.

Anisotropic material is one which exhibits dissimilar properties or structures when viewed from different directions, for example, the shape of a rod is anisotropic because its characteristic dimensions vary along its length and across its diameter.

Clearly the definition of both isotropy and anisotropy requires a specification of scale because various properties and structures may be observed at different scales, for example, the direction of fibers at a macroscopic scale, the shape of pores at a microscopic scale or the molecular level interactions at a mesoscopic scale. In case of polymers, the molecular anisotropy is very present due to the anisotropic angular distribution of the chemical bonds in a polymer chain, or the polymer chains alignment with the fiber axis in fibrous scaffolds, or the polymer chain incorporation into folded lamellar crystals which is a feature of semi-crystalline polymers such as polycaprolactone (PCL) or polyethyleneglycol (PEG). The internal structure of polymer biomaterials may be affected by diverse additives and processing characteristics. (Mitchell & Tojeira, 2013)

Many of the natural tissues are anisotropic and viscoelastic due to different mechanical loading environments. Bone is a prominent example that possesses anisotropy both in morphology and mechanical properties and that is due to the complex porous structure that differs across the bone and mechanical properties that are higher axially than transversely, for example, trabecular bone has longitudinal modulus (129.07 ± 49.48) MPa, while transverse modulus is only (38.23 ± 20.18) MPa. The viscoelasticity is one of the specific properties of natural bones and is strictly connected to its porous structure. In addition, the bone has unique properties of remodeling to adapt its microstructure to external mechanical stress. Therefore, tissue differentiation and bone regeneration might be

influenced by the porosity and pores distribution, Young's modulus and dissolution rate of the biomaterial, and load condition of the scaffold which are properties that may be anisotropic and vary in different directions. (Hoque, 2017)

3.1 Effect on cell behavior

Most types of cells are capable of sensing the orientation, texture, and physical properties of biomaterials, most importantly scaffolds. (Mitchell & Tojeira, 2013) The interaction and response of cells with their physical environment is mediated by a phenomenon called contact guidance which is known to affect cellular behaviors such as adhesion, morphology, migration, and differentiation. These changes in cell function are achieved with a process known as mechanotransduction which integrates and converts various physical cues in a cell's surrounding environment into biochemical, intracellular signaling responses. (Nikkhah et al., 2012) Among a number of cellular structures that are involved in the probing and sensing of the microenvironment[4], the integrins are the most important in the field of tissue engineering since they mediate contacts between cells and adhesive proteins located in the ECM, optionally on the surface of scaffolds (Ke et al., 2017; Wilson et al., 2005). This kind of mechanotransduction initiates with transmembrane integrins binding via adhesive proteins to the substrate outside the cell which then transmits force across the cytoplasmic membrane to the focal adhesion complex (FAC) that links to intracellular components, as shown in Figure 7. Following FAC formation can potentially signal via several downstream pathways and amplifications that lead to morphological and behavioral changes since it can activate several signaling molecules, including G-proteins, phosphatases, kinases, and other regulators that may be involved in modulation of transcription factors and gene expression. The most significant are actin dynamics regulators, such as the RhoGTPase that play a pivotal role in cell shape, polarity, and migration. Integrins also transmit environmental physical forces directly through its physical connection with the cytoskeletal actin filaments that further mediate force transduction from the cell membrane to the nucleus, leading to the reorganization of nuclear architecture. (Arvind & Huang, 2017) By understanding how cells interact with their physical environment, it may be possible to control cellular behavior by producing substrates with unique physical properties. However, despite its significance, this

[4] Integrins in cell–ECM contact, cadherins in cell–cell adhesion, stretch-sensitive ion channels, Tyr kinase receptors, and G protein-coupled receptors are the cellular structures involved in the probing and sensing of the cell environment. (Nikkhah et al., 2012)

phenomenon is still not completely analyzed and the underlying mechanisms of how physical stimuli contribute to the regulation of cellular behaviors have yet to be fully understood. (Nikkhah et al., 2012)

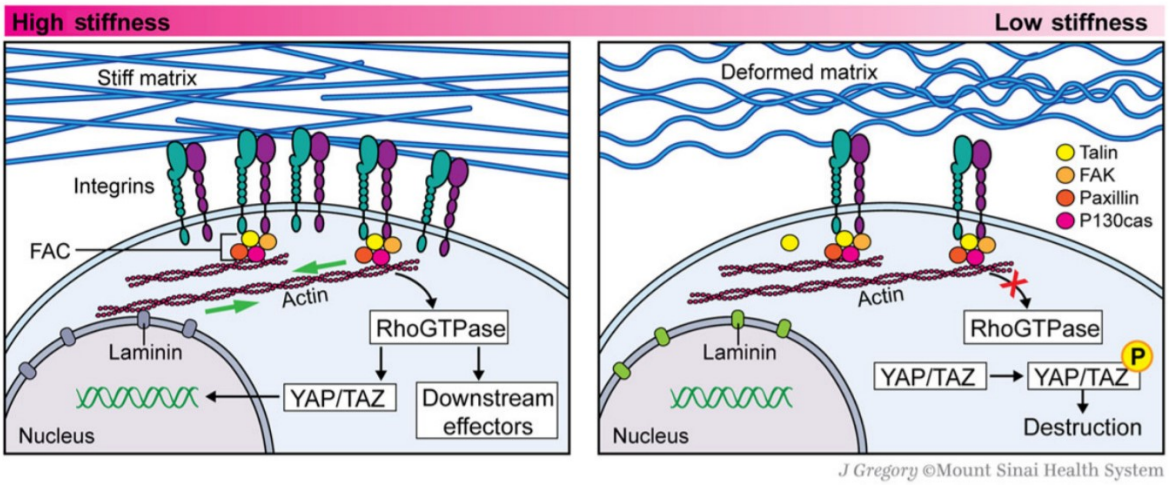

Figure 7 A schematic illustration of cell–ECM mechanotransduction where cells respond via integrin signaling to high and low stresses based on underlying substrate stiffness. (Arvind & Huang, 2017)

3.1.1 Under static cultivation conditions

Cultivation of cells under the static conditions is a commonly used method to obtain a basic knowledge of cellular behavior *in vitro*. (Nokhbatolfoghahaei et al., 2020) In the case of static cultivation of cells on the surface of anisotropic scaffolds, topographic anisotropy of the constructs represents the most important factor affecting cell motility, alignment, and functions. (Mitchell & Tojeira, 2013) The effect of biomaterial topography on the cytocompatibility has been already discussed in the subchapter 2.3 'Topography and morphology'. This part of the theory is focused on the impact of topographical anisotropy in comparison to its isotropy.

The main principle of how cells react to the structural anisotropy initiates with cells spreading and sensing the topographical features of the underlying substrate. Its specific anisotropic organization, arrangement, availability, and distribution of binding sites for integrins ultimately through a series of intracellular signaling cascades involving FAC and cytoskeletal actin filaments alter the cytoskeletal organization and force balance which in turn changes cell function and morphology. Hence, the topography, as well as the ECM, conveys biophysical signals over a broad range of length scales, for example, at the micron level, it influences cellular and supracellular characteristics, such as cell morphology,

migration, or tissue organization, whereas, at the nanometer length scale, it affects sub-cellular behaviors, such as the organization of the cell adhesion molecule receptors. (Nikkhah et al., 2012) Grooved surfaces, aligned fibers, micro-channels, and cell-inspired topographies are the commonly used anisotropic features of scaffold surfaces. When comparing isotropic and anisotropic scaffold geometries, cell attachment and consequent proliferation often are more prominent using the anisotropic scaffold. One of the reasons may be an enlarged specific surface area, due to which a greater amount of adhesive proteins can adsorb, improving the adhesion of cells. However, this does not have to be necessarily true depending on the specific surface area of the compared isotropic surface. (Mitchell & Tojeira, 2013) Another and much more important reason is the mimicking of the ECM and the cell natural environment since many of the natural tissues are anisotropic. (Hoque, 2017) For example, many studies have aimed to simulate the *in vivo* anisotropic structure of the myocardium through a series of topographical features because contractile properties of cardiac tissues are directly related to cellular orientation and elongation. (Nikkhah et al., 2012) In the study of Bursac et al. (2002), cardiomyocytes cultured on microabraded channels on a PVC substrate took their native *in vivo* phenotype - aligned actin fibers, parallel sarcomeric arrangements[5], and nuclear elongation. Furthermore, the tissue exhibited faster propagation of action potential along the long axis of abrasions and a directionally-dependent contractile behavior. (Bursac et al., 2002) However, not only cardiomyocytes but the majority of cell types cultured on grooved features elongates, orientates, and aligns along the major axis of grooves, especially with decreasing groove width and increasing groove depth. (Nikkhah et al., 2012)

In addition to the morphologic changes, many cell types have also shown changes in migration speeds and directions; cells have a higher average migration speed on microgrooved substrates in comparison to flat surfaces and migrate along with the higher anisotropy toward the denser regions of the topographical features. The physical structure and geometry of the cell surroundings restrict sites of adhesion and directs migration through the contact guidance. Cell motility is essential in natural processes, such as morphogenesis, embryonic development, cancer metastasis, or wound healing, as well as in regenerative medicine including tissue engineering. (Nikkhah et al., 2012) Furthermore, it was found that anisotropic scaffolds, compared to the isotropic scaffolds, support a higher metabolic activity of the tendon cells, which is an import assessment parameter

[5] A sarcomere is the basic unit of a muscle composed mainly of actin and myosin that cooperate to generate contraction and relaxation of the muscle. (Cho et al., 2020)

that informs about the health of the neo-formed tissue. The transport of nutrients and drugs to cells adhered inside the scaffold structures depends on many factors such as the diffusing molecule itself (size, charge, spatial configuration), the volume fraction of these molecules in the environment, but also on the design the scaffold since the directional components of the diffusion coefficient strongly depend on the porosity and structural anisotropy, for example in the case of fibrous mats – the volume fraction of fibers and the degree of fiber alignment. (Mitchell & Tojeira, 2013)

When discussing fibrous scaffolds, it should be known that the engineering of scaffolds with control over fiber orientation is essential and a prerequisite for controlling cell growth and related functions. (Murugan & Ramakrishna, 2007) In response to nanotopography of aligned fibers, morphological changes, cytoskeletal rearrangements, and nuclear elongation have been reported in many cell types including axon extrusion enhancing from neuronal stem cells. Yin et al. (2010) fabricated an electrospun poly(L-lactic acid) (PLLA) fibrous scaffolds with random and aligned fibers that then seeded with human tendon stem/progenitor cells (hTSPCs) with a multipotent differentiation capacity. However, it remains a great challenge to ensure their differentiation into tendon-forming cells and avoid ossification *in vivo*, which hinders their application. It is known that hTSPCs reside within a niche where the ECM comprises primarily parallel collagen fibers; therefore, the uniaxial oriented electrospun nanofibers should mimic this natural environment and help to regulate hTSPC function and differentiation. The fluorescence microscopy and SEM micrographs, which may be seen in Figure 8, showed that hTSPCs were well attached to both scaffolds but with significantly different morphology: a stellate-patterned phenotype on the randomly-oriented nanofibers (Figure 8B, F) but the classic fibroblastic phenotype on the aligned nanofibers (Figure 8A, E) expressing a spindle-shaped morphology gradually more elongated parallel to the nanofibers direction. Further, the nanofibers influence the cell-matrix interactions, their amount, and distribution which play an important role in regulating cell functions such as migration, proliferation, and differentiation. The expression of all integrin subunits was upregulated after culture on the aligned scaffold and the filament-like extensions, which were suspected to be focal adhesions, from the cell body attached to the nanofibers appeared especially at the extremities of the elongated cells on aligned scaffolds (Figure 8C) whereas a lower degree of integrin subunits expressed on the randomly-oriented scaffolds and the filament-like structures were seen on any parts of the cells (Figure 8D). It was also confirmed the effect

of matrix anisotropy on the cell nuclei that became more elongated and uniformly oriented in the direction of the nanofibers (Figure 8E) in comparison to the nuclei of the cells cultured on the randomly-oriented scaffolds (Figure 8F). To examine hTSPC attachment and proliferation, cell density was measured at days 1, 3, 7, 11, and 14 and there was no statistical difference between the scaffolds with random and aligned fibers (Figure 8G). Results of differentiation tests suggest that the use of aligned nanofibers not only promotes hTSPC differentiation to the teno-lineage but also significantly hinders the osteo-lineage differentiation of hTSPCs when cultured under osteogenic conditions which reflect the fact that an aligned nanotopography exerts an instructive function as effectively as chemical cues. (Yin et al., 2010)

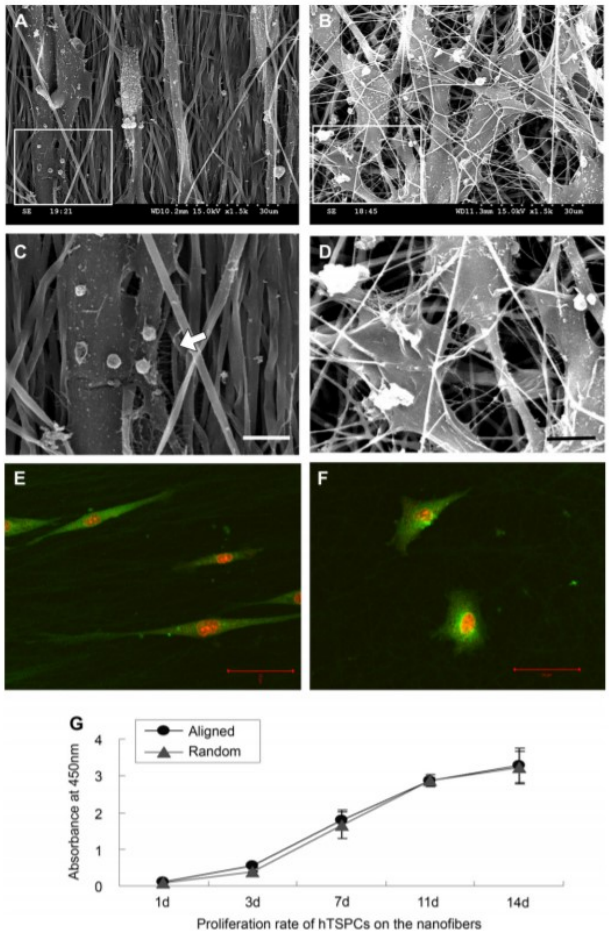

Figure 8 Morphological changes of hTSPCs growing on the scaffolds with (A, C, E) aligned fibers or (B, D, F) randomly-oriented fibers. (A, B): SEM images of hTSPCs. (C, D): High magnifications of boxed areas in A, B. (Arrow in C): filament-like structures. (E, F): Confocal micrographs of CFDA-stained hTSPCs. (G): Cell proliferation on the scaffolds with aligned fibers or randomly-oriented fibers. Scale bars: 30 μm (A, B), 5 μm (C, D), and 50 μm (E, F). (Yin et al., 2010)

3.1.2 Under dynamic cultivation conditions

Nowadays, tissue engineering researchers rely on the vision of producing scaffolds with appropriate mechanical properties similar to the host tissue *in vivo*, mostly meaning viscoelastic and anisotropic, which are capable to tune tissue regeneration at a cellular level. Relating to electrospun scaffolds, Yin et al. (2010) fabricated nonwoven mats with aligned fibers biomimicking tendon anisotropic properties. As measurement results show in Figure 9, the load–strain curve of the PLLA scaffold with aligned fibers was similar to the native rabbit tendon, which is composed of aligned collagen fibers. Both curves comprised (I) a toe region, (II) a linear region, and (III) a microfailure region – instability in the curve just before failure (Figure 9G). For comparison, the load-strain curve of the electrospun scaffold with randomly-oriented fibers did not have such typical regions (Figure 9F). (Yin et al., 2010)

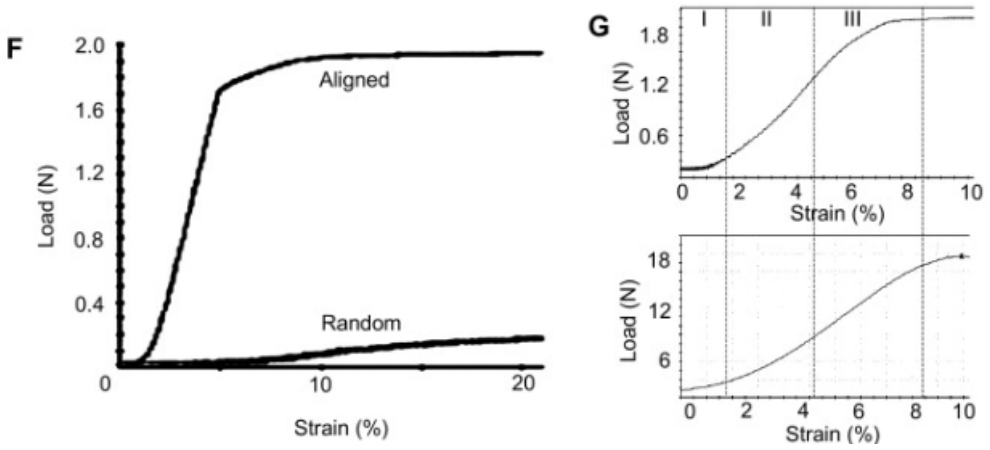

Figure 9 The load-strain curves of (F) the electrospun PLLA scaffolds with aligned and randomly-oriented fibers, (G) aligned scaffold (upper) and rabbit native tendon (lower), which are composed of toe (I), linear (II), and failure (III) regions. (Yin et al., 2010)

Although many studies have already focused on the impact of the scaffold mechanical properties anisotropy on different cell lines, the majority of *in vitro* investigations are conducted under static cultural settings, the main drawbacks of which are: neglecting the pivotal role of mechanical stimulations together with a restricted diffusive transport of nutrients to the scaffold core. In comparison to the static cultivation conditions, dynamic-based bioreactors are designed to mimic the mechanical stimuli of the natural *in vivo* tissue environment that are directly sensed by mechanosensitive compartments of cells and tissues and may act as an active force for directing cellular function including stem cell

differentiation. Of the designed bioreactor systems, the most straightforward and commonly used bioreactors are shear-loading devices, such as spinner flasks, rotating wall vessels, and perfusion bioreactors. These are based on applying hydrodynamic shear stress to cells by streaming of culture medium fluid within the bioreactor chamber and the scaffold secured therein. However, it has been evidenced that bioreactors utilizing a combination of forces, for example, perfusion plus rotation, significantly enhance cell growth and differentiation, at least the osteogenic one. Hence the tissue engineering using combined practical approaches is an attractive strategy. (Nokhbatolfoghahaei et al., 2020) In addition to the mentioned shear stress and rotation, there may be other external forces that act on the cell cytoskeleton, such as tensile and compression forces, as well as cell-induced contractile forces. All these forces are transmitted to cells through the adhesion sites, actomyosin pathways, and cell stress fibers, and play a central role in determining tissue morphology and properties. This was observed, for example, in Rosenfeld et al. (2016) study where external mechanical stretching regimens applied on a co-culture of fibroblasts and endothelial cells seeded within fibrin gel fabricated uniaxially between two polydimethylsiloxane (PDMS) microposts to support vascular network creation were studied. The resulting orientation of vessel-like structures varied depending on the form of applied forces, as shown in Figure 10: cyclic stretching resulted in diagonal vessels, static stretching in vertical vessels, and free-floating scaffolds in randomly orientated vessels. Furthermore, a positive correlation between the intensity of force and vessel elongation was noted. (Rosenfeld et al., 2016)

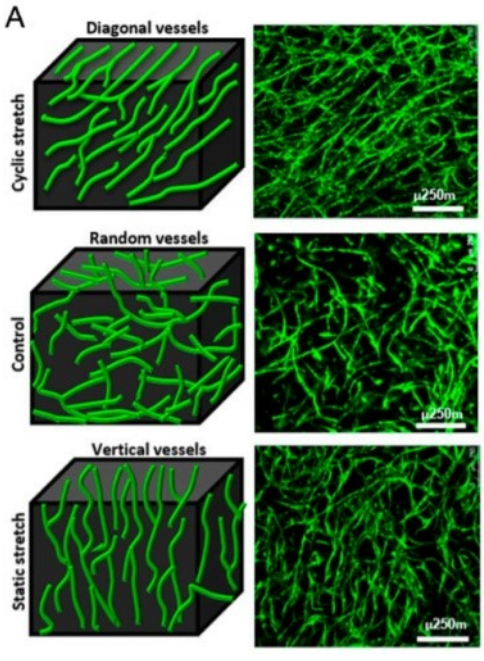

Figure 10 The orientation of vessel-like structures varying depending on the form of forces applied: cyclic stretching resulted in diagonal vessels, free-floating scaffolds in randomly orientated vessels, and static stretching in vertical vessels. Scale bars: 250 μm. (Rosenfeld et al., 2016)

One of the few studies that assessed the impact of anisotropic properties of scaffolds on cells under dynamic conditions was accomplished by Lee et al. (2005) who inoculated cell line of human ligament fibroblasts (hLFs) on electrospun PU sheets with various anisotropy and after 48-h static cultivation, 5% uniaxial strain was applied for 24 h at a frequency of 12 cycles/min. Photographs of the cells on the nanofibrous scaffolds before and after applying the strain may be seen in Figure 11. Before the stretching, the hLFs on a scaffold with aligned fibers (Figure 11A) took spindle shapes, oriented in the direction of the fibers and synthesized significantly more collagen even though the proliferation did not differ statistically comparing to the hLFs seeded on randomly-oriented fibers (Figure 11D) that were neither spindle-shaped nor oriented. After stretching the scaffolds, the cells spread on the randomly-oriented fibers reorganized their cytoskeleton into the spindle shapes (Figure 11E). Between the strained and unstrained hLFs on aligned fibers was no significant histological difference (Figure 11B, C) except for the amount of generated ECM in the intercellular regions which was higher around the hLFs exposed to strain in the longitudinal direction. The results suggest that spindle-shaped hLFs oriented along aligned nanofibers under longitudinal strain is preferable in producing parallel-oriented ECM observable in intact ligaments. (Lee et al., 2005)

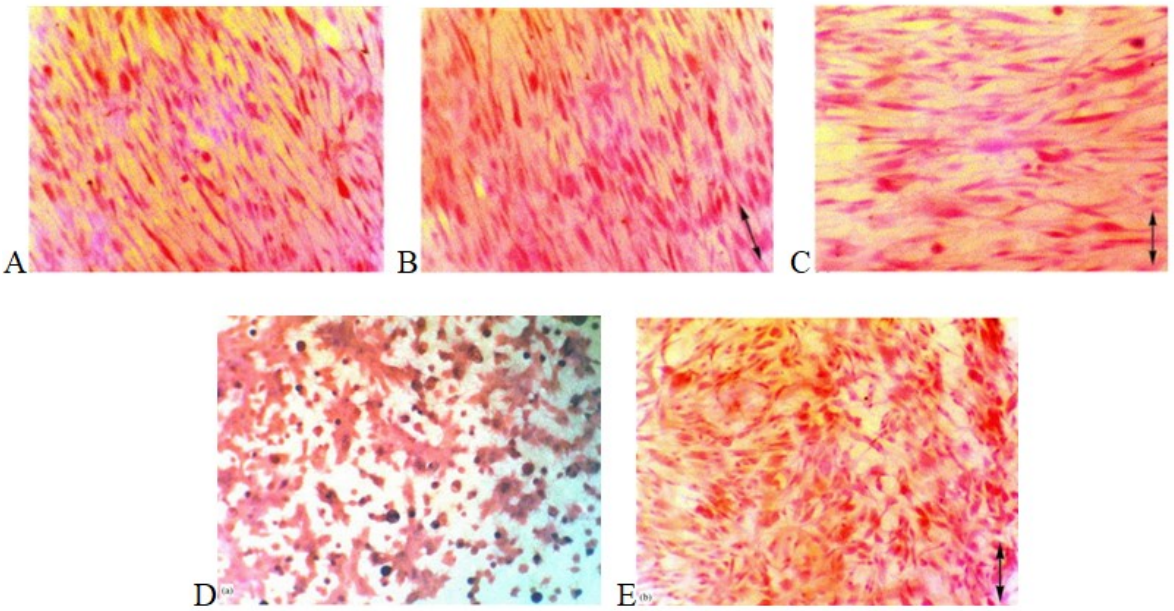

Figure 11 Morphology of fibroblasts grown on (A, B, C) aligned nanofibers: (A) before stretching, (B) after longitudinal stretching, and (C) after perpendicular stretching, and on (D, E) randomly oriented nanofibers: (D) before stretching and (E) after stretching. The direction of stretching is represented by "↔". (Lee et al., 2005)

3.2 Fabrication techniques for anisotropic scaffolds

In pursuit of understanding how cells interact with their physical environment, conventional and additive manufacturing techniques together with macro-, micro- and nanofabrication technologies are being widely used to construct scaffolds with unique anisotropic physical properties. Conventional techniques are capable of creating highly interconnected porous nets or micro-channel morphologies that are suited as biomedical scaffolds and often with a less costly fabrication. (Mitchell & Tojeira, 2013) One of the ways, how to introduce anisotropy through into a conventionally fabricated foam is by incorporating fibers that are being oriented during processing. When 10 wt% 2.5 mm PGA fibers were included in a PLGA foam, the compressive modulus in the axial direction (32 MPa) was obtained up to six times higher than that in the transverse direction (5 MPa). On the other hand, additive techniques, such as rapid prototyping, allow scaffold manufacturing with uniform, defined and variable pores sizes and shapes, and accuracy of their interconnectivity. Other advantages of the advanced fabrication techniques are excellent reproducibility, ability to produce virtually any kind of structure within the capacity of the used specific technique (Hoque, 2017), and that they do not require toxic solvents or pore-forming chemicals which may endanger patient health. (Mitchell & Tojeira, 2013)

Rapid prototyping and solid free-form fabrication have already proven their potential in the scaffold fabrication for the use in the field of tissue engineering due to the capability of producing the scaffolds with such structure and properties that reliably mimic the natural tissue. (Hoque, 2017) These layer-by-layer processes can reproduce highly complex three dimensional (3D) scaffolds using the computer-aided design (CAD) systems or the medical imaging files, such as magnetic resonance imaging (MRI) or computed tomography (CT). A variety of techniques may be utilized for the production of polymer scaffolds with anisotropic structure and properties by rapid prototyping.

One of the most used is fused deposition modeling (FDM) that processes materials above their melting point temperature that pass through a nozzle and deposit onto an elevating platform in the shape of a strand that subsequently cools down and solidifies. However, there is also a method called 3D fiber deposition (3DF) that, on the other hand, uses room temperature conditions which makes it promising to produce cell-laden scaffolds. In both cases, to form a 3D porous scaffold, each layer is deposited in a different configuration, for example, different patterns are obtained by laying microfilaments in

different deposition angles, such as 0º/90º or 0º/60º, which is the main parameter that affects the scaffold anisotropy. Fiber diameter, extrusion rate, and writing speed are the other controllable parameters of the FDM process. (Mitchell & Tojeira, 2013)

Stereolithography is another widely used rapid prototyping technique where photosensitive monomeric resins are polymerized or polymeric resins cross-linked using a UV laser. (Nikkhah et al., 2012) Three different methods of stereolithography were indicated: mask-based, focusing beam, and ink-jet-based processes. In the first mask-based method, UV light crosses patterned mask and the patterned light further irradiates the surface layer of the photosensitive material. In the second focusing beam method, the UV beam directly draws a path on the surface layer of the photosensitive material. In the third ink-jet-based method, which is largely applied to tissue engineering, the photosensitive material layer is firstly jetted and then cured by UV irradiation immediately. (Mitchell & Tojeira, 2013)

Another advanced method that could be used for polymeric scaffolds production is the polymer solution phase separation. As the name suggests, a homogenous polymer solution separates into a polymer-rich and polymer-poor phases which may be induced by cooling the bimodal solubility curve that represents the thermodynamic equilibrium of liquid-liquid demixing or by the exposure to a nonsolvent (Ishigami et al., 2014) or an immiscible solvent (Mitchell & Tojeira, 2013). After the polymer solidified by glass transition or crystallization, used dilutants, solvents, or nonsolvents are then extracted by solvent exchange and evaporation (Ishigami et al., 2014) or lyophilization (Mitchell & Tojeira, 2013). Both these approaches produce isotropic microcellular scaffolds; however, it is possible to obtain anisotropic structures when a uniaxial thermal gradient is applied between two opposing sides of the matrix. In this case, the insulation of the walls during the phase separation causes crystal formation longitudinally to the thermal gradient and so microchannels are created instead of the common ellipsoidal pores. These microchannels are oriented in the same axis, their diameter may be tuned by adjusting the polymer/solvent ratio and the thermal gradient, and their microstructure, which can be ladder-like or microtubular, is affected by the solvent choice. (Mitchell & Tojeira, 2013) These scaffolds with oriented microchannels show anisotropy in both structure and mechanical properties since they demonstrate higher longitudinal than transverse modulus. (Hoque, 2017)

3.2.1 Electrospinning

In the field of tissue engineering, the use of electrospun materials as scaffolds is a promising and rapidly growing area of research for generating replacements to damaged tissues. The success of electrospun scaffolds lies in a straightforward, cost-effective, and versatile method of engineering well-defined nanofibrous scaffolds that hold promise in serving as a synthetic ECM providing not only structural support for the cells but also guiding their growth in the three-dimensional space which may lead to creating of a specific tissue. (Murugan & Ramakrishna, 2007) Electrospun scaffolds offer highly customizable mechanical and microtopological properties that may be adjusted by a simple set-up of electrospinning process parameters. (Fee et al., 2016)

Electrospinning repose the injection of a polymer solution, which is stored in a syringe and pumped at a constant flow rate through a nozzle while a specific voltage is applied to create an electric field between the nozzle tip and a collector, as shown in Figure 12. A charge accumulates at the solution surface at the tip of the nozzle and when a critical voltage is reached that overcame the solution surface tension, a conically shaped structure known as the Taylor cone starts to form, and fiber is driven to draw a chaotic conical path in direction of the collector. During the flight time, the solvent evaporates and a solid fiber with a diameter in the nanometer scale is formed and finally at the collector creates a highly porous nonwoven mat. By set-upping and adjusting of several processing parameters, such as voltage, electric current, injection rate, and environmental factors, such as temperature and humidity, some characteristics of the electrospun scaffolds may be customized, such as porosities or fiber diameters, among other features. In the conventional electrospinning apparatus, a collector has a plate form capturing the disoriented fiber which leads to the isotropic scaffold formation. To obtain scaffolds with aligned fibers and certain anisotropy, a cylindrical collector is rotating with the tangential velocity slightly higher than the flight velocity of the electrospun fibers which leads to tensioning and orientation of the fibers. (Mitchell & Tojeira, 2013)

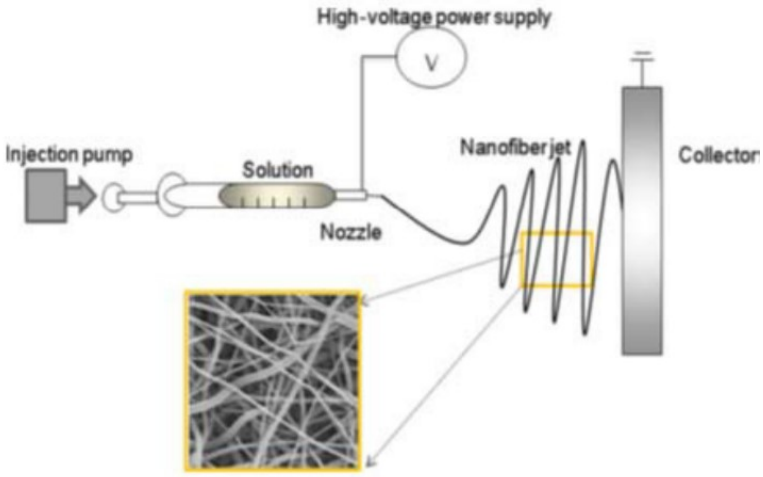

Figure 12 An electrospinning process scheme with a chaotic fiber orientation SEM image. (Mitchell & Tojeira, 2013)

The nonwoven mats anisotropy was dealt with by Fee et al. who fabricated electrospun fibers, made of polycaprolactone (PCL) and type A gelatin in a 90/10 (w/w) ratio, using the rotating cylindrical collector whose surface velocity was modulated to produce scaffolds with varying degrees of fiber alignment and anisotropy (Figure 13A–D) and using the stationary flat collector as a reference which is known to produce scaffolds with randomly oriented fibers and isotropic mechanical properties (Figure 13E). SEM images of electrospun mats were taken and analyzed to quantify. Results are summarized in a table (Figure 13F) that displays an increased fiber alignment expressed as the Von Mises distribution parameter **κ** with increasing collector velocity. The mechanical properties of the scaffolds were determined from uniaxial tensile testing that showed an increased degree of anisotropy with increasing alignment parameter κ (Figure 14B). The degree of anisotropy was defined as the ratio of the moduli measured in the parallel and the perpendicular directions to the direction of fiber alignment (Figure 14A). The electrospun scaffolds from the three highest collection speeds had a high degree of anisotropy since they had significantly different moduli in the directions parallel and perpendicular to the direction of fiber alignment. It is apparent that the electrospinning process can yield nonwoven mats with mechanical anisotropy directly modulated by nanofiber alignment within the scaffold. (Fee et al., 2016)

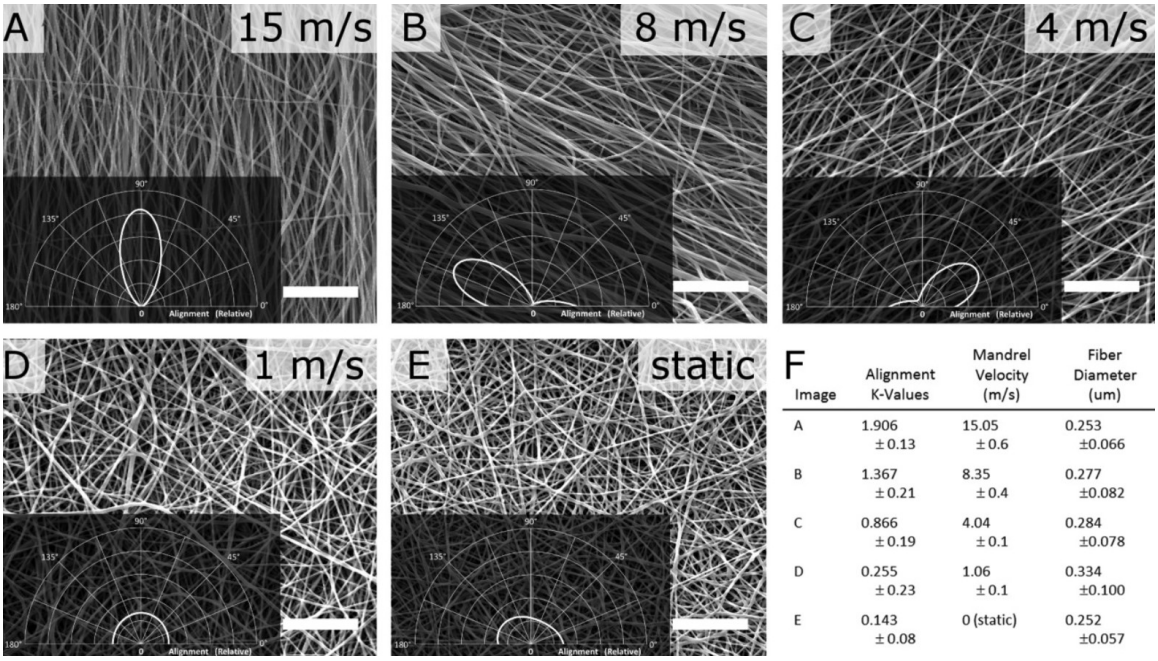

Image	Alignment K-Values	Mandrel Velocity (m/s)	Fiber Diameter (um)
A	1.906 ±0.13	15.05 ±0.6	0.253 ±0.066
B	1.367 ±0.21	8.35 ±0.4	0.277 ±0.082
C	0.866 ±0.19	4.04 ±0.1	0.284 ±0.078
D	0.255 ±0.23	1.06 ±0.1	0.334 ±0.100
E	0.143 ±0.08	0 (static)	0.252 ±0.057

Figure 13 The SEM images (scale = 10 μm) of electrospun scaffolds collected on (A–D) the rotating cylindrical collector with different velocities and (E) the stationary planar collector. The inset plots display the Von Mises distribution representing the fiber alignment. (F): Table with means ± standard deviations of the fiber alignment, collector velocity, and fiber diameter. (Fee et al., 2016)

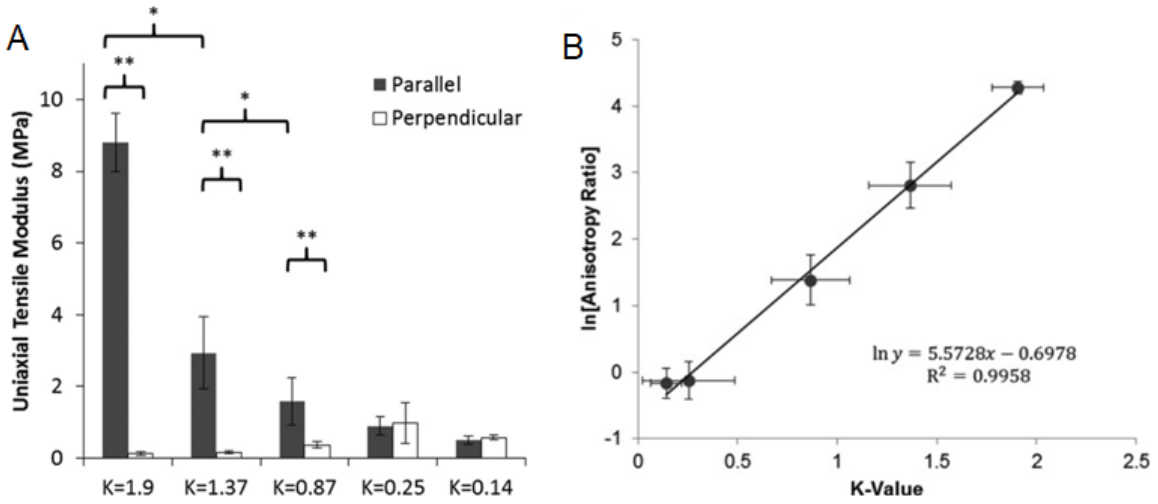

Figure 14 (A): Results of the uniaxial testing of scaffolds with different fiber alignment parameter κ showing elastic modulus for the directions parallel and perpendicular to the direction of fiber alignment (* – one-way ANOVA, Tukey post-hoc, $p < 0.05$; ** – $p < 0.05$, 2-sample t-test). (B): The linear dependence of the alignment parameter κ on the log of the anisotropy ratio (defined as the ratio of the modulus in the parallel and the perpendicular direction). (Fee et al., 2016)

4 SURFACE MODIFICATIONS OF POLYMERIC BIOMATERIALS

Interaction of any biomaterial with cells, tissues, biological fluids, or immune system is complex and affected by many different properties of biomaterial and the environment simultaneously. Therefore, when a material is not properly modified, this interaction is not ideal, which may lead to unwanted consequences. For example, orthopedic implants should ideally after implantation bind directly to the bone, but actually untreated orthopedic implants get encapsulated with fibrous tissue after implantation, which may lead to implant failure. (Unadkat et al., 2011)

In order to prevent these and other failures, considerable efforts have been invested in various biomaterial treatments. Generally, bulk or surface treatments may be used to achieve the desired cellular interactions with the biomaterial. In the case of polymer biomaterials, bulk modification is usually accomplished by copolymerization or by attaching a functional group to the polymer chain before the production of biomedical products, such as scaffolds. The disadvantage of these bulk modifications is that it usually changes the mechanical properties and processing possibilities of the treated polymeric biomaterials. (Ma, 2008) Surface treatments are used more often because it is a post-production process with a great advantage of the improvement of the surface properties while keeping the benefits of bulk properties of treated biomaterial simultaneously. (Michaljaničová et al., 2016) There are many different ways to modify and functionalize biomaterial surfaces and they could be divided into six groups: chemical, biological, physical, mechanical, combined, and special treatments.

4.1 Chemical modifications

Chemical treatments lead to chemical modifications of the biomaterial surface but that may also affect physical properties such as surface energy and wettability, mechanical properties such as hardness and elasticity, and other surface properties of the treated biomaterial. Polymers, in comparison to other materials, have an advantage in a diversity of chemical modifications that can be accomplished on them, for example, chemical crosslinking of the polymer surface (Tallawi et al., 2015) or surface grafting of suitable molecules via covalent bonds to the polymer chains. Amino acid grafting has been found to facilitate cell adhesion and proliferation on the surface of modified polymers. (Slepička et al., 2012)

Grafting of polyhydroxyethylmethacrylate (PHEMA), polyethyleneglycol (PEG), or zwitterionic (betaines) hydrophilic brushes or hydrogels onto the surface are used to improve the blood compatibility of the biomaterial due to the ability of these coatings to strongly bound a hydration layer that suppresses blood protein adsorption and its denaturation. (Maitz et al., 2019) Similar hemocompatible results, but with a different approach, might be gained by surface attachment of highly hydrophobic octadecyl groups or by coating with non-adhesive silicon-based, fluorocarbon, or polyurethane materials. (Bronzino & Peterson, 2015) In general, surface coatings, which are nowadays widely used to modify polymer biomaterials, may be based on various chemical structures and can change almost any of the surface properties. Besides, coatings might also be applied to more complex 3D structures, for example by immersing a porous scaffold in gelatin in a solvent mixture - dioxane, water. (Ma, 2008)

Focusing on enhancing the cytocompatibility of biomaterials made by chemical modifications that lead to increased binding of adhesive proteins to the surface, the preparation of the carbon layers on PTFE by chemical vapor deposition from acetylene may serve as an example. The cytocompatibility of coated PTFE, which was demonstrated on endothelial cells growth, was comparable to the cytocompatibility of tissue PS commonly used as the standard in cultivation *in vitro*, while pristine un-treated PTFE showed itself cytotoxic. (Kubová et al., 2007)

However, the cytocompatibility of polymer biomaterials may be changed by classical chemical treatments with acids, bases, and other chemicals. As was shown in the study of Ke et al., 2017, alkaline treatment of poly(3-hydroxybutyrate) (PHB) membranes using KOH or NaOH bases break the ester bonds to produce carboxylic groups on the surface which increases hydrophilicity, protein adsorption, and proliferation of human osteoblasts. It is also possible to introduce amino groups on the PHB surface by ethylenediamine treatment that decreases the hydrophobicity and improves the attachment of porcine urothelial cells. The chemical etching has major advantages in its simplicity and low cost, but the functionality is affected by many factors, such as reaction time, reagents concentrations, and crystallinity of the polymer substrate. (Ke et al., 2017)

Some chemical treatments may cause surface roughness changes. This could be used for controlled morphological modifications of biomaterials that may enlarge the surface area, help mimic ECM, increase tissue growth, and specify stem cell differentiation. (Tallawi et al., 2015) For example, time-sequenced dosing of a mixture of good solvent

(tetrahydrofuran, THF) and bad solvent (2-ethoxyethanol, ETH) on the surface of a rotating polymer substrate (tissue polystyrene, PS) causes changes in surface roughness, and the size and depth of the irregularities can be affected by sequencing variations, temperature or solvent concentrations (see Figure 15). (Wrzecionko et al., 2017)

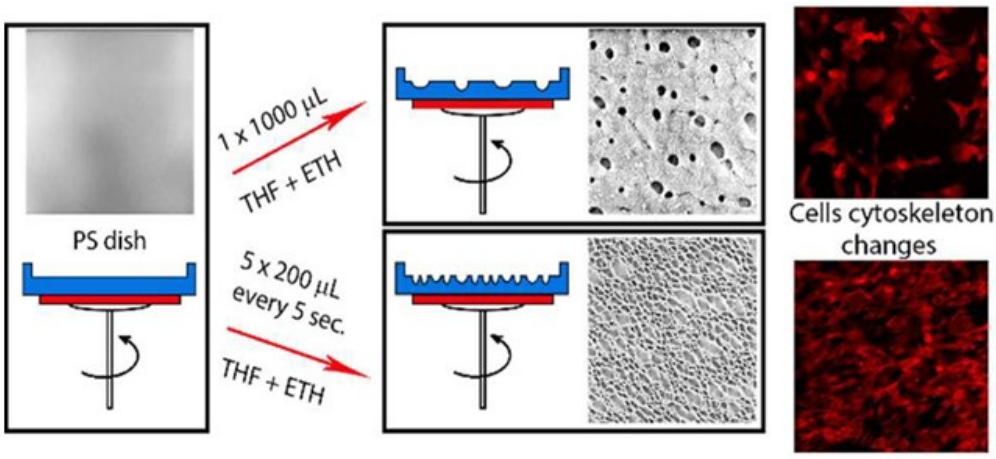

Figure 15 Surface morphology of original tissue PS and two differently structured samples in the schemes and SEM images (134 × 134) µm. Cytoskeletons of mouse fibroblasts cultivated on the structured samples are on the right in fluorescence microscope images (magnification: 100×, red color - actin). (Wrzecionko et al., 2017)

4.2 Biological modifications

Biological treatments modify biomaterial surfaces with bio-substances that change the biological activity of the treated surface. (Tallawi et al., 2015) These biological treatments mostly are based on immobilization of the bio-substances on the biomaterial surface which is applied with a limitation in the clinical success due to a gradual loss of their activity caused by saturation, consumption, and degradation during storage and physiological turn over *in vivo*. However, the life-time of biomolecules on the biomaterial surface may be increased via the reservoir capacity of the device. (Maitz et al., 2019)

Biomolecules introduced on the surface increase the biomaterial cytocompatibility and stimulate specific cellular responses by mimicking the natural extracellular matrix. Accordingly, collagen is one of the most commonly used structural proteins to construct the biomimetic layers. (Ke at al., 2017) However, it is possible and also effective to treat polymer surfaces with other various proteins and peptides, such as gelatin (Van Vlierberghe et al., 2011), albumin, and fibrinogen, or with polysaccharides, such as algin (Bronzino & Peterson, 2015) and chitosan, or with glycoproteins, such as laminin and

fibronectin (Ke at al., 2017), or with specific antibodies, growth factors, and other biomolecules. (Maitz et al., 2019) In clinical applications where blood is in contact with biomaterials, such as prosthetic valves, artificial vascular grafts, heart and heart-lung machines, or hemodialysis membranes and tubes, it is desirable to treat a surface with antithrombotic agents[6]. (Bronzino & Peterson, 2015) Furthermore, surface bioactivated by albumin exhibits good hemocompatibility because albumin serves as a transport molecule for bilirubin and fatty acids in the natural bloodstream. (Maitz et al., 2019)

4.3 Physical modifications

Physical treatments lead to physical modifications of the biomaterial surface, wettability primarily, but they may also affect surface chemistry, morphology, and biocompatibility. The most commonly used treatment for polymer biomaterials is plasma. Plasma treatment of the polymer surface creates radicals, ions, molecules, or molecular fragments in excited states that increase surface energy and may facilitate subsequent grafting of the surface with other bioactive agents, or they may recombine into more stable structures (functional groups). The modification results have been found to depend strongly on the type of plasma used, which can be gas, vacuum arc, or laser type (in the case of gas, also depends on the type of gas used - Ar, He, Ne, N_2, H_2O, CO_2, SO_2, NH_3, halogens, or their mixtures), and also on the plasma exposure time and discharge power that affect the depth of modification, which could be a few tens or hundreds of nanometres.

In addition to plasma, other important and commonly used treatments for modification of polymer surface are corona discharge, irradiation with UV, X, gamma rays, by electron or ion beams. Further, it should be known that some of the physical techniques, such as pyrolysis, UV-light irradiation, plasma discharge, and ion implantation, may cause carbonization of the polymer surface, which also affects the cell adhesion and proliferation. (Slepička et al., 2012) Another possible way to prepare a polymer-carbon structure is the deposition of carbon layers, that could have different forms (diamond-like carbon, amorphous hydrogenated carbon, amorphous carbon, pyrolytic graphite, and fullerene), onto the sample surface. The reparation of such carbon layers may be carried out by physical vapor deposition. (Kubová et al., 2007) For example, radiofrequency glow discharge plasma decomposition was used to coat polycarbonate samples with diamond-like carbon films that, as reported, improve blood biocompatibility. Amorphous

[6] Antithrombotic agents, such as anticoagulants (heparin, warfarin) or antiplatelets (aspirin, clopidogrel), reduce platelet aggregation and prevent the formation of blood clots. (Watson, 2002)

hydrogenated carbon films, that have also a positive effect on hemocompatibility, can be produced by plasma immersion ion implantation or magnetron sputtering. Also, there are next various physical methods of a thin layer deposition on the polymer surface, such as plasma polymerization, evaporation induced by heating or electron bombardment, sputtering (Slepička et al., 2012), atomic layer deposition, and many other techniques (Bose et al., 2018).

As well as selective chemical treatment, some physical treatments may also be used to modify the surface morphology of polymeric biomaterials. The irradiation of UHMWPE, which is used in orthopedic implants (Paita & Dahotre, 2008), by 532 nm wavelength laser reduces the surface roughness closely to 1 μm, which is proximately optimal roughness to bone bonding to the implant surface. (Chauhan et al., 2019) Using laser beam treatment was also studied in the field of tissue engineering. It has been found that aromatic polymers such as polyetheretherketone (PEEK), polyetherimide (PEI), and polyethersulfone (PES) have a high absorption coefficient and that periodic structures of scaffold surface have a positive impact on cytocompatibility. (Michaljaničová et al., 2016) The illumination of the surface of PS foil by the polarized UV laser beam can induce the formation of self-organized ripple structure with certain depth and periodicity (see Figure 16), the dependence of which can be described by

$$\Lambda = \frac{\lambda}{n - sin(\theta)} \tag{2}$$

where Λ is the periodicity of the ripple structures, λ is the wavelength of the excitation laser light, n is the effective refractive index of the polymer material and θ is the incidence angle of the laser beam.

The formula (2) and Figure 16 show that the period of the surface ripples depends on the angle of incidence of the radiation and the laser wavelength. Furthermore, the direction of the ripples is related to laser beam polarization. All these characteristics have an impact on the adhesion, proliferation, and alignment of the cells on the irradiated PS foils. (Rebollar et al., 2008)

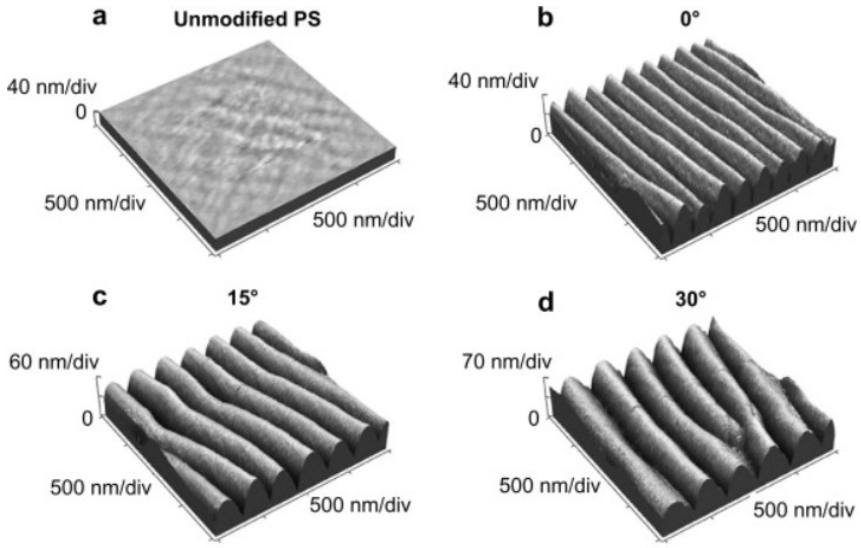

Figure 16 AFM images of PS (a) smooth unmodified foil and (b–d) irradiated samples under different angles of laser beam incidence: (b) 0° (Λ = 200 nm), (c) 15° (Λ = 270 nm), and (d) 30° (Λ = 340 nm). (Rebollar et al., 2008)

4.4 Mechanical modifications

Mechanical treatments naturally lead only to changes in morphology and topography of treated biomaterial. Grit-blasting, sandblasting (Bose et al., 2018), polishing, grinding, and abrasion (Hikkhah et al., 2012) of the polymer surface can serve as examples of such a mechanical modification. Its main effect is an increase in tissue growth by enlarging the surface area. (Tallawi et al., 2015) However, those mechanical methods, as well as already mentioned chemical etching, have a disadvantage in the impossibility to fully define the geometry of the patterns, the topography. This may be only done with computer numerical control (CNC) approaches by using lasers, which were slightly discussed before in physical treatments, or machinating technologies, such as micro-drilling, which are considered mechanical treatments. (Henriques et al., 2017) Controlled topographic patterns allow specifying cellular responses including stem cell differentiation which was largely correlated by Unadkat et al., 2011. In cases where tissue integration is desired, it has to be understood that macro, micro, and even nanoscale parameters have an impact on cell adhesion, proliferation, and migration. However, it is should be noted that in some cases textured surfaces impair the function of biomaterials, such as articulating surfaces or cardiovascular devices. (Bose et al., 2018)

4.5 Combined and special modifications

Not every treatment has to be strictly chemical, biological, physical, or mechanical. Many modifying methods combine different approaches to achieve the desired surface properties results. Very commonly used is a combination of chemical and physical methods, for example, photochemical techniques, when the polymeric surface is treated with hydrochloric acid or concentrated sulfuric acid and subsequently exposed to UV light or it is exposed to UV radiation in a reactive ammonia atmosphere. (Curtis et al., 1983) Another favorite double combined treatment is electrochemical deposition (Bose et al., 2018) and there are many others but triple and multiple combinations are also used, for example, a positive impact on human fibroblast proliferation showed a PHBV sample which was treated by oxygen plasma, then grafted with acrylic acid, followed by insulin immobilization mediated with a reaction using a water-soluble carbodiimide. (Ke et al., 2017) These methods enhance the cytocompatibility by the creation of new functional groups on the polymer surface. (Slepička et al., 2012)

Some lithographic methods, which are used for nanopatterning of polymer surfaces, may be considered as combined treatments as well. Photolithography, which was one of the first fabrication methods applied to the field of biology, is based on a spin-coated layer on the substrate of a light-sensitive polymer called photoresist that is selectively exposed to UV light, X-rays or electron beams that causes cross-linking, polymerization, or degradation of the exposed material. Stereolithography, which uses UV laser to polymerize photosensitive monomeric or polymeric resins, and two-photon absorption lithography, where an ultrafast laser is focused on photocurable resins, are mask-less fabrication methods that have been used to create nerve guidance conduits more than to generate topographies for biological studies. The pattern is then developed through various means which results in the dissolution of selected areas, such as isotropically or anisotropically etching using dry or wet chemical etching processes. Soft lithography with advantages of low cost and ease of use refers to a set of techniques, which use elastomeric polymers to develop patterns based on embossing, molding, and printing methods. In soft lithography, polydimethylsiloxane (PDMS) is the most widely used material due to its biocompatibility, transparency for optical imaging, and permeability to oxygen and carbon dioxide. Various soft lithography topographies have been utilized in the biological sciences to study mechanobiology and to modulate cell behavior. (Nikkhah et al., 2012)

II. ANALYSIS

5 AIMS AND OBJECTIVES

The experimental part of this master's thesis focuses on the cytocompatibility of polymeric samples, specifically electrospun polyurethane (PU) nanofiber nonwoven mats both in their pristine isotropic unmodified form and in their modified alternatives.

Stated objectives of the practical part were:

1) Production of the PU samples by electrospinning.
2) Determination of cytotoxicity of sample extracts.
3) Modification of the samples:
    - orientation of fibers in the PU mats to reach anisotropy,
    - coating with polypyrrole (PPy) to enhance electro-conductivity,
    - coating with gelatin and albumin to increase cytocompatibility.
4) Determination of changes made by modifications:
    - SEM photography of (un)oriented fibers in the PU mats,
    - defining effects of PPy, albumin, and gelatin coatings on cytocompatibility.
5) Observation of the influence of the samples on the behavior of mouse fibroblast cell line and mouse embryonic stem cell line under static, tensile-dynamic, and electric cultivation conditions.
6) Qualification and quantification of the cytocompatibility of the polymeric samples and their modified forms.
7) Evaluation of the obtained results.

The main aim of this analysis was to supplement the knowledge about the influence of PU nanofibrous material characteristics and their (an)isotropy on the cytocompatibility, especially under tensile-dynamic cultivation conditions. The reason for this is that so far, cell growth on fibrous materials has mostly been observed under static and non-tensile dynamic cultivation conditions, although tensile stress is a matter of course in the natural cellular environment.

6 MATERIALS AND METHODS

6.1 Samples preparation and modification

6.1.1 Production

Three types of PU nanofibrous nonwoven mats, which were observed in this master's thesis, were produced using electrospinning in cooperation with the Centre of Polymer Systems in Zlín, Czech Republic:

- **sample 1 – Desmopan 385 S**

Desmopan 385 S was dissolved in a solvent mixture of dimethylformamide (DMF) and methylisobutylketon (MIBK) in a ratio of 3:1 to a concentration of 12.5 %. The final solution had a viscosity of 1.3 Pa.s and a conductivity of 31.5 mS/cm due to the addition of sodium chloride (NaCl). Then the solution was loaded into syringes that were filling 32 jets in total. The solution was extruded into a high-voltage electric field (75 kV). A planar collector with a backing film drawn at a speed of 0.1 m/min was located 19 cm from the jets. The final product had 4 deposited layers with a basis weight of 9.01 g/m^2.

- **sample 2 – Desmopan 439 T**

Desmopan 439 T was dissolved in a solvent mixture of DMF and MIBK in a ratio of 2:1 to a concentration of 13 %. The final solution had a viscosity of 1.88 Pa.s and a conductivity of 98.4 mS/cm due to the addition of tetraethylammoniumbromide (TAEB). Then the solution was loaded into syringes that were filling 32 jets in total. The solution was extruded into a high-voltage electric field (75 kV). A planar collector with a backing film drawn at a speed of 0.1 m/min was located 19 cm from the jets. The final product had 4 deposited layers with a basis weight of 5.46 g/m^2.

- **sample 3 – Permuthane SU-22-542**

Permuthane SU-22-542 was dissolved in DMF to a concentration of 20 %. The final solution had a viscosity of 1.19 Pa.s and a conductivity of 101.8 mS/cm due to the addition of TAEB. Then the solution was loaded into syringes that were filling 32 jets in total. The solution was extruded into a high-voltage electric field (65 kV). A planar collector with a backing film drawn at a speed of 0.1 m/min was located 19 cm from the jets. The final product had 4 deposited layers with a basis weight of 7.25 g/m^2.

6.1.2 Extraction

Extracts of the electrospun PU mats were prepared according to ISO 10993-12 standards. The tested materials were cut into small pieces and stored in the culture medium (6 cm^2/1 mL of the medium) for 24 hours at 37 °C with stirring. The parent 100 % extracts were then diluted in the culture medium to obtain a series of dilutions with concentrations of 75 and 50 %. All extracts were used up to the next 24 hours.

6.1.3 Purification and orientation

The PU mats produced by electrospinning were rinsed and stirred in ultrapure water for at least 7 days, while the water changed every few days, to wash out residual monomers and loose additives necessary for material synthesis and processing. The sample purification may reduce its cytotoxicity. Then the samples were dried for 1 hour in a dryer set on 50 °C. Subsequently, fibers in the PU mats were manually oriented above 150 °C heat source and secured to microscope cover glasses with tape. Un-oriented samples also were fixed in the same way. Overhangs were cut off to gain a united surface area (22 × 22) mm. These prepared samples were placed in 6-well plates for more convenient handling. The orientation of fibers in the PU mats was important to mimic the anisotropic properties of the natural tissues. Scanning electron microscopy was used to picture the effectiveness of this manual way of fibers orientation.

6.1.4 Coating with polypyrrole

The coating of the PU samples with electro-conductive polypyrrole (PPy) was used to mimic the electrically conductive properties of the natural cellular environment. PPy has been chosen for its higher conductivity in comparison to other conductive polymers, and quick and facile synthesis of PPy coatings. The polypyrrole (PPy) was synthesized by using pyrrole as a monomer and one of two different polymerization initiators:

- Ammonium persulfate (APS)
- Ferric chloride (FeCl3)

Solutions of monomer (0.2 M) and polymerization initiator (0.25 M) in ultrapure water were prepared and allowed to stand for about 1 hour at room temperature to dissolve the compounds well and stabilize the temperatures of both solutions. Next, the solutions were mixed and poured into cell culture PS dishes (empty or containing the samples) without delay. The polymerization reaction was carried out for about 10–15 seconds at

room temperature. The longer polymerization time is unwanted because of the PPy powdering. The PPy coatings were thoroughly rinsed with 0.2 M hydrochloric acid and methanol and allowed to dry overnight at room temperature. Before any other processing, the necessary sterilization of the samples surfaces was accomplished by UV illumination of both sides for 30 minutes.

6.1.5 Coating with albumin and gelatin

Solutions of albumin (40 mg/mL) and gelatin (0.1 %) in ultrapure water were applied on the PPy coatings to increase its cytocompatibility. The surfaces were covered with:

- 1 mL of albumin solution only (Alb)
- 1 mL of gelatin solution only (Gel)
- 0.5 mL of both albumin and gelatin solutions together (Alb/Gel)

The proteins were allowed to adhere to the surfaces from the solutions for 20 minutes. Then the solutions with residual proteins were aspirated and surfaces were allowed to dry out at room temperature for another 20 minutes at least. After this phase, the samples were prepared for cell cultivation.

6.2 Cell lines and cultivation means

6.2.1 Mouse fibroblast cell line

One of the used cell lines was mouse fibroblast cell line NIH/3T3 (ATCC CRL-1658, USA). Fibroblasts are heterogeneous cells of mesenchymal origin with diverse appearances, activities, and locations. In biological laboratories, mouse fibroblasts are commonly used due to their easy accessibility, rapid growth rates, and various experiment possibilities. (Qui et al., 2016).

For the NIH/3T3 mouse fibroblast cell line culture medium, Dulbecco's modified eagle medium (DMEM) was used as a basis, to which a fetal calf serum (in an amount of 10 % of the total volume of the medium) and antibiotics – Penicillin/Streptomycin of concentration 100 μg/mL (in an amount of 1 % of the total volume of the medium with the serum together) were added. Cells were cultivated in the incubator with controlled atmosphere (5 % CO_2), temperature 37 °C, and constant relative humidity. To prepare cells for experiments, the medium was carefully aspirated from the culture vessel where the NIH/3T3 mouse fibroblast cell line was grown. Cells were rinsed with phosphate-buffered

saline (PBS) in an amount of 0.2 mL/cm^2. Thereafter, the buffer was aspirated and then 0.1 mL/cm^2 of trypsin was added to the cells. The culture vessel containing the cells and trypsin was placed in the incubator for a sufficient time (maximum 20 minutes) to release all cells from the plastic surface which was continuously checked by phase-contrast microscope. After the cells were completely released, the medium was added to the flask in the same amount as trypsin (0.1 mL/cm^2). The resulting solution (cell-medium-trypsin) was pumped into a tube, which was then capped and placed in a pre-tempered centrifuge (37 °C, 3 minutes, 1100 rpm – rounds per minute). The resulting supernatant was aspirated and cells were diluted with the medium to a desired concentration.

6.2.2 Mouse embryonic stem cell line

Another of the used cell lines was mouse embryonic stem cell line R1 (Nagy et al., 1993). These embryonic stem cells, which are derived from the inner cell mass of the developing mouse blastocyst, can self-renew in vitro while preserving the developmental potential to reconstitute all embryonic lineages, so-called 'naive' pluripotency, which provides an important promise in areas, such as regenerative medicine and tissue engineering. (Waisman et al., 2019).

For the R1 mouse embryonic stem cell line culture medium, Dulbecco's modified eagle medium (DMEM) was used as a basis, to which a fetal calf serum (in an amount of 16.5 % of the total volume of the medium), antibiotics – Penicillin/Streptomycin of concentration 100 μg/mL (in an amount of 1 % of the total volume of the medium with the serum together), 100 mM non-essential amino acids, 0,05 mM b-mercaptoethanol, and leukemia inhibitory factor (LIF) of concentration 5 ng/mL were added. Cells were propagated in an undifferentiated state by culturing on gelatinized tissue culture dishes in the complete medium. The gelatinization was performed using 0.1 % porcine gelatin in water. Cells were cultivated in the incubator with controlled atmosphere (5 % CO_2), temperature 37 °C, and constant relative humidity. To prepare cells for experiments, the medium was carefully aspirated from the culture dishes where the R1 mouse embryonic stem cell line was grown. Cells were rinsed twice with 2 mL of phosphate-buffered saline (PBS) two times. Thereafter, 150 μL of trypsin was added to the cells and then the culture dishes containing the cells and trypsin was placed in the incubator for a sufficient time (maximum 2 minutes) to release all cells from the plastic surface which was continuously checked by phase-contrast microscope. After the cells were completely released, the medium was added to reach a desired concentration.

6.2.3 Cultivation with sample extracts

Cytotoxicity of sample extracts was determined using the mouse fibroblast cell line. Fibroblasts in a concentration of 1×10^5 cells per 1 mL of the culture medium were seeded in microtitration plates to pre-incubate. Then the medium was aspirated and replaced by the extracts of the PU mats diluted with the medium to the following concentrations: 100, 75, and 50 % of parent extracts. References contained the medium without extracts. Repetitions were performed five times. Plates were put in the incubator for 24 hours then MTT assay followed.

6.2.4 Cultivation on sample surfaces under static conditions

The static cultivation of cells on the surface of the PU mats was performed with both of the used cell lines. Fibroblasts or embryonic stem cells in a concentration of 1×10^5 cells per 1 mL of the culture medium were seeded onto the sterilized and coated samples and references to adhere and pre-incubate. After 2 hours, the aliquot part of the medium was added to complete 2 mL volume. Repetitions were performed four times. The samples were put in the incubator for 3–5 days with medium restitution every 2 days. The state of the cells on the reference surfaces was regularly checked with the phase contrast optical microscope. The cultivation was followed by MTT assay and optical or fluorescence microscopy.

6.2.5 Cultivation on sample surfaces under tensile-dynamic and electric conditions

In this master's thesis, a bioreactor, which is shown in Figure 17, was used to apply hydrodynamic shear stress together with tensile strain and/or electric current to a scaffold with adhered cells. These stimuli should mimic cell environment properties in natural tissues. In the purpose of scaffold attachment within the chamber of the bioreactor, an inner frame was constructed using 3D printing in cooperation with the Department of Physics and Materials Engineering, Faculty of Technology, Tomas Bata University in Zlín, Czech Republic.

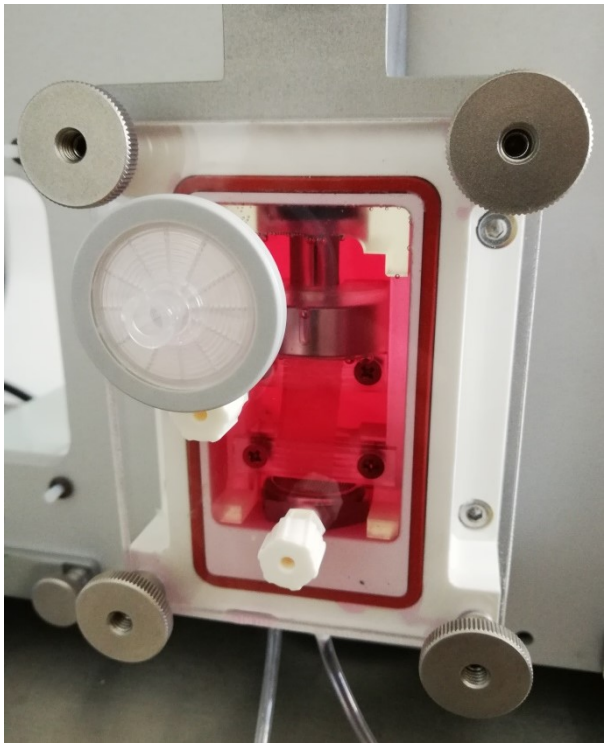

Figure 17 Photo of the bioreactor with the 3D-printed inner frame holding and stretching electrospun PU sample seeded with mouse embryonic stem cells while a culture medium is streaming throughout.

The tensile-dynamic cultivation of cells on the surface of the PU mats was performed with both of the used cell lines. Fibroblasts or embryonic stem cells in a concentration of 1×10^5 cells per 1 mL of the culture medium were seeded onto the sterilized sample and references to adhere and pre-incubate. After 2 hours, 2 mL of the medium was added to the sample, after which the cells were allowed to proliferate in a biological incubator for another 3 days. Subsequently, the sample with cells was removed from the medium and carefully secured to the inner frame of the bioreactor which was then filled with the culture medium, closed, attached and connected to a whole construction and a computer, and placed in the incubator. The bioreactor was planned on running for 3 days, during which a cyclic stretching or an electric current or both were supposed to be applied to the scaffold with cells. The set-up conditions would be: 1 mm stretching with a speed of 0.5 mm/sec for 15 minutes followed by 1 hour of static rest, and electric voltage 0.1 V. At the end of the experiment, the bioreactor would be stopped, opened, the medium aspirated, and the sample with cells carefully removed and placed in a tissue plastic for following qualification and quantification.

6.3 Obtaining of results

6.3.1 Scanning electron microscopy

The morphology of the samples, specifically the fiber alignment in the (un)oriented electrospun PU nonwoven mats, was studied using a scanning electron microscope (SEM) Phenom Pro.

6.3.2 Optical microscopy

In addition to the regular checks of the cell states, the phase contrast optical microscope was employed to obtain cell proliferation results from coated and seeded PS dishes. The optical microscope enables quick and easy observation of living cells. Nevertheless, the possibility of using optical microscopy is limited by the translucency of the samples. Therefore, the PU samples had to be analyzed by fluorescence microscopy.

6.3.3 Fluorescence microscopy

Fluorescence microscopy was used for a further determination of cell morphology. First, the cell samples were rinsed with PBS and after aspiration they were fixed, permeabilized, and stained with fluorescent dyes. Fixation was performed with 2 mL of 4 % formaldehyde in ultrapure water for 15 min, then the formaldehyde was aspirated and the cells rinsed again with PBS. The cell membrane permeabilization was ensured by the addition of 2 mL of 0.5 % Triton in PBS, which was allowed to act for 5 min. Subsequently, Triton was aspirated and the cells were washed three times with PBS. For staining of fixed cells, 2 mL of PBS was first pipetted into which fluorescent dyes were added in the dark: ActinRed (1 drop/mL) and Hoechst (20 µL/mL). The samples were left in the dark for 20 minutes. During this time, ActinRed bound to the proteins contained in the cytoskeleton of the cells and Hoechst penetrated the nuclei of the cells where it bound to the DNA. After this time, PBS with dyes was aspirated and replaced with 2 mL of pure PBS. Then the samples of PU mats secured to the microscope cover glasses were carefully inverted. In this phase, the cells were prepared to be observed by a phase-contrast inverted fluorescent microscope.

6.3.4 MTT assay

MTT assay was used to determine cell viability and to specify the PU extracts cytotoxicity as well as the cytocompatibility of different surfaces. This colorimetric

method is based on the reduction of 3-(4,5-dimethylthiazol-2-yl)-2,5-diphenyltetrazolium bromide (MTT) by mitochondrial enzymes of living cells. To complete the MTT assay, a culture medium was aspirated, cells were washed with PBS and then 3 mL of medium and MTT solution in ultrapure water (5 mg/mL) was applied in a ratio of 9:1. MTT was allowed to interact with the cells for at least 4 hours in a biological incubator. After that time, medium with the excess MTT was aspirated and replaced with an equal amount of dimethylsulfoxide (DMSO) for 15 minutes. Then the absorbance values were measured on a photometer at 570 nm with the reference wavelength set at 690 nm. The results are presented as a reduction of cell viability in percentage when compared to the cells cultivated on reference surfaces or, in the case of extracts, in pure medium without the PU extracts.

6.4 Used chemicals

These chemicals were used to perform the experimental part of this master's thesis: polyurethane (PU; Desmopan 385 S and Desmopan 439 T – Covestro AG, Germany; Permuthane SU-22-542 – Stahl, Netherlands), dimethylformamide (DMF; Brenntag, Poland), tetraethylammoniumbromide (TEAB; Penta chemicals, Czech Republic), sodium chloride (NaCl; Penta chemicals, Czech Republic), methylisobutylketon (MIBK; Penta chemicals, Czech Republic), Dulbecco's modified eagle medium (DMEM; PAA Laboratories GmbH, Austria; Gibco™, USA), antibiotics – Penicillin/Streptomycin (GE Healthcare HyClone, Great Britain), fetal calf serum (BioSera, France; Gibco™, USA), non-essential amino acids (Gibco™, USA), b-mercaptoethanol (Sigma-Aldrich; USA), leukemia inhibitory factor (LIF; Chemicon, USA), porcine gelatin (Sigma-Aldrich; USA), Dulbecco's phosphate buffered saline (PBS; BioSera, France), trypsin (PAA Laboratories GmbH, Australia), pyrrole (Sigma-Aldrich; USA), ferric chloride ($FeCl_3$; IPL, Czech Republic), hydrochloric acid (HCl; Penta chemicals, Czech Republic), methanol (Penta chemicals, Czech Republic), bovine gelatin (Sigma-Aldrich; USA), bovine serum albumin (Sigma-Aldrich; USA), 3-(4,5-dimethylthiazol-2-yl)-2,5-diphenyltetrazolium bromide (MTT; Duchefa Biochemie, Netherlands), dimethylsulfoxide (DMSO; Duchefa Biochemie, Netherlands), formaldehyde (Penta chemicals, Penta chemicals, Czech Republic), triton X 100 (Sigma-Aldrich, Austria), fluorescent dyes: ActinRed 555 (Life Technologies, USA) and Hoechst 33258 (Sigma-Aldrich, Austria).

6.5 Used apparatus and equipment

These apparatus and equipment were used to perform the experimental part of this master's thesis: electrospinning device Nanospider (Elmarco, Czech Republic), scanning electron microscope Phenom Pro (SEM; Phenom-World, Netherlands), laminar box with controlled air circulation HERAsafe (Thermo Scientific, USA), laboratory centrifuge Eppendorf 5702 R (Eppendorf, Germany), biological incubator HERAcell 150i (Thermo Scientific, USA), stimulation bioreactor (EBERS Medical Technology, Spain), phase-contrast inverted fluorescent microscope Olympus IX 81 (Olympus, Japan) with camera Leica DFC480 (Leica Microsystems, Japan), photometer NanoQuant infinite M200PRO (Tecan, Switzerland), autoclave Tuttnauer 3870 ELPV (Tuttnauer, USA), ultrapure water system Puranity TU3UV+ (VWR, Sweden), water bath (Memmert, Germany), automatic pipettes and micropipettes (Eppendorf, Germany), analytical scales AS 220.R2 (RADWAG, USA), tissue plastic (TPP, Switzerland), and other laboratory equipment.

7 RESULTS

For the sake of clarity, the results are divided into three sections regarding:

1. PU mats and their (an)isotropy
2. Surface modifications with PPy, albumin, and gelatin
3. Cell cultivation under different conditions

7.1 Electrospun samples and orientation

This subchapter shows the analysis results of the three different electrospun PU nanofiber nonwoven mats:

- sample 1 – Desmopan 385 S
- sample 2 – Desmopan 439 T
- sample 3 – Permuthane SU-22-542

At first, the cytotoxicity of extracts of these samples was examined by the MTT assay. After the manual orientation of fibers in these samples, its effectiveness was checked by scanning electron microscopy. Then the impact of these three different PU samples and their (an)isotropic properties on the mouse fibroblast cell line was observed using fluorescence microscopy.

7.1.1 Sample 1

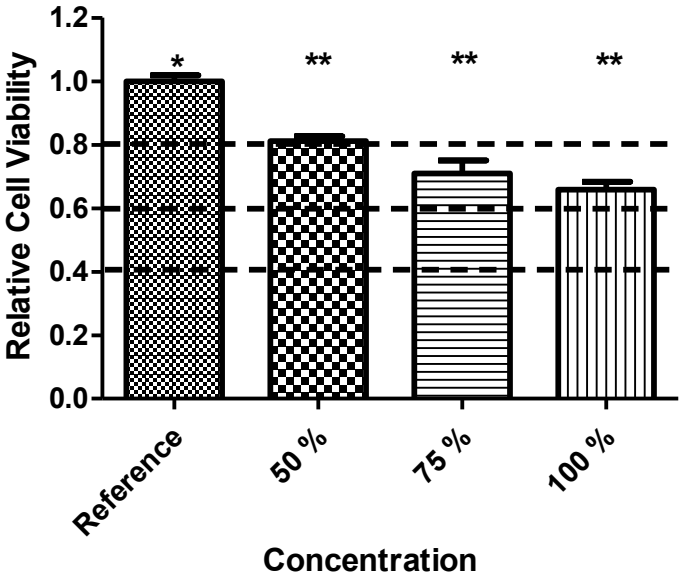

Figure 18 Results of MTT assay referring to the cytotoxicity of the sample 1 extracts (a different number of stars indicates a statistically significant difference, one-way ANOVA, $p < 0.05$).

The results of the sample 1 extract cytotoxicity are shown in Figure 18. Concentrated extract (100 %) gave mild cytotoxicity. As the extract dilutes, the cytotoxicity decreases. The 50 % extract ended on the 0.8 cell viability relative to the reference – cells cultivated in pure medium without the PU extract. The results were tested using one-way ANOVA, Tukey's multiple comparison test, which proved that the means of the measured values are statistically significantly different between reference and 50 % extract concentrations at a probability value of $p < 0.05$ and between reference and 75 % or 100 % extract concentrations at a probability value of $p < 0.001$.

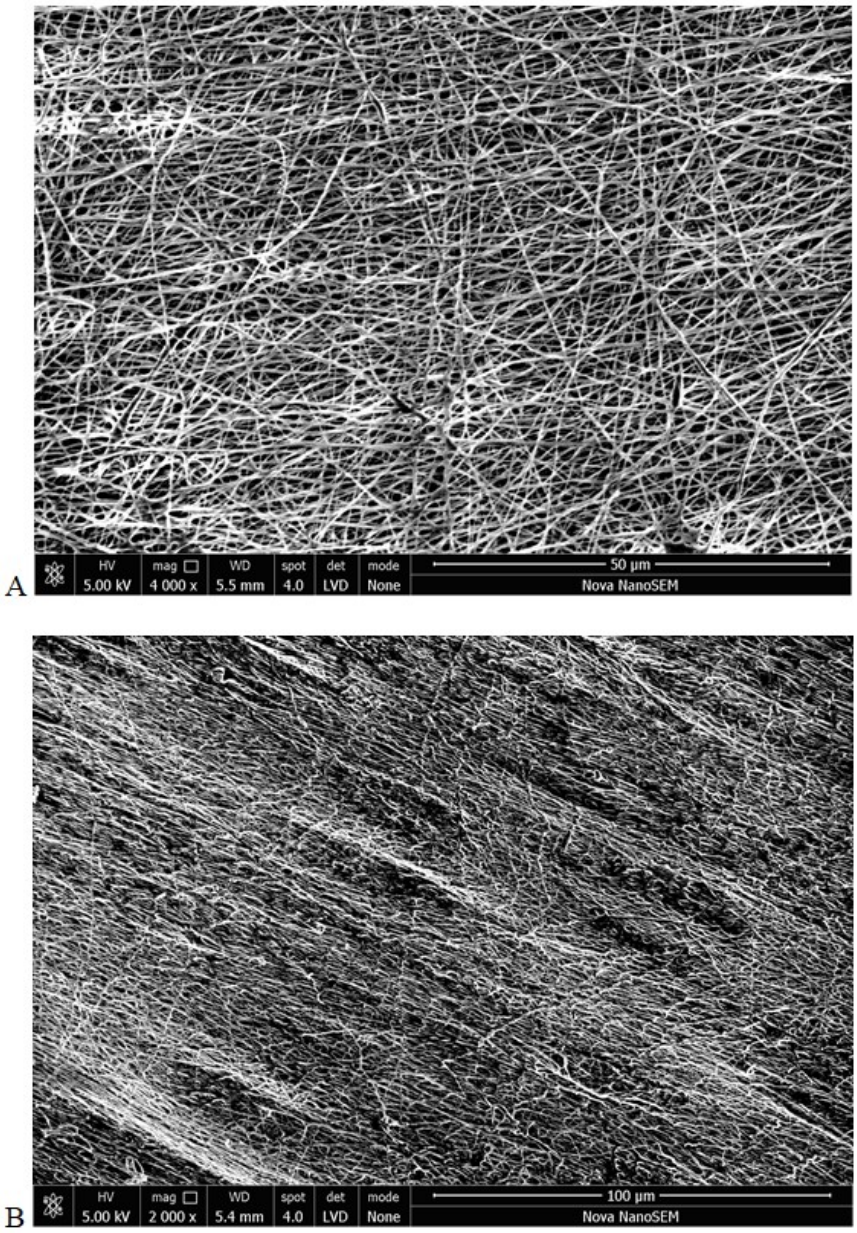

Figure 19 The SEM photographs of PU nonwoven mat, sample 1, in its (A) original form with un-oriented fibers, (B) modified form with oriented fibers.

The difference between the original isotropic sample 1 (Figure 19A) and its oriented anisotropic modification (Figure 19B) is significant. Although some fibers are torn after mechanical orientation, the majority length of the fibers lays in one direction.

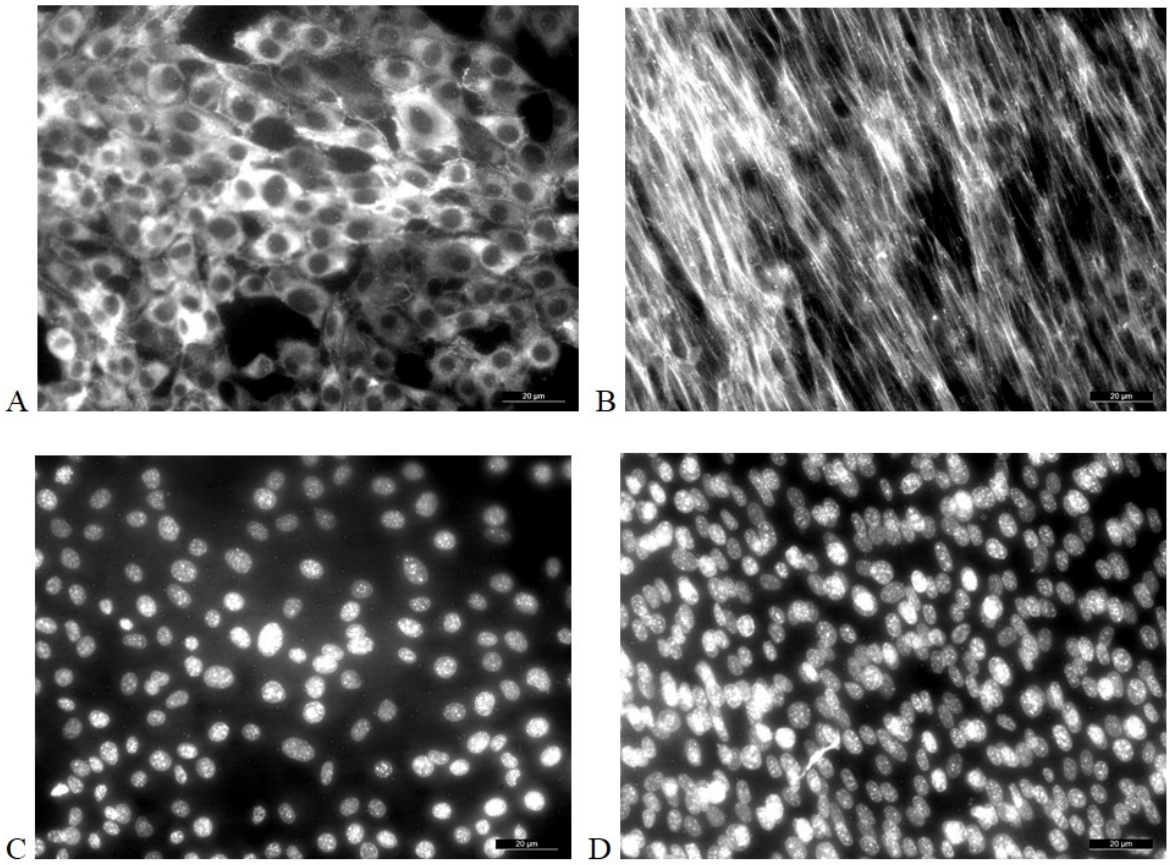

Figure 20 The fluorescence microscopy photographs of mouse fibroblasts (NIH/3T3) cultivated on the sample 1 in its (A, C) original form with un-oriented fibers, (B, D) modified form with oriented fibers; (A, B) ActinRed – actin, (C, D) Hoechst – DNA.

The morphology of fibroblasts grown on the surface of sample 1 can be seen in Figure 20. Concerning the estimation of cell number, the modified form of this sample with oriented fibers (on the right) suited mouse fibroblasts better than the original un-oriented mat (on the left). The effect of the fiber orientation on the cell morphology is visible preferably in the upper photos (20A vs. 20B) where the clear difference in the cytoskeletons may be seen. Uneven distribution of round-shaped cells showed on the isotropic un-oriented sample. Whereas, cells that grew on the anisotropic oriented samples had taken prolonged shapes in the exact direction of the orientation of fibers. Many of these cells showed also elongated nuclei (20D) in comparison to the rounded cell nuclei on the pristine sample (20C).

7.1.2 Sample 2

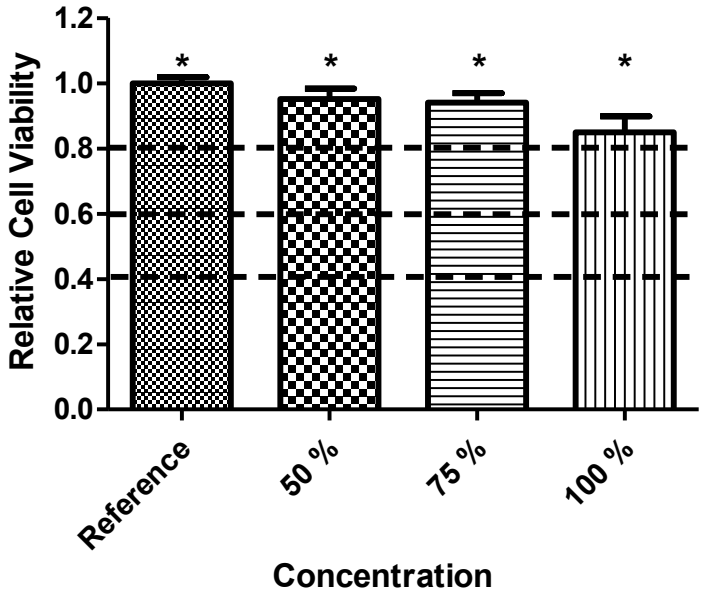

Figure 21 Results of MTT assay referring to the cytotoxicity of the sample 2 extracts (a different number of stars indicates a statistically significant difference, one-way ANOVA, $p < 0.05$).

The results of the sample 2 extract cytotoxicity are shown in Figure 21. Extracts in any concentration (nor the 100 % one) were not cytotoxic as the cell viability was almost as high as in the case of the reference – cells cultivated in pure medium without the PU extracts. The results were tested using one-way ANOVA, Tukey's multiple comparison test, which showed that the means of the measured values are not statistically significantly different.

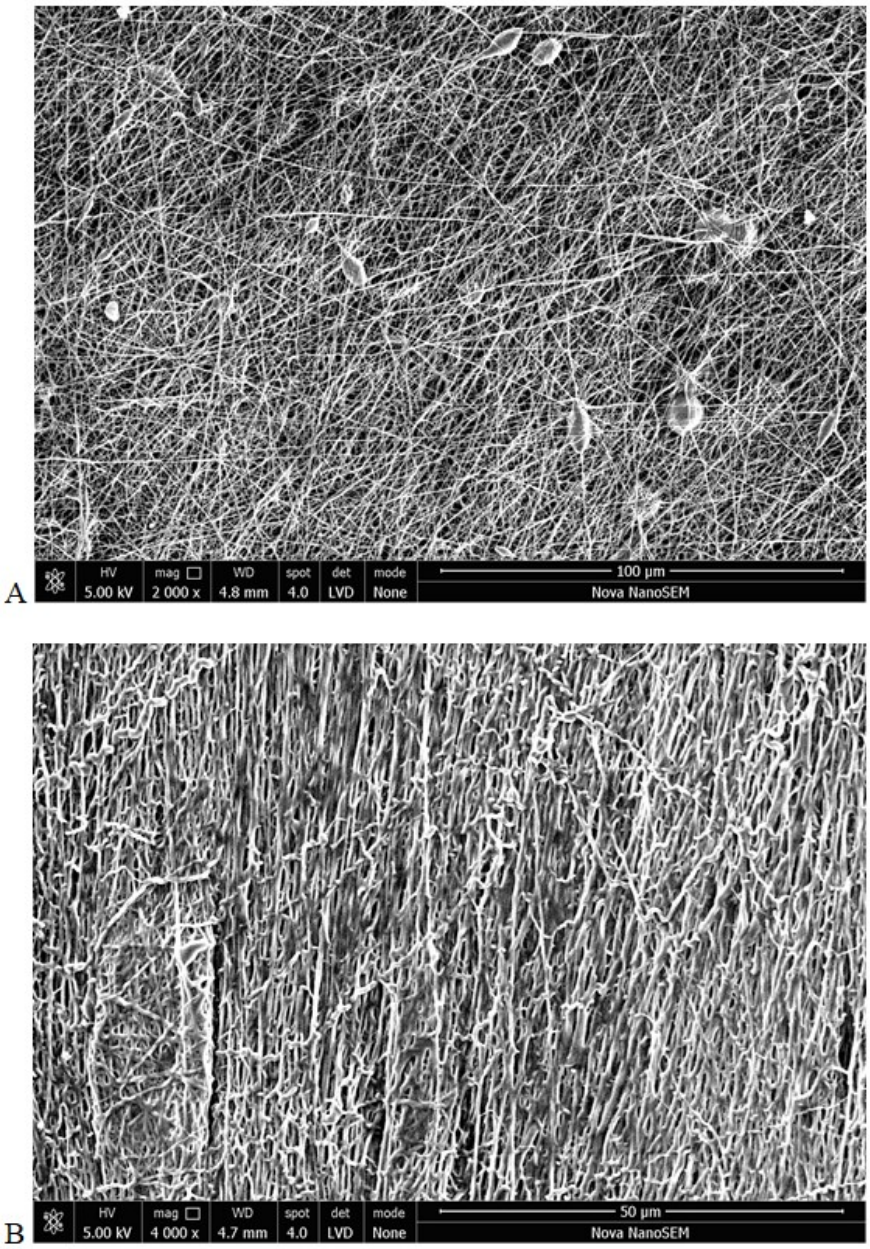

Figure 22 The SEM photographs of PU nonwoven mat, sample 2, in its (A) original form with un-oriented fibers, (B) modified form with oriented fibers.

The SEM photographs show the difference between the original form of the sample 2 (Figure 22A), which consists of randomly oriented fibers with a few nodules, against the modified sample 2 (Figure 22B) with oriented fibers. Although some fibers are torn after mechanical orientation, the majority length of the fibers lays in one direction.

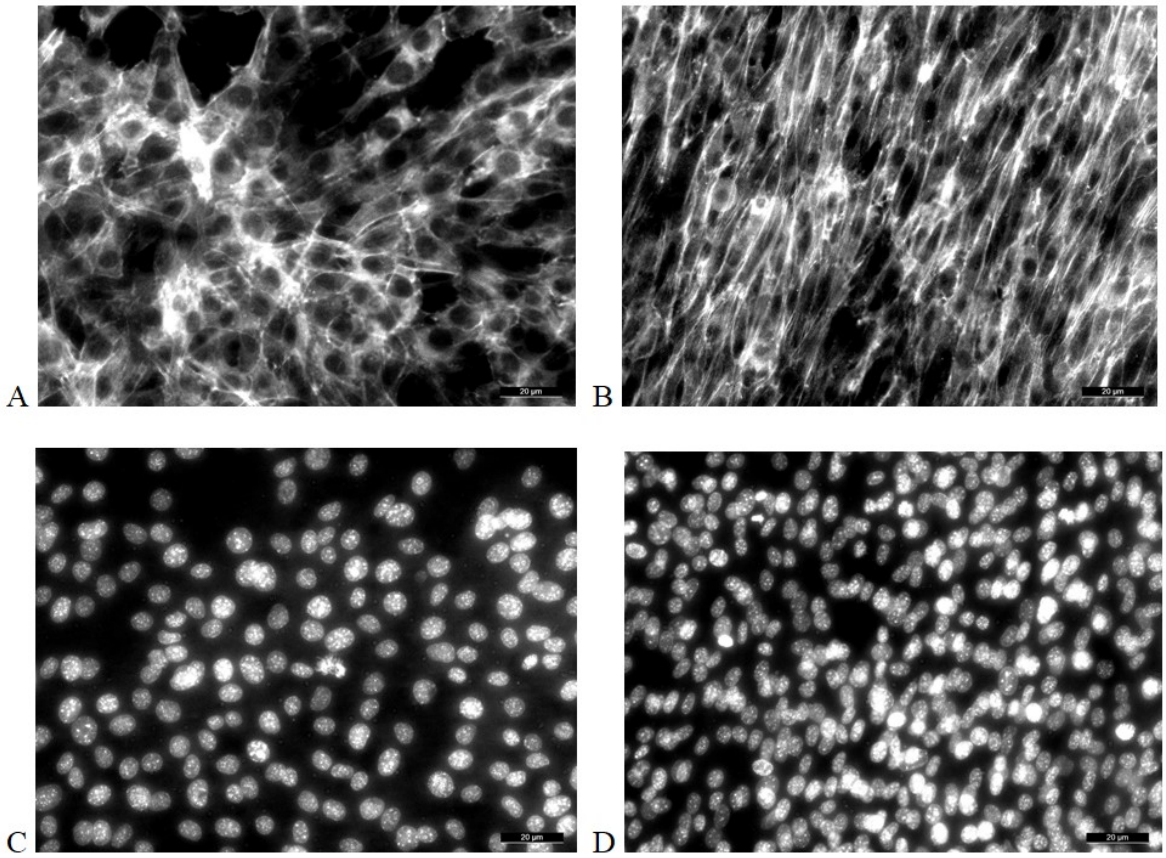

Figure 23 The fluorescence microscopy photographs of mouse fibroblasts (NIH/3T3) cultivated on the sample 2 in its (A, C) original form with un-oriented fibers, (B, D) modified form with oriented fibers; (A, B) ActinRed – actin, (C, D) Hoechst – DNA.

Mouse fibroblasts that grew on the sample 2 are shown in Figure 23. Based on the estimation of cell number, oriented fibers in the mat (on the right) are more sufficient for mouse fibroblast proliferation than the randomly-oriented fibers (on the left). The impact on the cell morphology is visible preferably in the upper photos (23A vs. 23B) where the significant difference in the cytoskeletons may be seen. Cultivation of fibroblasts on the un-oriented fibers led to the creation of stellate-patterned morphology similar to the morphology of fibroblasts grown on the reference smooth cell culture PS dishes. While cultivation on the oriented fibers resulted in cells with elongated shapes, more even distribution on the surface, and orientation in the direction of the fibers. Some of these cells showed also prolonged nuclei (23D) in comparison to the rounded cell nuclei on the isotropic un-oriented mat (23C).

7.1.3 Sample 3

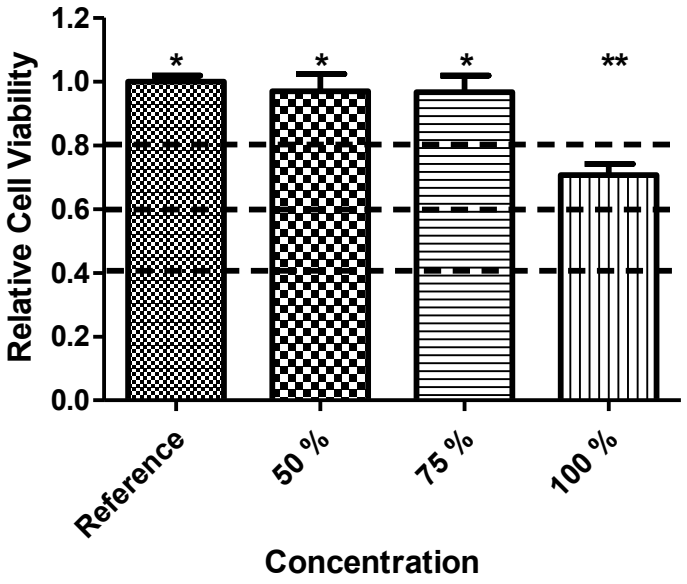

Figure 24 Results of MTT assay referring to the cytotoxicity of the sample 3 extracts (a different number of stars indicates a statistically significant difference, one-way ANOVA, $p < 0.05$).

The results of the sample 3 extract cytotoxicity are shown in Figure 24. The extracts in concentrations 50 and 75 % were not cytotoxic. However, the concentrated extract (100 %) demonstrated mild cytotoxicity based on the cell viability relative to the reference – cells cultivated in pure medium without the PU extracts. The results were tested using one-way ANOVA, Tukey's multiple comparison test, which proved that the means of the measured values are statistically significantly different between 100 % and 75 % or 50 % extract concentrations at a probability value of $p < 0.05$ and between reference and 100 % extract concentration at a probability value of $p < 0.001$.

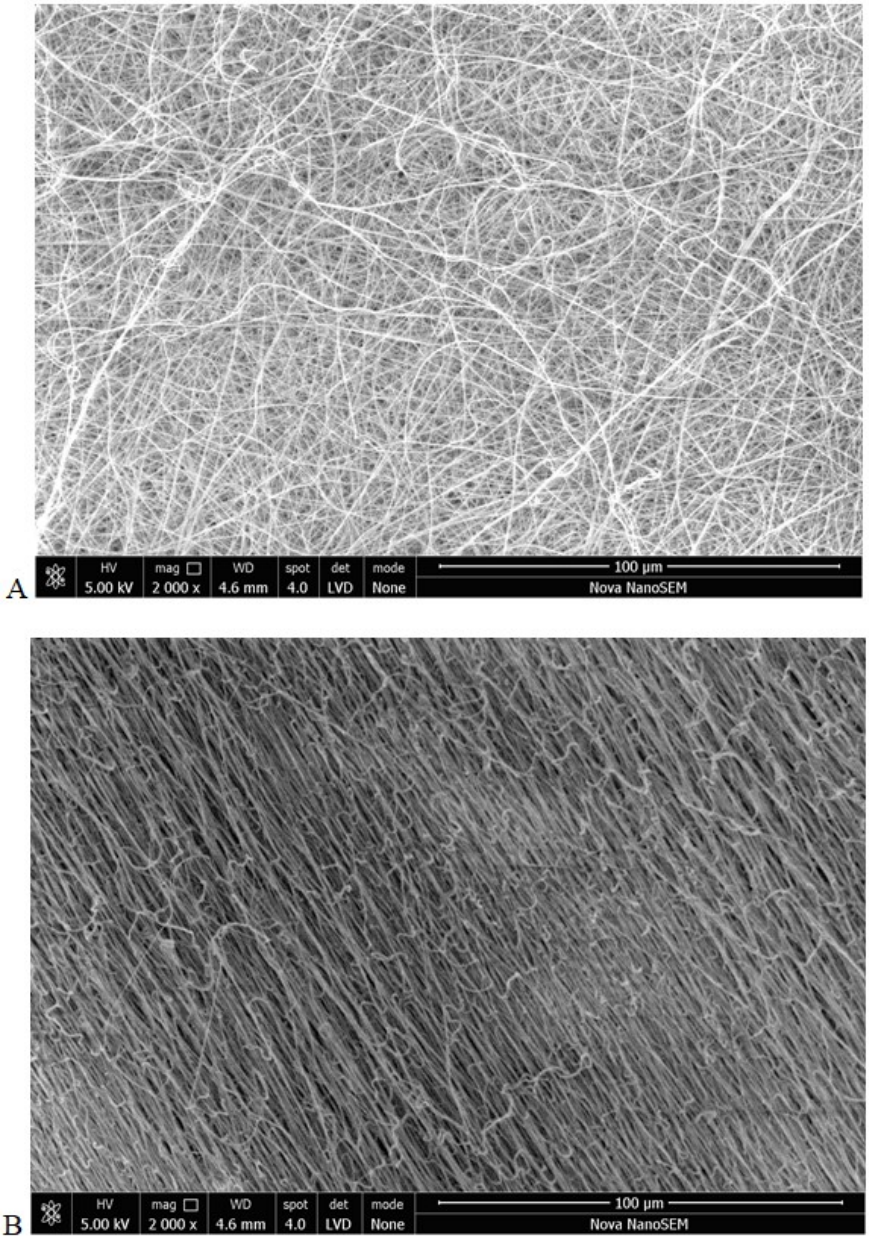

Figure 25 The SEM photographs of PU nonwoven mat, sample 3, in its (A) original form with un-oriented fibers, (B) modified form with oriented fibers.

The difference between the original isotropic sample 3 (Figure 25A) and its oriented anisotropic modification (Figure 25B) is evident. Although some fibers are torn after mechanical orientation, the majority length of the fibers lays in one direction.

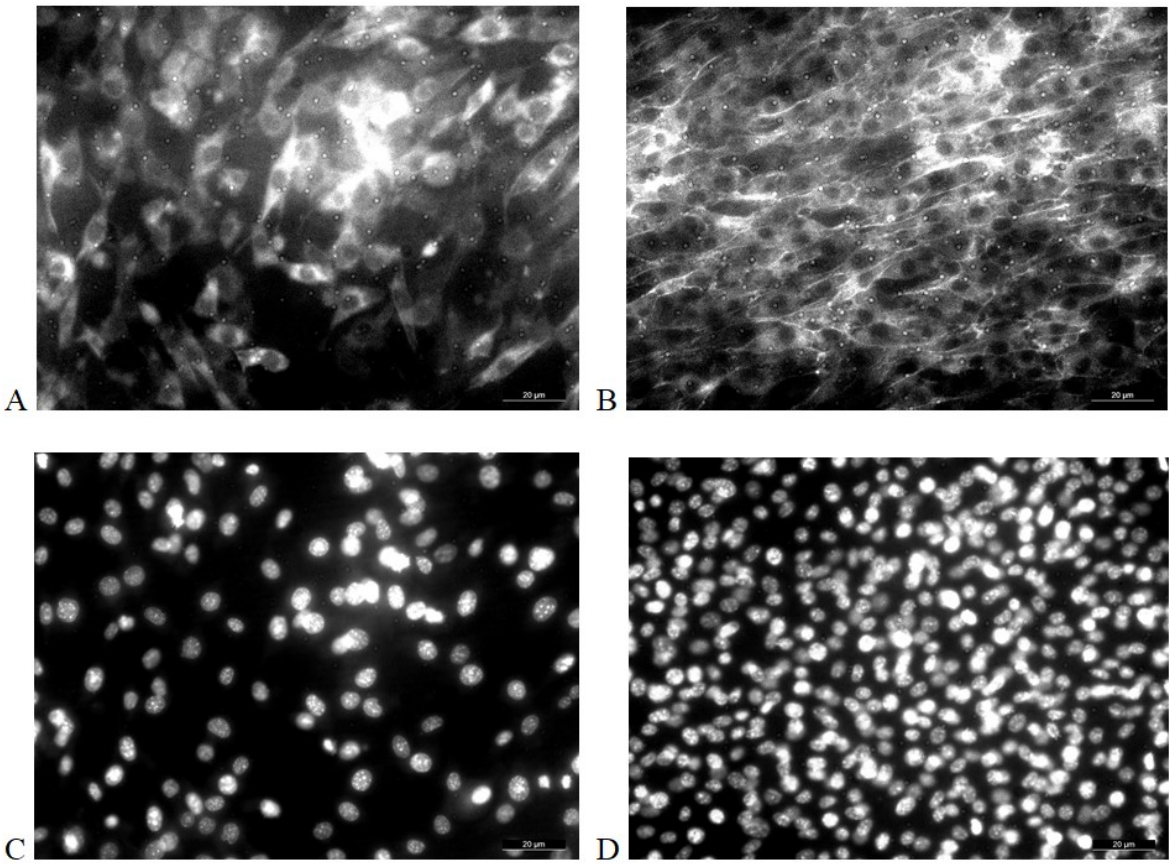

Figure 26 The fluorescence microscopy photographs of mouse fibroblasts (NIH/3T3) cultivated on the sample 3 in its (A, C) original form with un-oriented fibers, (B, D) modified form with oriented fibers; (A, B) ActinRed – actin, (C, D) Hoechst – DNA.

The morphology of fibroblasts cultivated on the sample 3 may be seen in Figure 26. According to the estimation of the number of the cells, mouse fibroblasts proliferate more on the surface of the oriented sample (on the right) than on the surface of the pristine un-oriented sample (on the left). The effect of the fiber orientation on the cell morphology is visible preferably in the upper photos (26A vs. 26B) where the significant difference in the cytoskeletons may be seen. Fibroblasts cultivated on the original PU mats with un-oriented fibers got lenticular morphology. In the case of the oriented mats, cells showed slightly prolonged shapes, but not as much as cells on the samples 1 and 2. Neither the nuclei of these cells are elongated, but instead retain their round shape (26D) as cell nuclei on the un-oriented mats (26C).

7.2 Surface coatings

This subchapter shows the analysis results of four different coatings and their various combinations. Firstly, electrically conductive polypyrrole (PPy) coatings were synthesized using pyrrole as monomer and two different polymerization initiators:

- ammonium persulfate (APS)
- ferric chloride ($FeCl_3$)

As the results show, the PPy cytocompatibility had to be increased which was reached by biofunctionalization of the surface by adhesion of selected proteins, peptides:

- albumin (Alb)
- gelatin (Gel)

The distinctions in the cytocompatibility (NIH/3T3 mouse fibroblast cell line) acquired by coating the cell culture PS dishes with mentioned PPy, albumin, and gelatin were observed by optical microscopy.

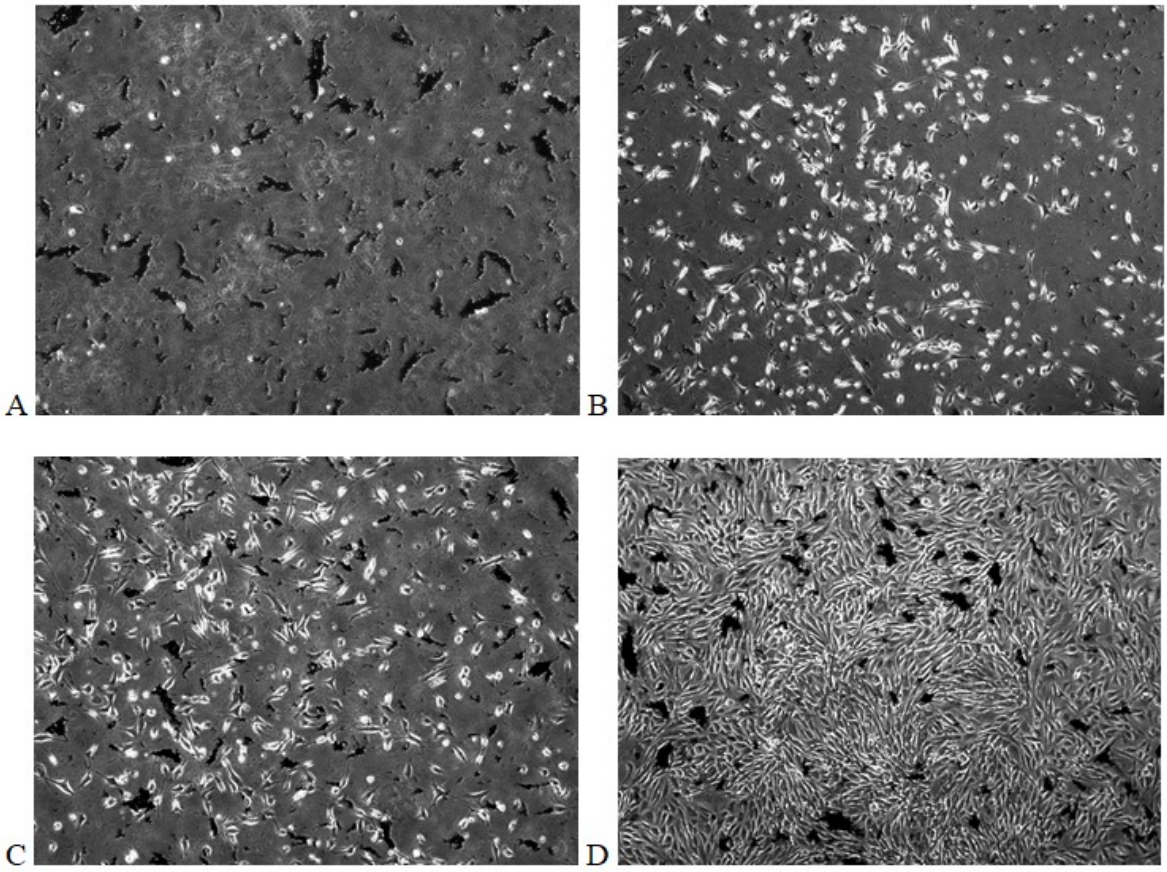

Figure 27 The optical microscopy photographs with 40× magnification of mouse fibroblasts (NIH/3T3) cultivated on cell culture PS dishes coated with PPy using APS as polymerization initiator: (A) PPy only, (B) PPy + Alb, (C) PPy + Gel, (D) PPy + Alb/Gel.

Fibroblasts cultivated on cell culture PS dishes coated with PPy using APS as the initiator are shown in Figure 27. As the photograph (27A) shows, PPy alone is not cytocompatible enough for the tested cell line of mouse fibroblasts. Coating with albumin (27B) resulted in a similar enhancement of PPy surface biocompatibility as with gelatin-coating (27C). Nevertheless, the combination of both albumin and gelatin (27D) brought the biggest cytocompatibility improvement.

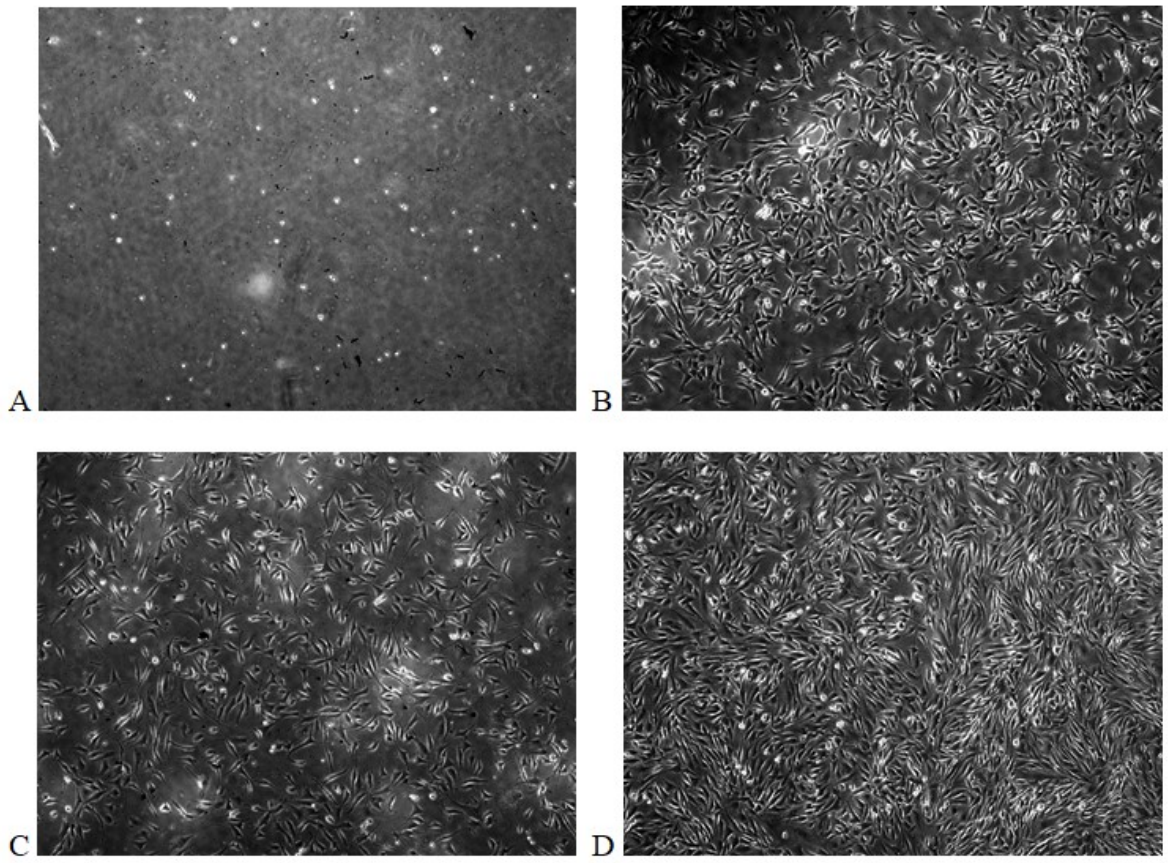

Figure 28 The optical microscopy photographs with 40× magnification of mouse fibroblasts (NIH/3T3) cultivated on cell culture PS dishes coated with PPy using $FeCl_3$ as polymerization initiator: (A) PPy only, (B) PPy + Alb, (C) PPy + Gel, (D) PPy + Alb/Gel.

The viability of fibroblasts cultivated on cell culture PS dishes coated with PPy using $FeCl_3$ as the initiator can be seen in Figure 28. This PPy alone (28A) is not cytocompatible with mouse fibroblasts. Coating with albumin (28B) or with gelatin (28C) increased the PPy cytocompatibility but the combination of both albumin and gelatin together (28D) gave the most significant improvement in cell adhesion and subsequent proliferation. When comparing the two types of observed PPy coatings (Figures 27 vs. 28), the results seem very similar, only this PPy with $FeCl_3$ tends to generate less powder possible to wash out.

7.3 Conditions of cell cultivation

This subchapter was supposed to show the analysis results of cell cultivation under four different conditions – static, tensile-dynamic, electric, and a combination of the last two.

Of the three observed electrospun PU nanofiber nonwoven mats, the sample 1 (Desmopan 385 S) was chosen as the most appropriate to perform these experiments. Despite its extract show mild cytotoxicity (Figure 18), the sample 1 was chosen due to the suitable mechanical properties, such as elasticity which is important in the tensile-dynamic cultivation, cohesion and rift resistance essential during the orientation process, and due to the most significant impact of fiber orientation on the fibroblast morphology (Figure 20). In addition to the orientation of fibers in the chosen PU mat that causes anisotropy, the sample was coated with PPy to enhance electro-conductivity of the polymeric substrate and with proteins to increase the surface cytocompatibility. Of the two types of observed PPy coatings, the PPy with $FeCl_3$ used as a polymerization initiator was chosen due to its higher electrical conductivity and less powder formation. The surface functionalization was secured by coating with both albumin and gelatin together due to the highest cytocompatibility of this combination (Figure 28). The results of mouse fibroblast cell line NIH/3T3 and mouse embryonic stem cell line R1 cultivation under static conditions on these modified polymer samples are shown hereinafter. Unfortunately, it was not possible to complete the cultivation under tensile-dynamic and electric conditions because of both the restriction related to SARS-CoV-2 pandemic and software technical issues.

7.3.1 Cultivation under static conditions

The results of static mouse fibroblast (NIH/3T3) and embryonic stem cell (R1) cultivation on the PU nonwoven mat (the sample 1), which was (un)oriented and (un)coated with PPy using $FeCl_3$ initiator and with both albumin and gelatin together, are shown hereinafter. The impact of these polymer surface modifications on the two cell lines was observed using fluorescence microscopy. Since all observed samples had the same culture surface area (22 × 22) mm, it was possible to perform not only qualification but also quantification by the MTT assay.

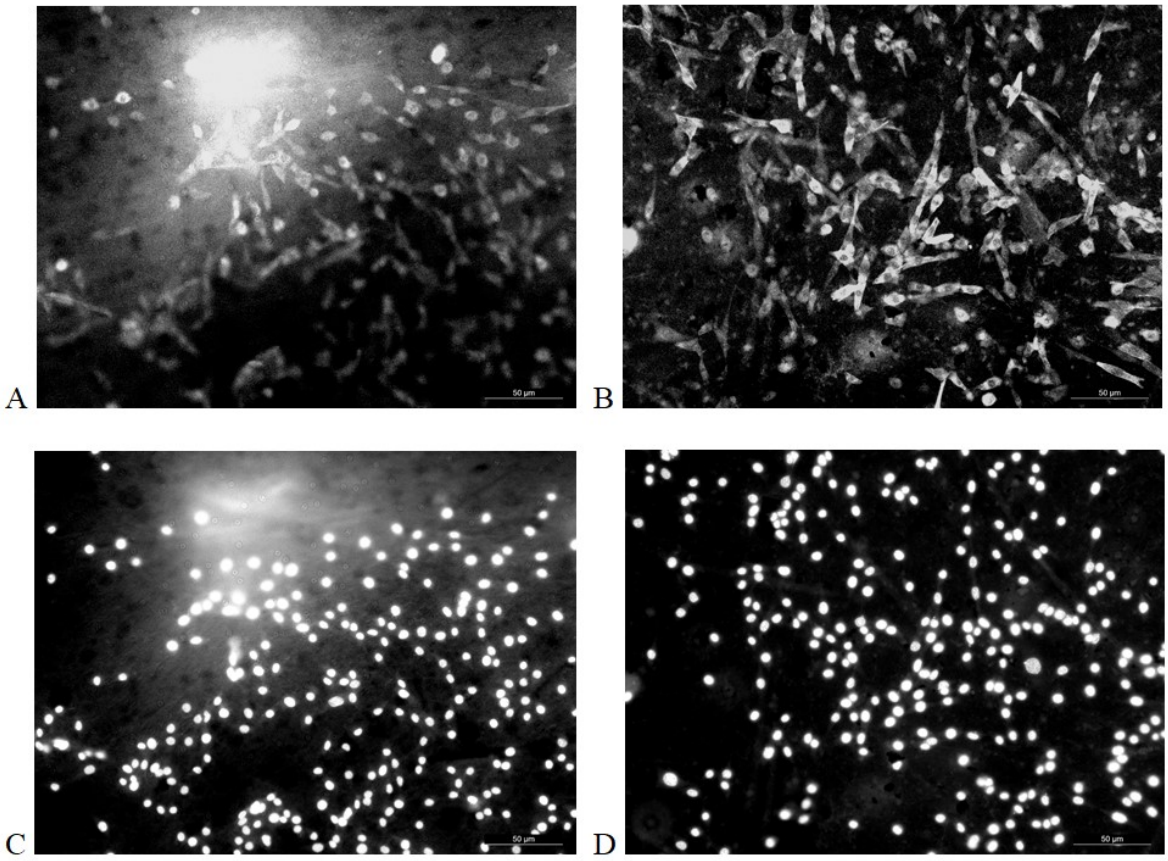

Figure 29 The fluorescence microscopy photographs of mouse fibroblasts (NIH/3T3) cultivated on the sample 1 in its original form with un-oriented fibers: (A, C) uncoated, (B, D) coated with PPY + Alb/Gel; (A, B) ActinRed – actin, (C, D) Hoechst – DNA.

Fibroblasts cultivated under static conditions on the surface of the isotropic PU mat are shown in Figure 29. Cells on the pristine sample, photographs of which are situated on the left, established preferably round-shaped cytoskeletons (29A) and also nuclei (29C). This morphology was expected in a view of results obtained in the sample 1 analysis (see Figure 20A, C). Isotropic samples, which were coated with PPy, albumin, and gelatin, are located on the right. Here, the cells took diverse shapes, from round to considerably elongate (29B) with a random direction because of the randomly oriented fibers in the substrate. Nuclei of these cells are classically rounded (29D).

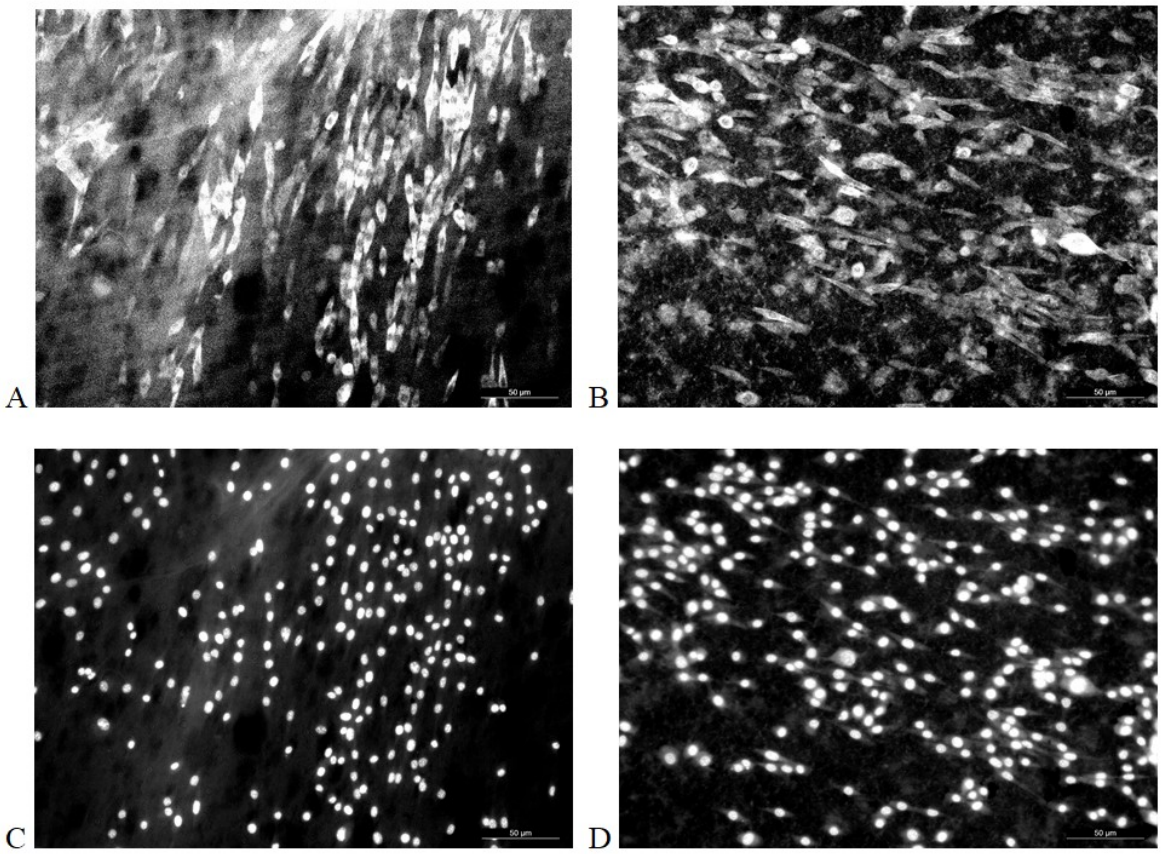

Figure 30 The fluorescence microscopy photographs of mouse fibroblasts (NIH/3T3) cultivated on the sample 1 in its modified form with oriented fibers: (A, C) uncoated, (B, D) coated with PPY + Alb/Gel; (A, B) ActinRed – actin, (C, D) Hoechst – DNA.

The morphology of fibroblasts cultivated under static conditions on the surface of the anisotropic PU mat with oriented fibers can be seen in Figure 30. Photographs of cells that grew on the oriented but un-coated sample are shown on the left. Their cytoskeletons (30A) and also most of the nuclei (30C) are elongated. However, the cell elongation effect is not as significant as in the sample 1 analysis (see Figure 20B, D) which was caused probably by a two days shorter time of cell cultivation. When focusing on the anisotropic sample treated with PPy, albumin, and gelatin, photographs of which are located on the right, the cells have taken various morphologies: round, lenticular, elongated (30B). In both cases, un-coated and coated, the cytoskeletons oriented strictly with the direction of fibers in the mats (30A vs. 30B). On the other hand, it seems that the surface treatment prevents the cell nuclei to elongate (30D) in comparison to the un-coated sample results (30C).

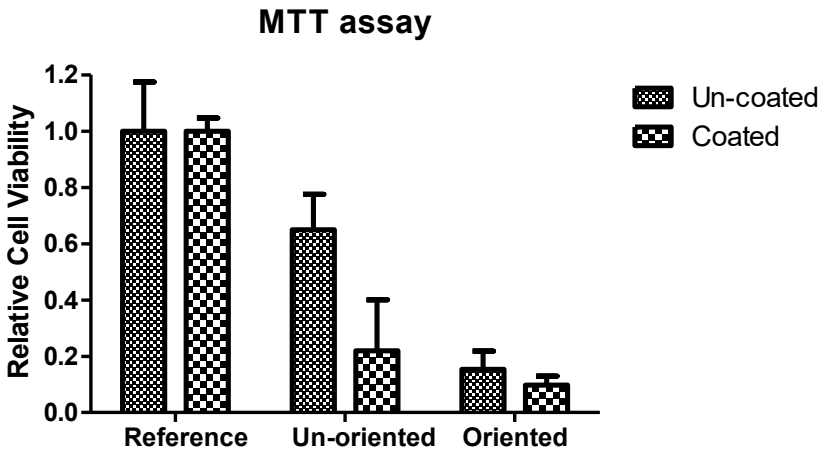

Figure 31 Results of MTT assay referring to the cytotoxicity of the samples under static cultivation conditions.

Cell quantification was performed by the MTT assay. Results are shown in Figure 31 where the number of viable cells is presented as the cell viability relative to the references which were the cell culture PS dishes clear or coated with PPy, albumin, and gelatin in the same way as the observed samples were. As the graph shows, the only sample comparable to the reference surface is the pristine isotropic un-oriented un-coated sample. It seems that the orientation of the fibers led to the reduction of viable cells, despite the previous results where it looked like the cells proliferated more on the oriented samples (see Figures 20, 23, and 26). The number of viable cells is also lower on the treated surfaces, but this was expected because of the poor cytocompatibility of PPy coatings (see Figures 27 and 28). However, it is still a success that albumin and gelatin enabled to increase the PPy cytocompatibility to a usable state.

Nevertheless, it should be known that several complications accompanied the MTT assay that could have affected the accuracy of the results. Firstly and most importantly, the dimethylsulfoxide (DMSO) used to complete the MTT assay dissolved all the PU samples and the PPy coating as well which unfavorably influenced the solution color, the absorbance of which was subsequently measured. Therefore, it was necessary to prepare blind samples with no cells seeded and measured results relate to them during the evaluation. Secondly, the number of repetitions was low, only three times for every column with the PU samples. Unfortunately, it was not possible to repeat the MTT assay with a higher repetition number because of the emergency state caused by the SARS-CoV-2 epidemic.

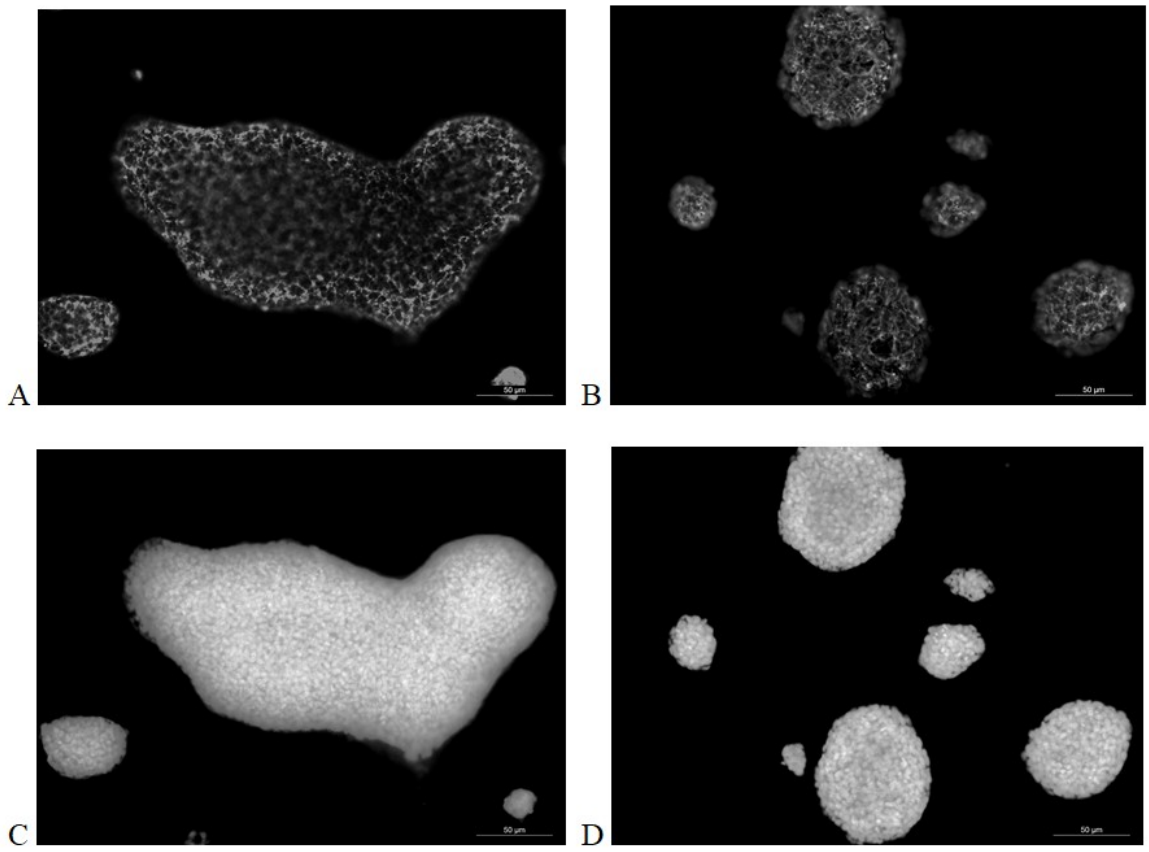

Figure 32 The fluorescence microscopy photographs of clusters of mouse embryonic stem cells R1 cultivated on the sample 1 in its original form with un-oriented fibers coated with: (A, C) Alb/Gel, (B, D) PPY + Alb/Gel; (A, B) ActinRed – actin, (C, D) Hoechst – DNA.

Mouse embryonic stem cells cultivated under static conditions on the surface of the isotropic PU mat are shown in Figure 32. For the sake of embryonic stem cells, all samples had to be coated with albumin and gelatin for higher compatibility. Photographs of cells on the sample including the PPy coating may be seen on the right (32B, D) whereas without the PPy on the left (32A, C). However, the cells behaved the same in both cases; there was no significant difference between the proliferation, cells managed to survive in an un-differentiated state (in the presence of medium containing LIF), and did not tend to grow apart on the surface at all, contrariwise they clustered.

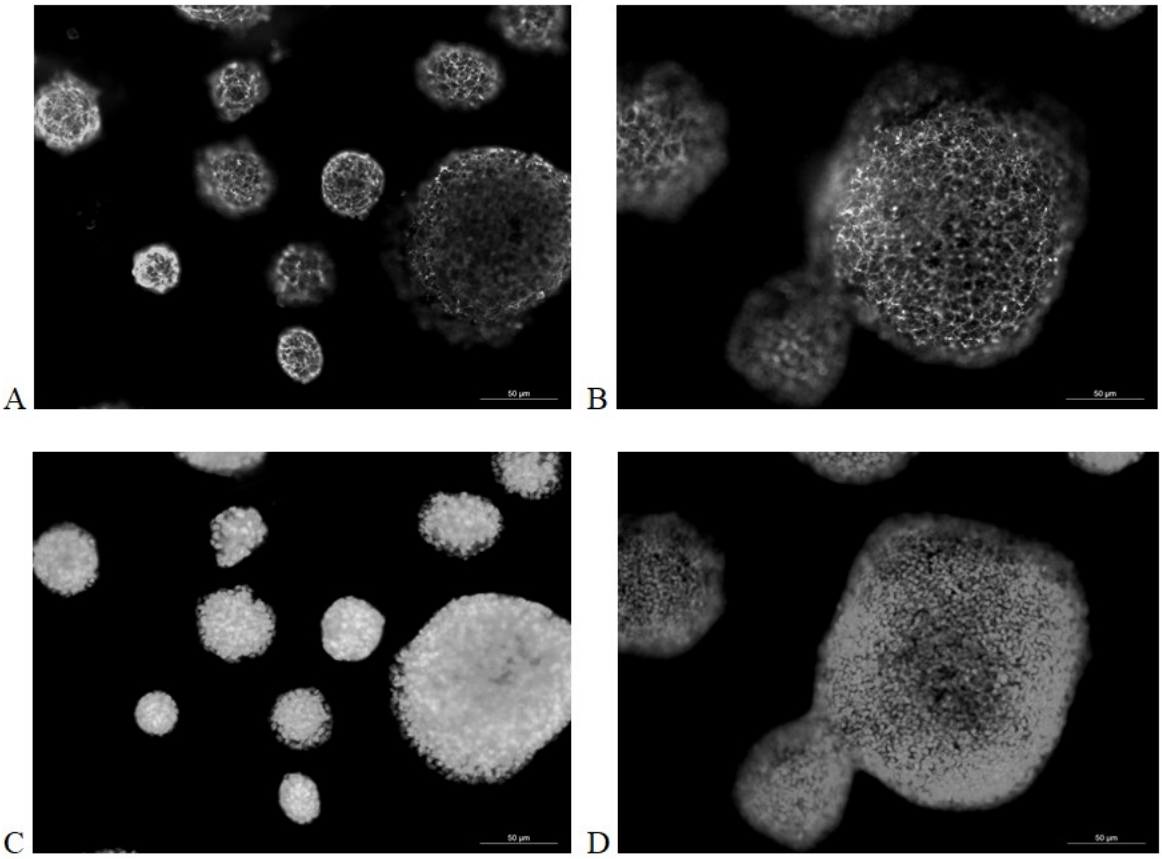

Figure 33 The fluorescence microscopy photographs of clusters of mouse embryonic stem cells R1 cultivated on the sample 1 in its modified form with oriented fibers coated with: (A, C) Alb/Gel, (B, D) PPY + Alb/Gel; (A, B) ActinRed – actin, (C, D) Hoechst – DNA.

The morphology of mouse embryonic stem cells cultivated under static conditions on the surface of the anisotropic PU mat with oriented fibers can be seen in Figure 33. For the sake of embryonic stem cells, all samples had to be coated with albumin and gelatin for higher compatibility. Cells behaved the same in both cases – on the sample without the PPy coating shown on the left (33A, C) either with the PPy coating located on the right (33B, D). There was no significant difference between the proliferation, cells managed to survive in an undifferentiated state (in the presence of medium containing LIF), and did not tend to grow apart on the surface at all, contrariwise they clustered. When comparing the fiber alignment (32 vs.33), the result seems quite similar.

8 DISCUSSION

Three types of electrospun PU nanofiber nonwoven mats were used as a subject of the experimental part of the master's thesis. The samples differ in used PUs, solvents, conductive additives, their ratios, and electric voltage during the electrospinning, which led to different basis weights of the nonwoven mats. Thermoplastic PU was stated as biocompatible by many studies, for example, Jaganathan et al. (2019). To verify this assertion and to get acquainted with the samples, the cytotoxicity of extracts was assessed. In summary, the results (Figures 18, 21, 24) showed only slight cytotoxicity, mild in maximum, no extract was neither moderate nor severe cytotoxic. Therefore, all three samples of PU electrospun mats may be considered cytocompatible as expected. However, 100 % extract of the sample 1 gave mild cytotoxicity close to the lower critic line (0.6 cell viability relative to the reference – cells cultivated in pure medium without the PU extracts). This outcome is sufficient on behalf of fibroblasts but for more susceptible embryonic stem cells not so much, hence it was necessary to ensure an improvement in the cytocompatibility of the sample before seeding the stem cells onto its surface. In agreement with Javaid et al. (2019), there always is a remained space for improvement of the biological behavior of petrochemical-based polyurethanes.

One of the many possible ways of biomaterial bioactivity improvement is to modify its topography so the surface imitates the natural cellular surroundings. The nanofibrous structure of electrospun mats is supposed to be excellent in mimicking the ECM. Nevertheless, attention should be paid to mechanical and structural anisotropy that increases with fiber alignment (Fee et al., 2016). The uniaxial orientation of fibers in the nonwoven mats is essential since most of the natural tissues are anisotropic (Hoque, 2017). Randomly-oriented fibers within the isotropic electrospun samples were aligned manually above 150 °C heat source with results shown in SEM images (Figures 19, 22, 25). The impact of the fiber alignment on the NIH/3T3 mouse fibroblast morphology is significant as demonstrated in all three samples (Figures 20, 23, 26). Fibroblasts cultivated on the isotropic sample with randomly-oriented fibers got rounded, lenticular, or stellate-patterned morphology, whereas cells that grew on the anisotropic sample with aligned fibers had taken prolonged spindle shapes in the exact direction of the fiber orientation. Many of these cells showed also elongated nuclei in comparison to the rounded cell nuclei on the pristine un-oriented sample. Cell cultivation on the aligned fibers also results in higher cell proliferation and more even distribution of cells on the surface. These results

confirm the claim of Yin et al. (2010), that cells respond to fiber orientation with morphological changes, cytoskeletal rearrangements, and nuclear elongation. The explanation probably lies in contact guidance and cell-matrix interactions, whose amount and distribution are influenced by the nanofiber alignment, and that plays an important role in regulating cell functions, including mentioned proliferation and migration (distribution).

Another PU bioactivity improvement manner was surface coating with an electrically conductive polymer that, according to Gajendiran et al. (2017), should help cells communicate with each other and hence improve cell growth. Specifically, polypyrrole (PPy) coatings were synthesized using two different oxidants: ammonium persulfate or ferric chloride. Although many studies stated PPy as cytocompatible material (Wang et al., 2004; Ravichandran et al., 2010) or low-cytotoxic (Hsu et al., 2008), cell death of NIH/3T3 mouse fibroblasts cultivated on PPy surfaces in this thesis showed otherwise (Figures 27A, 28A). When comparing the cytocompatibility of the two types of observed PPy coatings with different oxidants, the results seem similarly bad. Under Ravichandran et al. (2010), the major limitation of the PPy cytocompatibility lies in its hydrophobicity that decreases the successful entrapping of proteins from the medium to the surface. This restriction may be influenced by using other oxidants and synthesis conditions, or there is also another path, which was carried out in this analysis, the surface coating with bio-substances that change the biological activity of the treated surface. (Tallawi et al., 2015) As the results show (Figures 27B–D, 28B–D), coating with albumin or gelatin increased the PPy biocompatibility considerably, but surprisingly, the combination of both albumin and gelatin together provided an even more significant improvement in cell proliferation. These positive results, which have likely been achieved due to the functional carboxyl and amino groups of proteins and peptides, are in compliance with studies of Wu et al. (2019) and Van Vlierberghe et al., (2011) that confirm the biocompatibility and cell-interactive properties of albumin and gelatin.

After the cytocompatibility of PPy overlay with albumin and gelatin on the surface of reference PS tissue dishes was confirmed, the next step was the coating of the electrospun mats. Despite its mild-cytotoxic concentrated extract (Figure 18), the sample 1 was evaluated as the most appropriate representative of the three observed electrospun PU nonwoven mats for following experiments due to a cohesion and rift resistance which is essential during the fiber orientation process, the most significant impact of fiber alignment on the fibroblast morphology (Figure 20), and the suitable mechanical properties, such as

elasticity which is important in the cultivation under tensile-dynamic conditions. Of the two types of observed PPy coatings, the PPy with $FeCl_3$ used as an oxidant was chosen due to its higher electrical conductivity and less powdering. The surface bioactivity was secured by coating with both albumin and gelatin together due to the effectiveness of this combination (Figure 28).

The way in which selected surface coatings affects the impact of fiber alignment on the mouse fibroblast cell line NIH/3T3 was observed by a fluorescence microscope (Figures 29, 30). As expected, cells cultivated on the pristine sample with un-coated randomly-oriented fibers established preferably round-shaped cytoskeletons and also nuclei. When the PPy, albumin, and gelatin coatings were applied, cell cytoskeletons demonstrated various shapes, from round to considerably elongate with a random direction because of the randomly-oriented fibers in the substrate; nuclei of these cells were classically rounded. Focusing now on the oriented but un-coated samples, most of the cells had elongated cytoskeletons and also most of the nuclei. In this case, the surface PPy, albumin, and gelatin coatings again led to various cell morphologies: round, lenticular, spindle-shaped; however, cell nuclei did not elongate and remained rounded. In both cases, un-coated and coated, the cells oriented strictly with the direction of fibers in the mats. In summary, the surface coatings significantly influenced cell morphology and prevented nuclei elongation, nevertheless, cell orientation maintained still according to fiber orientation.

Since all of these samples had the same culture surface area (22 × 22) mm, it was also possible to perform cell quantification using the MTT assay. The results (Figure 31) determined that the only sample that could compare to the reference surfaces, which were the cell culture PS dishes clear or coated, is the pristine isotropic un-oriented un-coated sample. It seems that the orientation of the fibers led to the reduction of viable cells, despite the previous results whereby guesstimate it seemed that the fibroblasts proliferated more on the oriented samples (Figure 20). The number of viable cells is also lower on the treated surfaces, but this was kind of expected because of the poor cytocompatibility of PPy coatings (Figure 28). Nevertheless, it is still a success that albumin and gelatin enabled to increase the PPy cytocompatibility up to a usable state. However, it should be known that several complications accompanied the MTT assay that could have affected the accuracy of the results. Firstly and most importantly, the dimethylsulfoxide (DMSO) used to complete the MTT assay dissolved all the PU samples and the PPy coating as well

which unfavorably influenced the solution color, the absorbance of which was subsequently measured. Therefore, it was necessary to prepare blind samples with no cells seeded and measured results relate to them during the evaluation. Secondly, the number of repetitions was low, only three times for every group with the PU samples. Unfortunately, it was not possible to repeat the MTT assay with a higher repetition number or to perform another quantification method, for example, ATP assay, because of the emergency state caused by the SARS-CoV-2 epidemic.

Furthermore, the R1 mouse embryonic stem cell line was cultivated on the surface of these electrospun PU mats (Figures 32, 33). For the sake of the cells, all samples had to be coated with albumin and gelatin for higher surface bioactivity. The embryonic stem cells behaved the same in all observed samples – there was no significant difference between the proliferation, cells managed to survive in an undifferentiated state (in the presence of medium containing LIF), and did not tend to grow apart on the surface at all, contrariwise they clustered. This means that neither the fiber orientation nor the PPy coating has a visible impact on the morphology of the embryonic stem cell in the undifferentiated state.

However, all aforementioned results were obtained from cell cultivation under static conditions and, as it is well known, the static cultivation is neglecting the pivotal role of mechanical stimulations that are a matter of fact in the natural tissue environment and may act as an active force for directing cellular morphology and functions including stem cell differentiation. (Nokhbatolfoghahaei et al., 2020) For this purpose, a bioreactor with a 3D printed inner attachment frame (Figure 17) was used in this master's thesis to apply hydrodynamic shear stress together with a tensile strain to a scaffold with cells. This should let manifest the effect of mechanical anisotropy of scaffold on cell behavior, similarly as was done in studies of Lee et al. (2005) or Rosenfeld et al. (2016). Furthermore, it was planned to undergo cultivation with an electric current applied which should help to show the impact of electrically conductive PPy coatings. According to Gajendiran et al. (2017), organic conductive polymers affect cell activities, improve cell growth, help cells communicate with each other, and can control stem cell differentiation under external electrical stimuli. Some of the latest studies that prove the effectiveness of electric current applied on (neural) stem cells were implemented by Yan et al. (2020) or Shrestha et al. (2019). Unfortunately, it was not possible to complete the cultivation under tensile-dynamic and electric conditions because of both the restriction related to SARS-CoV-2 pandemic and bioreactor software issues.

CONCLUSION

The main topic of this master's thesis was the cytocompatibility of polymeric biomaterials and material properties and modifications affecting it. The attention of the experimental part was particularly driven to electrospun polyurethane (PU) nanofiber nonwoven mats. All three tested PU samples exhibited only slight and mild cytotoxicity, so they may be considered cytocompatible as expected. However, a space for improvement of the bioactivity remained, especially in terms of their surface properties. Thus, several modifications were suggested and implemented. First, the uniaxial orientation of fibers in the PU mats was provided to mimic structural and mechanical anisotropy of the natural extracellular matrix. The impact of the fiber alignment on the morphology of mouse fibroblasts was significant. Not only cytoskeletons but also cell nuclei demonstrated prolonged shapes with a uniform orientation strictly along the fibers. Second, the samples were coated with two types of polypyrrole-based coatings (PPy) in order to enhance electrical conductivity. Although the PPy was supposed to improve cell growth, the results showed conversely the cell death of mouse fibroblasts in both cases. Therefore, the third surface modification was carried out to increase the cytocompatibility. As the results manifest, the most significant improvement in cell proliferation was achieved with a combination of albumin and gelatin applied together. After the application of these coatings on the PU samples, mouse fibroblasts were prevented from cytoskeleton and nuclei elongation but the orientation of the cells maintained still according to the fiber direction. In the case of mouse embryonic stem cells, neither the fiber alignment nor the PPy coating had a visible impact on the clusters of the stem cells. Furthermore, the quantification of fibroblasts was performed but sadly, it was found that the MTT assay is not an entirely suitable method because dimethylsulfoxide dissolved the PU samples and the PPy coatings which led to the results against expectations. Another objective of the analysis was to supplement the knowledge about the influence of the PU samples and their modifications on the cytocompatibility under tensile-dynamic or/and electric cultivation conditions. Unfortunately, it was not possible to fully complete these experiments because of both the restriction related to SARS-CoV-2 pandemic and bioreactor software issues. Even though the aims were not completely accomplished, the results of this master's thesis may help in further deepening of current knowledge about the impact of polymeric surface properties on cell behavior and hence contribute to scaffold design optimization on behalf of specific tissue growth achievement.

BIBLIOGRAPHY

Adamow, A., Szukalski, A., Sznitko, L., Persano, L., Pisignano, D., Camposeo, A., & Mysliwiec, J. (2020). Electrically controlled white laser emission through liquid crystal/polymer multiphases. Light: Science & Applications, 9(1). doi: 10.1038/s41377-020-0252-9

Bassett, C., Pawluk, R., & Becker, R. (1964). Effects of electric currents on bone *in vivo*. Nature, 204(4959), 652-654. doi: 10.1038/204652a0

Bonartsev, A., Bonartseva, G., Reshetov, I., Kirpichnikov, M., & Shaitan, K. (2019). Application of Polyhydroxyalkanoates in Medicine and the Biological Activity of Natural Poly(3-Hydroxybutyrate). Acta Naturae, 11(2), 4-16. doi: 10.32607/20758251-2019-11-2-4-16

Bose, S., Robertson, S., & Bandyopadhyay, A. (2018). Surface modification of biomaterials and biomedical devices using additive manufacturing. Acta Biomaterialia, 66, 6-22. doi: 10.1016/j.actbio.2017.11.003

Bousalem, S., Yassar, A., Basinska, T., Miksa, B., Slomkowski, S., Azioune, A., & Chehimi, M. (2003). Synthesis, characterization and biomedical applications of functionalized polypyrrole-coated polystyrene latex particles. Polymers For Advanced Technologies, 14(11-12), 820-825. doi: 10.1002/pat.401

Bronzino, J., & Peterson, D. (2015). Biomedical Engineering Fundamentals (4th ed.). Boca Raton: CRC Press. ISBN 978-1-4398-2519-8

Bursac, N., Parker, K., Iravanian, S., & Tung, L. (2002). Cardiomyocyte Cultures With Controlled Macroscopic Anisotropy. Circulation Research, 91(12). doi: 10.1161/01.res.0000047530.88338.eb

Castner, D. (2017). Biomedical surface analysis: Evolution and future directions (Review). Biointerphases, 12(2), 02C301. doi: 10.1116/1.4982169

Chauhan, N., Jangid, N., Kaur, N., Rathore, B., Gholipourmalekabadi, M., & Mozafari, M. (2019). Medicines: Polymers for. In M. Mishra, Encyclopedia of Polymer Applications (pp. 1679-1691). Boca Raton: CRC Press. doi: 10.1201/9781351019422-140000298

Cho, H., Kim, T., Hong, T., & Park, Y. (2020). Ratchet-integrated pneumatic actuator (RIPA): a large-stroke soft linear actuator inspired by sarcomere muscle contraction. Bioinspiration & Biomimetics, 15(3), 036011. doi: 10.1088/1748-3190/ab7762

Curtis, A., Forrester, J., McInnes, C., & Lawrie, F. (1983). Adhesion of cells to polystyrene surfaces. The Journal Of Cell Biology, 97(5), 1500-1506. doi: 10.1083/jcb.97.5.1500

Fee, T., Downs, C., Eberhardt, A., Zhou, Y., & Berry, J. (2016). Image-based quantification of fiber alignment within electrospun tissue engineering scaffolds is related to mechanical anisotropy. Journal Of Biomedical Materials Research Part A, 104(7), 1680-1686. doi: 10.1002/jbm.a.35697

Fonner, J., Forciniti, L., Nguyen, H., Byrne, J., Kou, Y., Syeda-Nawaz, J., & Schmidt, C. (2008). Biocompatibility implications of polypyrrole synthesis techniques. Biomedical Materials, 3(3), 034124. doi: 10.1088/1748-6041/3/3/034124

Fu, J., Wang, Y., Yang, M., Desai, R., Yu, X., Liu, Z., & Chen, C. (2010). Mechanical regulation of cell function with geometrically modulated elastomeric substrates. Nature Methods, 7(9), 733-736. doi: 10.1038/nmeth.1487

Gajendiran, M., Choi, J., Kim, S., Kim, K., Shin, H., Koo, H., & Kim, K. (2017). Conductive biomaterials for tissue engineering applications. Journal Of Industrial And Engineering Chemistry, 51, 12-26. doi: 10.1016/j.jiec.2017.02.031

Gogoi, D., Choudhury, A., Chutia, J., Pal, A., Khan, M., & Choudhury, M. et al. (2014). Development of advanced antimicrobial and sterilized plasma polypropylene grafted muga (antheraea assama) silk as suture biomaterial. Biopolymers, 101(4), 355-365. doi: 10.1002/bip.22369

Henriques, B., Sampaio, M., Buciumeanu, M., Souza, J., Gomes, J., Silva, F., & Carvalho, O. (2017). Laser surface structuring of Ti6Al4V substrates for adhesion enhancement in Ti6Al4V-PEEK joints. Materials Science And Engineering: C, 79, 177-184. doi: 10.1016/j.msec.2017.04.157

Hirsh, S., McKenzie, D., Nosworthy, N., Denman, J., Sezerman, O., & Bilek, M. (2013). The Vroman effect: Competitive protein exchange with dynamic multilayer protein aggregates. Colloids And Surfaces B: Biointerfaces, 103, 395-404. doi: 10.1016/j.colsurfb.2012.10.039

Hoque, M. (2017). Robust formulation for the design of tissue engineering scaffolds: A comprehensive study on structural anisotropy, viscoelasticity and degradation of 3D scaffolds fabricated with customized desktop robot based rapid prototyping (DRBRP)

system. Materials Science And Engineering: C, 72, 433-443. doi: 10.1016/j.msec.2016.11.019

Horbett, T. (2018). Fibrinogen adsorption to biomaterials. Journal Of Biomedical Materials Research Part A, 106(10), 2777-2788. doi: 10.1002/jbm.a.36460

Hsu, C., Zhang, L., Peng, H., Travas-Sejdic, J., & Kilmartin, P. (2008). Scavenging of DPPH free radicals by polypyrrole powders of varying levels of overoxidation and/or reduction. Synthetic Metals, 158(21-24), 946-952. doi: 10.1016/j.synthmet.2008.06.017

Humpolíček, P., Radaszkiewicz, K., Kašpárková, V., Stejskal, J., Trchová, M., & Kuceková, Z. et al. (2015). Stem cell differentiation on conducting polyaniline. RSC Advances, 5(84), 68796-68805. doi: 10.1039/c5ra12218j

Imbeau, J. What is the extra-cellular matrix (ECM) – figure [online] available from http://www.dr-jacques-imbeau.com/extracellularmatrix.html, [cit. 02/22/2020]

Ishigami, T., Nii, Y., Ohmukai, Y., Rajabzadeh, S., & Matsuyama, H. (2014). Solidification Behavior of Polymer Solution during Membrane Preparation by Thermally Induced Phase Separation. Membranes, 4(1), 113-122. doi: 10.3390/membranes4010113

Jaganathan, S., Prasath Mani, M., Ayyar, M., & Rathanasamy, R. (2019). Biomimetic electrospun polyurethane matrix composites with tailor made properties for bone tissue engineering scaffolds. Polymer Testing, 78, 105955. doi: 10.1016/j.polymertesting.2019.105955

Javaid, M., Zia, K., Khera, R., Jabeen, S., Mumtaz, I., & Younis, M. et al. (2019). Evaluation of cytotoxicity, hemocompatibility and spectral studies of chitosan assisted polyurethanes prepared with various diisocyanates. International Journal Of Biological Macromolecules, 129, 116-126. doi: 10.1016/j.ijbiomac.2019.01.084

Ke, Y., Liu, C., Zhang, X., Xiao, M., & Wu, G. (2017). Surface Modification of Polyhydroxyalkanoates toward Enhancing Cell Compatibility and Antibacterial Activity. Macromolecular Materials And Engineering, 302(11), 1700258. doi: 10.1002/mame.201700258

Kersten, R., van Gaalen, S., de Gast, A., & Öner, F. (2015). Polyetheretherketone (PEEK) cages in cervical applications: a systematic review. The Spine Journal, 15(6), 1446-1460. doi: 10.1016/j.spinee.2013.08.030

Kubová, O., Švorčík, V., Heitz, J., Moritz, S., Romanin, C., Matějka, P., & Macková, A. (2007). Characterization and cytocompatibility of carbon layers prepared by photo-induced chemical vapor deposition. Thin Solid Films, 515(17), 6765-6772. doi: 10.1016/j.tsf.2007.02.014

Kulkarni, M., Junkar, I., Humpolíček, P., Capáková, Z., Radaszkiewicz, K., & Mikušová, N. et al. (2017). Interaction of nanostructured TiO2 biointerfaces with stem cells and biofilm-forming bacteria. Materials Science And Engineering: C, 77, 500-507. doi: 10.1016/j.

Kupka, V. (2015). Modification of Polyurethanes by Biologically Active Substances. (Doctoral dissertation, 98 p.) Faculty of Chemistry, University of Technology, Brno, Czech Republic.

Lee, C., Shin, H., Cho, I., Kang, Y., Kim, I., Park, K., & Shin, J. (2005). Nanofiber alignment and direction of mechanical strain affect the ECM production of human ACL fibroblast. Biomaterials, 26(11), 1261-1270. doi: 10.1016/j.biomaterials.2004.04.037

Lis-Bartos, A., Smieszek, A., Frańczyk, K., & Marycz, K. (2018). Fabrication, Characterization, and Cytotoxicity of Thermoplastic Polyurethane/Poly(lactic acid) Material Using Human Adipose Derived Mesenchymal Stromal Stem Cells (hASCs). Polymers, 10(10), 1073. doi: 10.3390/polym10101073

Ma, P. (2008). Biomimetic materials for tissue engineering. Advanced Drug Delivery Reviews, 60(2), 184-198. doi: 10.1016/j.addr.2007.08.041

Maitz, M., Martins, M., Grabow, N., Matschegewski, C., Huang, N., & Chaikof, E. et al. (2019). The blood compatibility challenge. Part 4: Surface modification for hemocompatible materials: Passive and active approaches to guide blood-material interactions. Acta Biomaterialia, 94, 33-43. doi: 10.1016/j.actbio.2019.06.019

Mani, M., Jaganathan, S., Khudzari, A., & Prabhakaran, P. (2019). Development of advanced nanostructured polyurethane composites comprising hybrid fillers with enhanced properties for regenerative medicine. Polymer Testing, 73, 12-20. doi: 10.1016/j.polymertesting.2018.11.014

Mani, M., Jaganathan, S., & Ismail, A. (2018). Appraisal of electrospun textile scaffold comprising polyurethane decorated with ginger nanofibers for wound healing applications. Journal Of Industrial Textiles, 49(5), 648-662. doi: 10.1177/1528083718795911

Maszybrocka, J., Stwora, A., Gapiński, B., Skrabalak, G., & Karolus, M. (2017). Morphology and surface topography of Ti6Al4V lattice structure fabricated by selective laser sintering. Bulletin Of The Polish Academy Of Sciences Technical Sciences, 65(1), 85-92. doi: 10.1515/bpasts-2017-0011msec.2017.03.174

Michaljaničová, I., Slepička, P., Rimpelová, S., Slepičková Kasálková, N., & Švorčík, V. (2016). Regular pattern formation on surface of aromatic polymers and its cytocompatibility. Applied Surface Science, 370, 131-141. doi: 10.1016/j.apsusc.2016.02.160

Mitchell, G., & Tojeira, A. (2013). Role of Anisotropy in Tissue Engineering. Procedia Engineering, 59, 117-125. doi: 10.1016/j.proeng.2013.05.100

Murugan, R., & Ramakrishna, S. (2007). Design Strategies of Tissue Engineering Scaffolds with Controlled Fiber Orientation. Tissue Engineering, 13(8), 1845-1866. doi: 10.1089/ten.2006.0078

Nagy, A., Rossant, J., Nagy, R., Abramow-Newerly, W., & Roder, J. (1993). Derivation of completely cell culture-derived mice from early-passage embryonic stem cells. Proceedings Of The National Academy Of Sciences, 90(18), 8424-8428. doi: 10.1073/pnas.90.18.8424

Nikkhah, M., Edalat, F., Manoucheri, S., & Khademhosseini, A. (2012). Engineering microscale topographies to control the cell–substrate interface. Biomaterials, 33(21), 5230-5246. doi: 10.1016/j.biomaterials.2012.03.079

Nokhbatolfoghahaei, H., Bohlouli, M., Paknejad, Z., R. Rad, M., M. Amirabad, L., & Salehi-Nik, N. et al. (2020). Bioreactor cultivation condition for engineered bone tissue: Effect of various bioreactor designs on extra cellular matrix synthesis. Journal Of Biomedical Materials Research Part A. doi: 10.1002/jbm.a.36932

Padmapriya, S., Sudha, V., & Harinipriya, S. (2019). Paratacamite doped polypyrrole for effective hydrogen storage. International Journal Of Hydrogen Energy, 44(13), 6773-6786. doi: 10.1016/j.ijhydene.2019.01.191

Paital, S., & Dahotre, N. (2008). Review of laser based biomimetic and bioactive Ca–P coatings. Materials Science And Technology, 24(9), 1144-1161. doi: 10.1179/174328408x341825

Pfaff, H., & Ing, D. (2000). Ceramic Component Failure and the Role of Proof Testing. Clinical Orthopaedics And Related Research, 379, 29-33. doi: 10.1097/00003086-200010000-00005

Puleo, D., & Bizios, R. (2009). Biological Interactions on Materials Surfaces. New York: Springer. ISBN 978-0-387-98160-4

Qiu, L., Lai, W., Stumpo, D., & Blackshear, P. (2016). Mouse Embryonic Fibroblast Cell Culture and Stimulation. BIO-PROTOCOL, 6(13). doi: 10.21769/bioprotoc.1859

Ravichandran, R., Sundarrajan, S., Venugopal, J., Mukherjee, S., & Ramakrishna, S. (2010). Applications of conducting polymers and their issues in biomedical engineering. Journal Of The Royal Society Interface, 7(suppl_5). doi: 10.1098/rsif.2010.0120.focus

Rebollar, E., Frischauf, I., Olbrich, M., Peterbauer, T., Hering, S., & Preiner, J. et al. (2008). Proliferation of aligned mammalian cells on laser-nanostructured polystyrene. Biomaterials, 29(12), 1796-1806. doi: 10.1016/j.biomaterials.2007.12.039

Rosenfeld, D., Landau, S., Shandalov, Y., Raindel, N., Freiman, A., & Shor, E. et al. (2016). Morphogenesis of 3D vascular networks is regulated by tensile forces. Proceedings Of The National Academy Of Sciences, 113(12), 3215-3220. doi: 10.1073/pnas.1522273113

Schmalz, G., & Bindslev, D. (2009). Biocompatibility of dental materials (p. 379). Berlin: Springer-Verlag Berlin Heidelberg. doi: 10.1007/978-3-540-77782-3

Seifert, B., Mihanetzis, G., Groth, T., Albrecht, W., Richau, K., & Missirlis, Y. et al. (2002). Polyetherimide: A New Membrane-Forming Polymer for Biomedical Applications. Artificial Organs, 26(2), 189-199. doi: 10.1046/j.1525-1594.2002.06876.x

Shrestha, B., Shrestha, S., Baral, E., Lee, J., Kim, B., Park, C., & Kim, C. (2019). π-Conjugated polyaniline-assisted flexible titania nanotubes with controlled surface morphology as regenerative medicine in nerve cell growth. Chemical Engineering Journal, 360, 701-713. doi: 10.1016/j.cej.2018.12.027

Slepička, P., Slepičková Kasálková, N., Bačáková, L., Kolská, Z., & Švorčík, V. (2012). Enhancement of Polymer Cytocompatibility by Nanostructuring of Polymer Surface. Journal Of Nanomaterials, 2012, 1-17. doi: 10.1155/2012/527403

Tallawi, M., Rosellini, E., Barbani, N., Cascone, M., Rai, R., Saint-Pierre, G., & Boccaccini, A. (2015). Strategies for the chemical and biological functionalization of

scaffolds for cardiac tissue engineering: a review. Journal Of The Royal Society Interface, 12(108), 20150254. doi: 10.1098/rsif.2015.0254

Thévenot, D., Toth, K., Durst, R., & Wilson, G. (2001). Electrochemical biosensors: recommended definitions and classification. Biosensors And Bioelectronics, 16(1-2), 121-131. doi: 10.1016/s0956-5663(01)00115-4

Unadkat, H., Hulsman, M., Cornelissen, K., Papenburg, B., Truckenmuller, R., & Carpenter, A. et al. (2011). An algorithm-based topographical biomaterials library to instruct cell fate. Proceedings Of The National Academy Of Sciences, 108(40), 16565-16570. doi: 10.1073/pnas.1109861108

Van Vlierberghe, S., Vanderleyden, E., Boterberg, V., & Dubruel, P. (2011). Gelatin Functionalization of Biomaterial Surfaces: Strategies for Immobilization and Visualization. Polymers, 3(1), 114-130. doi: 10.3390/polym3010114

Vogler, E. (1998). Structure and reactivity of water at biomaterial surfaces. Advances In Colloid And Interface Science, 74(1-3), 69-117. doi: 10.1016/s0001-8686(97)00040-7

Vroman, L., & Adams, A. (1969). Findings with the recording ellipsometer suggesting rapid exchange of specific plasma proteins at liquid/solid interfaces. Surface Science, 16, 438-446. doi: 10.1016/0039-6028(69)90037-5

Waisman, A., Sevlever, F., Elías Costa, M., Cosentino, M., Miriuka, S., Ventura, A., & Guberman, A. (2019). Cell cycle dynamics of mouse embryonic stem cells in the ground state and during transition to formative pluripotency. Scientific Reports, 9(1). doi: 10.1038/s41598-019-44537-0

Wang, X., Gu, X., Yuan, C., Chen, S., Zhang, P., & Zhang, T. et al. (2004). Evaluation of biocompatibility of polypyrrole *in vitro* and *in vivo*. Journal Of Biomedical Materials Research, 68A(3), 411-422. doi: 10.1002/jbm.a.20065

Watson, R. (2002). ABC of antithrombotic therapy: Antithrombotic therapy in acute coronary syndromes. BMJ, 325(7376), 1348-1351. doi: 10.1136/bmj.325.7376.1348

Wilson, C., Clegg, R., Leavesley, D., & Pearcy, M. (2005). Mediation of Biomaterial–Cell Interactions by Adsorbed Proteins: A Review. Tissue Engineering, 11(1-2), 1-18. doi: 10.1089/ten.2005.11.1

Woo, K., Chen, V., & Ma, P. (2003). Nano-fibrous scaffolding architecture selectively enhances protein adsorption contributing to cell attachment. Journal Of Biomedical Materials Research, 67A(2), 531-537. doi: 10.1002/jbm.a.10098

Wrzecionko, E., Minařík, A., Smolka, P., Minařík, M., Humpolíček, P., & Rejmontová, P. et al. (2017). Variations of Polymer Porous Surface Structures via the Time-Sequenced Dosing of Mixed Solvents. ACS Applied Materials & Interfaces, 9(7), 6472-6481. doi: 10.1021/acsami.6b15774

Wu, M., Zhong, C., Deng, Y., Zhang, Q., Zhang, X., & Zhao, X. (2019). Resveratrol loaded glycyrrhizic acid-conjugated human serum albumin nanoparticles for tail vein injection II: pharmacokinetics, tissue distribution and bioavailability. Drug Delivery, 27(1), 81-90. doi: 10.1080/10717544.2019.1704944

Yan, H., Wang, Y., Li, L., Zhou, X., Shi, X., Wei, Y., & Zhang, P. (2020). A micropatterned conductive electrospun nanofiber mesh combined with electrical stimulation for synergistically enhancing differentiation of rat neural stem cells. Journal Of Materials Chemistry B, 8(13), 2673-2688. doi: 10.1039/c9tb02864a

Yin, Z., Chen, X., Chen, J., Shen, W., Hieu Nguyen, T., Gao, L., & Ouyang, H. (2010). The regulation of tendon stem cell differentiation by the alignment of nanofibers. Biomaterials, 31(8), 2163-2175. doi: 10.1016/j.biomaterials.2009.11.083

LIST OF ABBREVIATIONS

AFM	Atomic force microscopy
Alb	Albumin
APS	Ammonium persulfate
DMF	Dimethylformamide
DNA	Deoxyribonucleic acid
ECM	Extracellular matrix
ETH	2-ethoxyethanol
FAC	Focal adhesion complex
FDM	Fused deposition modeling
Gel	Gelatin
GTP	Guanosine triphosphate
hLF	Human ligament fibroblast
hTSPC	Human tendon stem/progenitor cell
LCPs	Liquid crystal polymers
MIBK	Methylisobutylketon
MSC	Mesenchymal stem cell
MTT	3-(4,5-dimethylthiazol-2-yl)-2,5-diphenyltetrazolium bromide
PBS	Phosphate buffered saline
PCL	Polycaprolactone
PDMS	Polydimethylsiloxane
PE	Polyethylene
PGA	Polyglycolic acid
PHB	Poly(3-hydroxybutyrate)
PLA	Polylactic acid
PLGA	Poly(lactic-co-glycolic) acid

PLLA	Poly(L-lactic acid)
PMMA	Polymethylemethacrylate
PP	Polypropylene
PPy	Polypyrrole
PS	Polystyrene
PTFE	Polytetrafluoroethylene
PU	Polyurethane
PVC	Polyvinylchloride
RGD	Arginine, Glycine, and Aspartate (Arg-Gly-Asp)
SEM	Scanning electron microscopy
TAEB	Tetraethylammoniumbromide
THF	Tetrahydrofuran
UHMWPE	Ultra-high molecular weight polyethylene

LIST OF FIGURES

Figure 1 Application of UHMWPE in (a) hip joint and (b) knee joint prostheses. (Paita & Dahotre, 2008) 11

Figure 2 A schematic illustration of a cell anchored in its natural environment. (Imbeau, online) 16

Figure 3 Schematic illustrations of three possible protein exchange processes as an interpretation of the Vroman effect. (Hirsh et al., 2013) 20

Figure 4 AFM images with the schematic illustration of the protein exchange process via transient complex. (Hirsh et al., 2013) 20

Figure 5 Morphology of human MSCs on different PLA chips. (A–D): Elongated cells aligned according to topographic features (fluorescence microscope, green - actin, red - nucleus, scale: 90 μm). (E–H): Cells with different morphologies (SEM scanning electron microscope, scale: 90 μm.) (I–J): Morphology of rounded cells on two different chips, which differ in cell membrane structure. (SEM, scale: 10 μm.) (Unadkat et al., 2011) 24

Figure 6 (a): PDMS micromolded elastomeric micropost arrays with three different heights in response to the horizontal traction force. (b): Dependence of the micropost deflection on the horizontal traction force. (c): Dependence of the nominal spring constant on the micropost height. (d–f): Human MSCs cultivated on the microposts of different heights and rigidity. SEM, scale: 100 μm (top), 50 μm (bottom left), 30 μm (bottom center) and 10 μm (bottom right). (Fu et al., 2010) 26

Figure 7 A schematic illustration of cell–ECM mechanotransduction where cells respond via integrin signaling to high and low stresses based on underlying substrate stiffness. (Arvind & Huang, 2017) 29

Figure 8 Morphological changes of hTSPCs growing on the scaffolds with (A, C, E) aligned fibers or (B, D, F) randomly-oriented fibers. (A, B): SEM images of hTSPCs. (C, D): High magnifications of boxed areas in A, B. (Arrow in C): filament-like structures. (E, F): Confocal micrographs of CFDA-stained hTSPCs. (G): Cell proliferation on the scaffolds with aligned fibers or randomly-oriented fibers. Scale bars: 30 μm (A, B), 5 μm (C, D), and 50 μm (E, F). (Yin et al., 2010) 32

Figure 9 The load-strain curves of (F) the electrospun PLLA scaffolds with aligned and randomly-oriented fibers, (G) aligned scaffold (upper) and rabbit native tendon (lower), which are composed of toe (I), linear (II), and failure (III) regions. (Yin et al., 2010) 33

Figure 10 The orientation of vessel-like structures varying depending on the form of forces applied: cyclic stretching resulted in diagonal vessels, free-floating scaffolds in randomly orientated vessels, and static stretching in vertical vessels. Scale bars: 250 μm. (Rosenfeld et al., 2016) 34

Figure 11 Morphology of fibroblasts grown on (A, B, C) aligned nanofibers: (A) before stretching, (B) after longitudinal stretching, and (C) after perpendicular stretching, and on (D, E) randomly oriented nanofibers: (D) before stretching and (E) after stretching. The direction of stretching is represented by "↔". (Lee et al., 2005) 35

Figure 12 An electrospinning process scheme with a chaotic fiber orientation SEM image. (Mitchell & Tojeira, 2013) 39

Figure 13 The SEM images (scale = 10 μm) of electrospun scaffolds collected on (A–D) the rotating cylindrical collector with different velocities and (E) the stationary planar

collector. The inset plots display the Von Mises distribution representing the fiber alignment. (F): Table with means ± standard deviations of the fiber alignment, collector velocity, and fiber diameter. (Fee et al., 2016) 40

Figure 14 (A): Results of the uniaxial testing of scaffolds with different fiber alignment parameter κ showing elastic modulus for the directions parallel and perpendicular to the direction of fiber alignment (* – one-way ANOVA, Tukey post-hoc, $p < 0.05$; ** – $p < 0.05$, 2-sample t-test). (B): The linear dependence of the alignment parameter κ on the log of the anisotropy ratio (defined as the ratio of the modulus in the parallel and the perpendicular direction). (Fee et al., 2016)..... 40

Figure 15 Surface morphology of original tissue PS and two differently structured samples in the schemes and SEM images (134 × 134) μm. Cytoskeletons of mouse fibroblasts cultivated on the structured samples are on the right in fluorescence microscope images (magnification: 100×, red color - actin). (Wrzecionko et al., 2017) 43

Figure 16 AFM images of PS (a) smooth unmodified foil and (b–d) irradiated samples under different angles of laser beam incidence: (b) 0° (Λ = 200 nm), (c) 15° (Λ = 270 nm), and (d) 30° (Λ = 340 nm). (Rebollar et al., 2008)..... 46

Figure 17 Photo of the bioreactor with the 3D-printed inner frame holding and stretching electrospun PU sample seeded with mouse embryonic stem cells while a culture medium is streaming throughout..... 55

Figure 18 Results of MTT assay referring to the cytotoxicity of the sample 1 extracts (a different number of stars indicates a statistically significant difference, one-way ANOVA, $p < 0.05$). 60

Figure 19 The SEM photographs of PU nonwoven mat, sample 1, in its (A) original form with un-oriented fibers, (B) modified form with oriented fibers. 61

Figure 20 The fluorescence microscopy photographs of mouse fibroblasts (NIH/3T3) cultivated on the sample 1 in its (A, C) original form with un-oriented fibers, (B, D) modified form with oriented fibers; (A, B) ActinRed – actin, (C, D) Hoechst – DNA. 62

Figure 21 Results of MTT assay referring to the cytotoxicity of the sample 2 extracts (a different number of stars indicates a statistically significant difference, one-way ANOVA, $p < 0.05$). 63

Figure 22 The SEM photographs of PU nonwoven mat, sample 2, in its (A) original form with un-oriented fibers, (B) modified form with oriented fibers. 64

Figure 23 The fluorescence microscopy photographs of mouse fibroblasts (NIH/3T3) cultivated on the sample 2 in its (A, C) original form with un-oriented fibers, (B, D) modified form with oriented fibers; (A, B) ActinRed – actin, (C, D) Hoechst – DNA. 65

Figure 24 Results of MTT assay referring to the cytotoxicity of the sample 3 extracts (a different number of stars indicates a statistically significant difference, one-way ANOVA, $p < 0.05$). 66

Figure 25 The SEM photographs of PU nonwoven mat, sample 3, in its (A) original form with un-oriented fibers, (B) modified form with oriented fibers. 67

Figure 26 The fluorescence microscopy photographs of mouse fibroblasts (NIH/3T3) cultivated on the sample 3 in its (A, C) original form with un-oriented fibers, (B, D) modified form with oriented fibers; (A, B) ActinRed – actin, (C, D) Hoechst – DNA. 68

Figure 27 The optical microscopy photographs with 40× magnification of mouse fibroblasts (NIH/3T3) cultivated on cell culture PS dishes coated with PPy using APS as polymerization initiator: (A) PPy only, (B) PPy + Alb, (C) PPy + Gel, (D) PPy + Alb/Gel. 70

Figure 28 The optical microscopy photographs with 40× magnification of mouse fibroblasts (NIH/3T3) cultivated on cell culture PS dishes coated with PPy using $FeCl_3$ as polymerization initiator: (A) PPy only, (B) PPy + Alb, (C) PPy + Gel, (D) PPy + Alb/Gel. 71

Figure 29 The fluorescence microscopy photographs of mouse fibroblasts (NIH/3T3) cultivated on the sample 1 in its original form with un-oriented fibers: (A, C) uncoated, (B, D) coated with PPY + Alb/Gel; (A, B) ActinRed – actin, (C, D) Hoechst – DNA. 73

Figure 30 The fluorescence microscopy photographs of mouse fibroblasts (NIH/3T3) cultivated on the sample 1 in its modified form with oriented fibers: (A, C) uncoated, (B, D) coated with PPY + Alb/Gel; (A, B) ActinRed – actin, (C, D) Hoechst – DNA. 74

Figure 31 Results of MTT assay referring to the cytotoxicity of the samples under static cultivation conditions. 75

Figure 32 The fluorescence microscopy photographs of clusters of mouse embryonic stem cells R1 cultivated on the sample 1 in its original form with un-oriented fibers coated with: (A, C) Alb/Gel, (B, D) PPY + Alb/Gel; (A, B) ActinRed – actin, (C, D) Hoechst – DNA.76

Figure 33 The fluorescence microscopy photographs of clusters of mouse embryonic stem cells R1 cultivated on the sample 1 in its modified form with oriented fibers coated with: (A, C) Alb/Gel, (B, D) PPY + Alb/Gel; (A, B) ActinRed – actin, (C, D) Hoechst – DNA.77

LIST OF EQUATIONS

(1) $F = k \cdot \Delta x = \left(\frac{3}{4}\pi E \frac{r^4}{L^3}\right) \cdot \Delta x$ 25

(2) $\Lambda = \frac{\lambda}{n - sin(\theta)}$ 45